



**INSTITUTO POTOSINO DE INVESTIGACIÓN  
CIENTÍFICA Y TECNOLÓGICA, A.C.  
POSGRADO EN CIENCIAS AMBIENTALES**

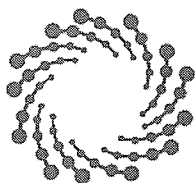
**Elucidating the role of graphene oxide on the  
methanogenic activity of anaerobic consortia**

Tesis que presenta  
**José Iván Bueno López**

Para obtener el grado de  
**Doctor en Ciencias Ambientales**

**Directores de Tesis:**  
**Dr. Francisco Javier Cervantes Carrillo**  
**Dr. José René Rangel Méndez**

San Luis Potosí, S.L.P., febrero de 2020



**IPICYT**

## Constancia de aprobación de la tesis

La tesis ***“Elucidating the role of graphene oxide on the methanogenic activity of anaerobic consortia”*** presentada para obtener el Grado de Doctor en Ciencias Ambientales fue elaborada por **José Iván Bueno López** y aprobada el siete de febrero del dos mil veinte por los suscritos, designados por el Colegio de Profesores de la División de Ciencias Ambientales del Instituto Potosino de Investigación Científica y Tecnológica, A.C.

**Dr. José René Rangel Méndez**  
Codirector de la tesis

**Dr. Francisco Javier Cervantes Carillo**  
Codirector de la tesis

**Dr. Felipe Alatríste Mondragón**  
Miembro del Comité Tutorial

**Dra. Fátima Pérez Rodríguez**  
Miembro del Comité Tutorial

**Dr. Virginia Hernández Montoya**  
Miembro del Comité Tutorial



## **Créditos Institucionales**

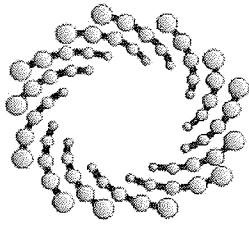
Esta tesis fue elaborada en la División de Ciencias Ambientales del Instituto Potosino de Investigación Científica y Tecnológica, A.C., bajo la dirección del Dr. Francisco Javier Cervantes Carrillo y del Dr. José René Rangel Méndez.

Durante la realización del trabajo el autor recibió una beca académica del Tecnológico Nacional de México y del Instituto Potosino de Investigación Científica y Tecnológica, A.C.

La investigación desarrollada en esta tesis fue financiada por el Consejo Nacional de Ciencia y Tecnología (CONACYT) a través del Fondo Fronteras de la Ciencia (Proyecto 1289).

El autor agradece el apoyo otorgado por la División de Ciencias Ambientales del Instituto Potosino de Investigación Científica y Tecnológica, A.C., para la presentación del trabajo en conferencias nacionales e internacionales.

El trabajo que se describe en el Capítulo IV se desarrolló durante una estancia corta en el departamento Chemical and Environmental Engineering de la Universidad de Arizona bajo la dirección de la Dra. Reyes Sierra Álvarez y con el soporte financiero de the National Science Foundation (NSF award # 1507446).



**IPICYT**

# Instituto Potosino de Investigación Científica y Tecnológica, A.C.

## Acta de Examen de Grado

El Secretario Académico del Instituto Potosino de Investigación Científica y Tecnológica, A.C., certifica que en el Acta 022 del Libro Primero de Actas de Exámenes de Grado del Programa de Doctorado en Ciencias Ambientales está asentado lo siguiente:

En la ciudad de San Luis Potosí a los 7 días del mes de febrero del año 2020, se reunió a las 10:00 horas en las instalaciones del Instituto Potosino de Investigación Científica y Tecnológica, A.C., el Jurado integrado por:

|  |                        |               |
|--|------------------------|---------------|
| <b>Dr. Felipe Alatraste Mondragón</b>          | <b>Presidente</b>      | <b>IPICYT</b> |
| <b>Dra. Virginia Hernández Montoya</b>         | <b>Secretaria</b>      | <b>ITA</b>    |
| <b>Dr. Francisco Javier Cervantes Carrillo</b> | <b>Sinodal externo</b> | <b>UNAM</b>   |
| <b>Dra. Fátima Pérez Rodríguez</b>             | <b>Sinodal</b>         | <b>IPICYT</b> |
| <b>Dr. José René Rangel Méndez</b>             | <b>Sinodal</b>         | <b>IPICYT</b> |

a fin de efectuar el examen, que para obtener el Grado de:

**DOCTOR EN CIENCIAS AMBIENTALES**

sustentó el C.

**José Iván Bueno López**

sobre la Tesis intitulada:

*Elucidating the role of graphene oxide on the methanogenic activity of anaerobic consortia*

que se desarrolló bajo la dirección de

**Dr. José René Rangel Méndez**  
**Dr. Francisco Javier Cervantes Carrillo (UNAM)**

El Jurado, después de deliberar, determinó

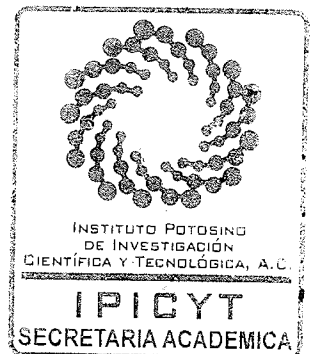
**APROBARLO**

Dándose por terminado el acto a las 12:20 horas, procediendo a la firma del Acta los integrantes del Jurado. Dando fe el Secretario Académico del Instituto.

A petición del interesado y para los fines que al mismo convengan, se extiende el presente documento en la ciudad de San Luis Potosí, S.L.P., México, a los 7 días del mes de febrero de 2020.

**Dr. Marcial Bonilla Marín**  
Secretario Académico

**Mtra. Ivonne Lizette Cuevas Vélez**  
Jefa del Departamento del Posgrado





---

## Dedicatorias

A mis padres y hermanas que han sido las personas que más han aportado desinteresadamente tiempo, amor, apoyo moral, económico y sacrificios para que pueda seguir avanzando en los aspectos académicos de mi vida y jamás han esperado obtener beneficio personal alguno.

A Alejandro Flores Días que gracias a sus “defectos” me ayudó a que continuara en este camino llamado vida y que seguramente sin esta intervención fortuita nada hubiera llegado hasta este punto.

A la memoria de la conciencia humana que es evidente que hace mucho tiempo que murió para dar paso al “progreso” y la “modernidad”.



---

## **Agradecimientos**

A mi familia por apoyarme y motivarme en todo momento y por aportar de todo tipo de recursos para que pudiera seguir adelante, sin ellos nada hubiera sido ni nada soy.

A mi tío Antonio López Valadez por financiar mi estancia en el extranjero y estar al pendiente de mí todo el tiempo que estuve en aquellas tierras estadounidenses.

A mis compañeros que fueron mis maestros en el laboratorio y coparticipes en la obtención de los resultados obtenidos en este trabajo, les agradezco inmensamente y soy consciente de que nadie puede lograr nada solo y que todo logro en la vida de una persona es el resultado de muchas que trabajan desinteresadamente detrás de ésta. En especial le doy gracias a Emilia Ríos, Esmeralda Vences, Alan Quezada, Eduardo Toral e Irma López. Gracias por compartir conmigo su conocimiento y su tiempo.



## Contents

|   |              |
|---|--------------|
| <b>Constancia de aprobación de la tesis</b> | <b>ii</b>    |
| <b>Créditos Institucionales</b>             | <b>iii</b>   |
| <b>Dedicatorias</b>                         | <b>v</b>     |
| <b>Agradecimientos</b>                      | <b>vi</b>    |
| <b>List of Tables</b>                       | <b>xi</b>    |
| <b>List of Figures</b>                      | <b>xii</b>   |
| <b>Resumen</b>                              | <b>xvii</b>  |
| <b>Abstract</b>                             | <b>xix</b>   |
| <b>Motivation of this research</b>          | <b>xxi</b>   |
| <b>Structure of this thesis</b>             | <b>xxiii</b> |
| <b>Chapter I. Introduction</b>              | <b>1</b>     |
| 1.1 Environmental concerns                  | 2            |
| 1.1.1 Global warming and climate change     | 2            |
| 1.2 Biorefinery                             | 4            |
| 1.3 Anaerobic digestion process             | 7            |
| 1.3.1 Principles of anaerobic digestion     | 7            |
| 1.4 Graphene Oxide                          | 11           |
| 1.4.1 Structure and chemistry               | 11           |
| 1.4.2 Reduced graphene oxide                | 12           |
| 1.5 Starch                                  | 14           |
|   | vii          |



|  |  |           |
|--|--|-----------|
| 1.5.1  | Structure and chemistry  | 14        |
| 1.6  | Known effects of graphene materials on anaerobic digestion       | 17        |
| 1.7  | Rationale  | 18        |
| 1.8  | Hypotheses   | 19        |
| 1.9  | Objectives   | 19        |
| 1.9.1  | General objective  | 19        |
| 1.9.2  | Specific objectives  | 20        |
| <b>Chapter II. Graphene oxide triggers mass transfer limitations on the methanogenic activity of an anaerobic consortium with a particulate substrate*</b> |  | <b>21</b> |
| 2.1  | Introduction   | 23        |
| 2.2  | Materials and methods  | 25        |
| 2.2.1  | Materials and chemical reagents                                  | 25        |
| 2.2.2  | Solutions  | 25        |
| 2.2.3  | Inoculum   | 26        |
| 2.2.4  | Characterization of materials                                    | 26        |
| 2.2.5  | Methanogenic activity tests                                      | 28        |
| 2.3  | Results and discussion   | 28        |
| 2.3.1  | Effects of GO on methanogenic sludge                             | 28        |
| 2.3.2  | Interactions between GO and starch affecting anaerobic digestion | 34        |
| 2.3.3  | Environmental relevance  | 40        |
| 2.4  | Conclusions  | 41        |



|  |           |
|--|-----------|
| <b>Chapter III. Enhanced methane production promoted by reduced graphene oxide in an anaerobic consortium supplied with particulate and soluble substrates</b> | <b>42</b> |
| 3.1 Introduction   | 43        |
| 3.2 Materials and methods  | 45        |
| 3.2.1 Materials and chemical reagents  | 45        |
| 3.2.2 Solutions  | 45        |
| 3.2.3 Chemical reduction of GO   | 46        |
| 3.2.4 Characterization of materials  | 46        |
| 3.2.5 Biological assays  | 48        |
| 3.3 Results and discussion   | 49        |
| 3.3.1 Physical characterization  | 49        |
| 3.3.2 Spectroscopic characterization   | 54        |
| 3.3.3 Acute effects of rGO materials on methanogenesis   | 57        |
| 3.4 Conclusions  | 61        |
| <b>Chapter IV. Effects of graphene oxide and reduced graphene oxide on acetoclastic, hydrogenotrophic and methylotrophic methanogenesis</b>                    | <b>62</b> |
| 4.1 Introduction   | 63        |
| 4.2 Materials and methods  | 66        |
| 4.2.1 Chemicals  | 66        |
| 4.2.2 Solutions  | 66        |
| 4.2.3 Chemical reduction of graphene oxide   | 67        |
| 4.2.4 Spectroscopic characterization of materials  | 67        |
| 4.2.5 Particle size distribution   | 68        |



---

|                                       |  |           |
|---------------------------------------|--|-----------|
| 4.2.6                                 | Batch sludge incubations                         | 68        |
| 4.3                                   | Results and discussion                           | 69        |
| 4.3.1                                 | Characterization of graphene materials           | 69        |
| 4.3.2                                 | Effects of GO and rGO on methanogenic activities | 73        |
| 4.4                                   | Conclusions                                      | 84        |
| <b>Chapter V. General discussions</b> |  | <b>85</b> |
| <b>Chapter VI. Final remarks</b>      |  | <b>91</b> |
| 6.1                                   | Concluding remarks                               | 92        |
| 6.2                                   | Perspectives                                     | 94        |
| 6.3                                   | Scientific products                              | 95        |
| 6.3.1                                 | Scientific publications                          | 95        |
| 6.3.2                                 | Congresses and symposia                          | 95        |
| <b>References</b>                     |  | <b>97</b> |



## List of Tables

|   |    |
|---|----|
| <b>Table II-1.</b> Concentration of acidic oxygenated functional groups (in milli-electron equivalents per g (meq/g)) in GO quantified by Boehm titration. ....   | 38 |
| <b>Table III-1.</b> Maximum methanogenic activity (MMA) obtained for experiments using glucose or starch and rGO with different reduction degrees .....   | 60 |
| <b>Table IV-1.</b> Calculated maximum methanogenic activity (MMA) <sup>a</sup> observed with different substrates in the presence of GO and rGO.....  | 75 |
| <b>Table IV-2.</b> Calculated maximum methanogenic activity (MMA) <sup>1</sup> observed with different substrates in the presence and absence of rGO <sub>2</sub> for granular and crushed sludge ..... | 83 |



## List of Figures

- Figure I-1.** Scheme of the biorefinery concept. Source: (Rabaçal et al., 2017)..... 6
- Figure I-2.** Stages of the anaerobic digestion. .... 8
- Figure I-3.** Models for interspecies electron transfer. Interspecies electron transfer between *Geobacter* species. Multiple lines of experimental evidence suggest that c-type cytochrome (red circles) and pili (lines) are important for the electron exchange and thus c-type cytochrome is hypothesized to make electrical contacts with as yet unknown cytochromes (orange triangle) of *G. metallireducens* or conductive pili (a). Electron transfer in conductive methanogenic aggregates. *Geobacter* species (orange), and possibly other syntrophic bacteria, are hypothesized to contribute to aggregate conductivity with conductive pili, but the mechanisms by which methanogens (blue) can consume the electrons have yet to be determined (b). Source:(Lovley, 2011) ..... 10
- Figure I-4.** Functional groups of graphene oxide. .... 12
- Figure I-5.** Graphene oxide (GO) is used as a starting material for the preparation of reduced graphene oxide (rGO). Epoxy and hydroxyl functional groups are randomly distributed on both sides of the starting GO sheet. Via a thermal annealing process (that is, thermal reduction), some of atoms are removed, resulting in nanopores formed in rGO materials with a variety of sizes. All



structures are represented as ball and stick with carbon, oxygen and hydrogen atoms in grey, red and white color, respectively. Source:(Lin and Grossman, 2015). ..... 13

**Figure I-6.** Proposed mechanism of microbial reduction of graphene oxide. Orange dots represent self-secreted electron mediators; blue circles with white dots represent multiheme-containing outer-membrane c-type cytochromes; the molecular structure of the heme group is shown in the dashed circle. Source: (Wang et al., 2011). ..... 14

**Figure I-7.** Starch and the powers of ten. The different levels of structural organization spanning five orders of magnitude. Source:(Pérez and Bertoft, 2010) ..... 15

**Figure I-8.** Scanning electron microscopy (SEM) and polarized light optical microscopy (insets) images of native starch granules from various cultivars: (a) taro; (b) chest- nut; (c) ginger; (d) manioc; (e) corn; (f) green banana; (g) wheat and (h) potato. Scale bars in all images: 20  $\mu$ m. Source: (Pérez and Bertoft, 2010)..... 16

**Figure II-1.** Cumulative methane production by anaerobic sludge supplied with glucose (a) and starch (b) as substrates at different GO concentrations (numbers displayed in series represent GO concentrations in mg/L). ..... 29

**Figure II-2.** SEM images of starch granules in dry powder (a) and the schematic growth rings around the hilum identified by the arrow (a inset); granules dispersed in water and dried before observation (b); and starch granules covered with GO sheets (c, d). ..... 31

**Figure II-3.** Size distribution obtained by dynamic light scattering of starch (gray) and GO (black) at pH 7 using deionized water as dispersant. .... 32

**Figure II-4.** SEM images showing size of starch granules previously dispersed in water (a), size of some blocklets from 103.5 nm to 257 nm (a inset), GO sheets from incubation with glucose (b) and GO without treatment dried at room temperature over 12 h before observation (b inset). .... 33

**Figure II-5.** SEM images of sludge obtained from the UASB reactor without treatment (a), where bacilli and cocci are the most abundant and with scarce presence of exopolysaccharides (b). Sludge flocs were covered by GO in the treatment with glucose and salt crystals show affinity for GO



(c). Similarly, cells in the treatment with starch show a GO wrapping that remains after cell dehydration (d). Image of sample taken from the treatment with starch and GO showing starch blocklets and GO sheets tangled up in exopolysaccharides threads (e)..... 35

**Figure II-6.** Zeta potential of starch, GO-starch mixture and GO with respect to pH. Deionized water was the dispersant. .... 36

**Figure II-7.** Dissociation potential (pKa) distribution of GO using deionized water as dispersant. .... 36

**Figure II-8.** High-resolution C1s X-ray photoelectron spectrum of GO. Dots represent experimental data; solid lines are fitted peaks that identify the different bond types of carbon, and dashed line shows  $\pi$ - $\pi^*$  transitions in aromatic rings (inset). .... 37

**Figure II-9.** High-resolution O1s X-ray photoelectron spectrum of GO. Grey scale solid lines represent deconvoluted peaks, while dots are the experimental data. .... 38

**Figure II-10.** FT-IR spectra of starch, graphene oxide (GO) and starch-GO mixtures with 1:2 and 1:1 ratio, respectively..... 39

**Figure III-1.** Size distribution of GO and rGO materials, bars represent the percentage of particles of a given size, while curves were added to make clearer the pattern of size distribution due to the reduction process ..... 50

**Figure III-2.** SEM images of untreated GO and the reduced materials obtained at increasing reduction time (rGO1, rGO2 and rGO4)..... 51

**Figure III-3.** SEM images of pristine starch granules (a), mixture of starch and GO (b), clusters found in samples with rGO4 (c), structures inside the clusters (d) and a sample of the bioassays using starch and rGO4 at low (e) and high magnification (f). .... 53

**Figure III-4.** Raman spectra of reduced and unreduced GO materials showing the main bands of carbonaceous materials. .... 55



**Figure III-5.** FTIR spectra of reduced and unreduced materials. Shaded areas indicate the regions of the oxygenated functional groups that underwent changes throughout the reduction process. 57

**Figure III-6.** Cumulative methane concentration using glucose (a) or starch (b) and their corresponding maximum methanogenic activity (MMA; b and d) Number displayed in the series legend indicate de concentration (mg/L) of rGO materials reduced 1, 2 and 4 hours, respectively, rGO1, rGO2 and rGO4. Letters on top of bars show statistical difference ( $p < 0.05$ ) respect to the control without rGO materials (letter a) and between treatments (letter b). Same set of letters means no statistically difference. .... 59

**Figure IV-1.** FTIR spectra of GO and rGO. Shaded areas indicate the regions of oxygenated functional groups that underwent changes through the reduction process. .... 70

**Figure IV-2.** Raman spectra of GO and rGO obtained by chemical reduction using ascorbic acid. .... 71

**Figure IV-3.** Core level C1s high resolution XPS spectra of (a) GO, (b) rGO obtained by chemical reduction using ascorbic acid. Dots and black solid line represent the experimental data, while gray and dotted lines are the deconvoluted components..... 72

**Figure IV-4.** Cumulative methane production related to acetoclastic (up), hydrogenotrophic (middle) and methylotrophic (down) activities using different concentrations of graphene oxide (GO) and reduced GO (rGO). Ctrl refers to control incubations performed without GO/rGO. Error bars represent the standard deviation of triplicates. .... 74

**Figure IV-5.** Core level C1s high resolution XPS spectra of GO materials recovered from (a) acetoclastic, and (b) methylotrophic experiments at the end of the incubation period. Dots and black solid line represent the experimental data, while gray and dotted lines are the deconvoluted components. .... 78

**Figure IV-6.** FTIR spectra of GO from abiotic incubations without sludge. Shaded areas highlight the regions of oxygenated functional groups of interest. .... 80



**Figure IV-7.** Comparative of cumulative methane production using granular sludge, crushed sludge and 300 mg/L of the rGO. Ctrl refers to control incubations performed without rGO. .... 82

**Figure V-1.** Comparison of the effect of GO and rGO4 on the anaerobic methanogenic consortium, using 100 mg/L of starch as substrate and 300 mg/L of each graphene material. Control is the treatment without graphene materials. .... 86

**Figure V-2.** Schematic representation of the possible interactions between starch (A) or cells (B) and the GO functional groups; as well as GO agglomeration due to the bridging effect of divalent cations in the basal medium that could involve organic matter (C; e.g. Exopolysaccharides) or cells directly (D). .... 88



## Resumen

**J. Iván Bueno-López. 2019. "Elucidando el papel del óxido de grafeno en la actividad metanogénica de los consorcios anaerobios". Tesis Doctoral, IPICYT, San Luis Potosí, México.**

El grafeno es un nanomaterial de gran interés debido a sus interesantes propiedades mecánicas, ópticas y eléctricas, ideales para el desarrollo de nuevos materiales y dispositivos en todos los campos de la tecnología; sin embargo, su producción a gran escala aun es costosa. Por lo tanto, se ha recurrido al uso de óxido de grafeno (GO) como precursor, el cual al ser reducido genera un GO reducido (rGO) que es similar al grafeno, pero que aún retiene algunos grupos oxigenados. Debido a las grandes cantidades que ya se están usando de GO y rGO en sustancias y productos, se espera que los efluentes de los procesos industriales que usan estos materiales como materia prima lleguen a las plantas de tratamiento de aguas residuales, que en un futuro deben convertirse en partes centrales de una bio-refinería, donde la biomasa reemplace al petróleo y los procesos biotecnológicos altamente eficientes y versátiles como la digestión anaerobia permitan la transformación de las materias primas y de este modo enfrentar los problemas ambientales causados por la dependencia del petróleo. La digestión anaerobia (AD) encaja perfectamente en este concepto al ser una tecnología prometedora para la generación de energía renovable y la obtención de componentes químicos; sin embargo, los efectos del GO y rGO sobre la AD son poco conocidos. Por lo tanto, es de suma importancia generar más conocimiento que permita aprovechar al máximo el potencial de la AD. En este sentido, el objetivo de este trabajo fue evaluar los efectos del GO y rGO sobre un consorcio anaerobio para determinar la existencia y efectos de las interacciones entre estos materiales y el tipo de sustrato, ya sea soluble y fácilmente fermentable, como la glucosa, o con uno particulado que requiere de hidrólisis, como el almidón. Además de estudiar cómo afecta la presencia de estos materiales de forma específica a las rutas metanogénica acetoclástica, hidrogenotrófica y metilotrófica. Los resultados señalan que el rGO produce una mejora al promover la transferencia directa de electrones entre especies (DIET)y/o el transporte de electrones entre exoelectrógenos y metanógenos, así como por favorecer la desintegración de



materia particulada (almidón). Por el contrario, el GO reduce la metanogénesis debido a que encapsula al almidón impidiendo su hidrólisis, mientras que las rutas acetoclástica e hidrogenotrófica son especialmente inhibidas debido a que los electrones derivados del sustrato son empleados para reducir el GO, lo que se comprobó mediante XPS. La información de este trabajo apunta a que el rGO predominará en los sistemas de tratamiento anaerobios y aporta conocimientos sobre los efectos y mecanismos involucrados. Además, ofrece indicios sobre la aplicación de la digestión anaerobia para modificar GO y la obtención de estructuras 3D de rGO.

**Palabras clave:** Digestión anaerobia, metanogénesis, óxido de grafeno, almidón.



## Abstract

**J. Iván Bueno-López. 2019. "*Elucidating the role of graphene oxide on the methanogenic activity of anaerobic consortia*". Doctoral Thesis, IPICYT, San Luis Potosí, Mexico.**

Graphene is a nanomaterial of great interest due to its interesting mechanical, optical and electrical properties, ideal for the development of new materials and devices in all fields of technology; however, its large-scale production is still expensive. Therefore, the use of graphene oxide (GO) as a precursor has been used, which is treated to generate a reduced GO (rGO) that is very similar to graphene, but still contains some oxygenated groups. Due to the large amounts of GO and rGO that are used in substances and products, it is expected that effluents from industrial processes, using this material as raw material, will reach wastewater treatment plants, which soon must become central parts of the biorefinery concept to face the environmental problems caused by the dependence on oil. Anaerobic digestion (AD) fits perfectly in the biorefinery model, being a promising technology for the generation of renewable energy and for obtaining building block chemicals; however, the effects of GO and rGO on AD are poorly understood. Therefore, it is of the utmost importance to generate more knowledge that allows the maximum potential of AD. In this sense, the objective of this work was to evaluate the effects of the GO and rGO on an anaerobic consortium to assess the effects of the interactions between these materials and the type of substrate. Experiments were conducted with soluble and easily fermentable substrates, such as glucose, and with a particulate one requiring hydrolysis, such as starch. Moreover, this dissertation is also focused on studying how the presence of these materials affects the acetoclastic, hydrogenotrophic and methylotrophic methanogenic routes. Results revealed that rGO produces an improvement on the methanogenic activity by promoting the direct interspecies electron transfer (DIET) and/or the transport of electrons between exoelectrogens and methanogens, besides to favor the disintegration of particulate matter (starch). On the contrary, GO decreased methanogenesis because it encapsulates starch granules, preventing their hydrolysis, while acetoclastic and hydrogenotrophic routes were specially inhibited because electrons derived from the substrate were used to reduce GO, which was confirmed by XPS. The information in this paper



---

suggests that rGO will predominate in the anaerobic treatment systems and provides knowledge on the effects and mechanisms involved, in addition to offering hint on other applications of AD such as GO modification and obtaining 3D structures of rGO.

**Keywords:** Anaerobic digestion, methanogenesis, graphene oxide, starch



## Motivation of this research

It is well known that oil, as a non-renewable resource, will be exhausted, but before its depletion there will be a high increase in costs. This will lead to an escalation in prices of practically all products, since in the current economy most of the goods are derived from oil, or they are transported or transformed by energy from fossil fuels. Even more importantly is the fact that emissions of greenhouse gases, such as CO<sub>2</sub>, have already caused global warming, which has unbalanced the global system of the Earth giving rise to the so-called climate change. This scenario will greatly affect human health and could even lead to the extinction along with the majority of the other existing species due to the event of massive extinction that can trigger. Therefore, it is imperative to eradicate the dependence on oil and to make a change of economy to one whose contribution of emissions is null in net terms and therefore is part of the recycling cycles of matter that nature carries out to maintain balance that sustains life. The above can be achieved by adopting the use of biorefinery as a central part of economic development, where biomass replaces oil and highly efficient and versatile biotechnological processes, such as anaerobic digestion, can be the core part in the transformation of raw materials for obtaining products with high added value.

Unfortunately, the predictions that have been made, even considering that the economy based on recycling and renewable resource: the biobased economy (bioeconomy) is installed at this moment, point out that the global average temperature will continue to rise exceeding the 1.5 °C established as the maximum goal of increase for the 21st century. A scenario in which there are serious adverse effects, such as sea level rise, melting of polar ice, territorial expansion of vector-borne diseases and the frequency of extreme weather events. However, it is necessary to act and make proposals to combat and adapt to climate change, thus we need the knowledge, provided by works like the present dissertation, on a system, such as anaerobic digestion that is highly complex and susceptible to being tuned to obtain products with high added value, especially from what is now considered waste.



The use of materials, such as graphene, graphene oxide and its derivatives are very extensive and the trend indicates that it will continue to increase due to the novel properties they present in applications, such as electronic devices, generation and use of energy, biomedical applications and even in the same processes of purification and treatment of water. However, these graphene materials will probably end up in wastewater treatment processes as pollutants. Especially, graphene oxide which is used as raw material for the synthesis of these materials, mainly through a reduction process using heat, light or chemicals, which may be of biological origin and in second place, reduced graphene oxide derived from the intended reduction process or from the unintended reduction within the effluents. In addition, more knowledge is needed about the interactions that may occur between graphene oxide or reduced graphene oxide and different types of substrates, since these determine the type of impact on anaerobic digestion and the fate of the graphene derivatives in the wastewater treatment plants or the environment. Also, the specific effects that these materials can have on the stages of anaerobic digestion and methanogenic routes are unknown.

This knowledge is key to ensure the efficiency of anaerobic digestion as a pollutant remover, biogas source and biochemical factory. In this sense, the present work investigates the effects of important variables, such as graphene oxide reduction degree and the type of substrate. Two types of substrates were investigated, one easily fermentable and completely soluble, represented by glucose, and another complex, which emulates the particulate organic matter, represented by the starch; as well as four carbon materials, starting with graphene oxide that is currently marketed and three additional materials with different reduction degree.



## Structure of this thesis

This dissertation is organized in five chapters, showing in the first place the basic concepts and the important definitions, in **Chapter I**, which allow the reader to obtain enough background to understand the importance of the development of this study and to interpret, in a general way, the results and the scope of the thesis. In the subsequent chapters the effects of oxidized and reduced graphene materials on the methanogenic activity of anaerobic consortia are studied with two types of substrates, one complex and insoluble (starch) and another simple and soluble (glucose). Additionally, the effects that these graphene derivatives have on the main methanogenic routes of an anaerobic consortium are also described. Specifically, **Chapter II** shows the results obtained from experiments in which graphene oxide and starch are used as a model of complex matter suspended in water systems. Additionally, these results are contrasted with those obtained using glucose, which is a soluble, readily fermentable sugar. On the other hand, **Chapter III** examines the results obtained with the same substrates, but modifying the chemical properties of the graphene materials through a chemical reduction to obtain reduced graphene oxide. Furthermore, in **Chapter IV**, the effects of both graphene oxide and reduced graphene oxide on the methanogenic acetoclastic, hydrogenotrophic and methylotrophic routes is investigated.

As a way of closing, **Chapter V** presents the general discussion of this dissertation emphasizing the main contributions of the study. Finally, **Chapter VI** presents the concluding remarks and perspectives of this work.



# **Chapter I**

## **Introduction**



## **1.1 Environmental concerns**

### **1.1.1 Global warming and climate change**

The current era presents great challenges for life on Earth, in general, because human activity has generated profound changes that are causing the planet to move to a new state of equilibrium, which has been called “Climate Change” and it refers to the alteration of the global natural phenomena that shape the climate and weather, caused by the “Global Warming”, which in turn is defined as the long-term increase in the temperature of the planet.

Global warming is due to the increase in the concentration of greenhouse gases, such as carbon dioxide (CO<sub>2</sub>), product of the excessive use of fossil fuels (Grasso, 2019) on which the current technology is based, both for obtaining energy and for creation of construction materials (e.g., plastics). The concentration of CO<sub>2</sub> has increased drastically since the industrial revolution, registering a concentration of 413.32 parts per million (ppm) in April 2019, much higher than the maximum concentration (300 ppm) of the 700,000 previous years (NOAA Earth System Research Laboratory, 2005).

Climate change obviously implies affecting the ecosystems in different ways, because directly, higher temperatures cause the increase in the level of the sea by thermal expansion and the melting of the ice at the poles, as well as modification of the distribution of the rain; also, greater amount of heat in the atmosphere implies that natural phenomena with greater devastating power, called extreme weather events (climate change). Nonetheless, biodiversity will be affected not only by the phenomena related to precipitation and the change of seasons, but also the fertility of the species is affected by temperature (Walsh et al., 2019). Humans, as a part of nature, will also be affected by climate change, being affected mainly by floods and droughts that will decrease the production of food, as well as by the increase of vector-borne diseases (Bartholy and Pongrácz, 2018).



According to studies, important negative effects are expected due to an increase in the temperature of even 1.5 °C, value that, according to the scientific community, will be reached and exceeded even in the case that the strategies of reduction of emissions of greenhouse gases are applied immediately, because to date the average increase in global temperature is already 0.8 °C and considering other more realistic scenarios in the prediction, it is obtained that the increase can be even higher than 5 °C (Bartholy and Pongrácz, 2018; National Centers for Environmental Information, 2019).

Developed and developing countries are the ones that contribute with most to CO<sub>2</sub> generation, with China and the USA being the first places in terms of the amount of emissions, but unfortunately undeveloped countries are the ones that will suffer more because of the lack of economic and technological resources. Within economic activities, agriculture/livestock and the oil and gas industries generate most emissions, contributing 50 % and 40 %, respectively (Dhillon and von Wuehlisch, 2013).

There are different proposals to fight climate change; however, they all imply a paradigm shift, which apparently, the different actors of the society are not willing to, even when the adverse effects are already noticeable. Corporations and governments do not have applied basic measures suggested by the scientific community to mitigate the damages; to make these issues worse, rulers and citizens of the most powerful nations and also with the highest emissions assure that global warming is a lie designed to affect their economy.

In spite of all the obstacles and interests against it, we must continue fighting to eliminate the dependence on oil, changing to the use of raw materials and renewable energy sources with neutral emissions of CO<sub>2</sub>. Obviously, the wise nature has been doing it for thousands of years and in the biomass has put all the mechanisms that allow an efficient cycling of carbon, now it is up to humanity to develop science and technology that allows to use them for the progress of their civilization. The set of knowledge and technology of this type is currently known as biorefinery and its implementation and development may involve the continuity of the human species on Earth.



## 1.2 Biorefinery

The concept of biorefinery can be easily understood by analogy with the oil refinery, in which various products such as chemicals, fuels and energy are generated; however, the difference with the biorefinery is that in the latter, raw materials are renewable resources such as biomass instead of oil. Properly, the definition of biorefinery, according to The International Energy Agency (IEA, 2012), is: "the sustainable processing of biomass into a spectrum of marketable products (food, feed, materials, chemicals) and energy (fuels, power, heat)".

The purpose of the biorefinery is to optimize the use of resources and reach zero-waste industrial processes, for which it requires the integration of multiple processes carried out either in a facility or in a cluster in which the waste of a process is used to obtain value-added products in others. To achieve this purpose, it is essential that the process, as well as its operating conditions, have flexibility that allows working with the available biomass stream.

Biorefineries can be classified into two types depending on the origin of their inputs: (1) biomass-producing-country type and (2) waste-material-utilization type; in the first type, agricultural products are used, while in the second type the waste from different sources is the raw material (Ohara, 2003; Rabaçal et al., 2017). Likewise, the processes within biorefinery can be classified according to Rabaçal et al., (2017) and Cherubini, (2010) into four types:

- 1) Thermochemical processes. They consist in the treatment of biomass with high temperatures in the absence of oxygen to produce gasification (>700 °C) and obtain Syngas (mixture of H<sub>2</sub>, CO, CO<sub>2</sub> and CH<sub>4</sub>) or pyrolysis (300-600 °C) to obtain bio-oil. Also, direct combustion of biomass is considered here.



- 2) Biochemical processes. These include the fermentation and anaerobic digestion of sugars, starch and derivatives of lignocellulosic materials to obtain mainly ethanol, hydrogen and methane, but there is much research focused on the production of many other compounds.
- 3) Chemical processes. They are the processes in which the biomass is transformed by means of reactions with other substances. There are several types of reactions that are grouped in this type of process, to date the most common are hydrolysis and transesterification.
- 4) Mechanical processes. These do not change the chemical structure and are the first step or pre-treatment of feedstock, they include all the treatments for particle size reduction, shape change and modification of the density.

The products that can be obtained from biorefinery can be classified into two large groups: energy products and material products. Energy products are those that can be used as fuels or to produce heat or electricity, for example, coal, biogas and biodiesel. The material products are the substances that are used for the synthesis of others or that have other applications different from those related to the production of energy due to their physical or chemical properties; Examples of these are materials such as paper, acids and organic solvents, fertilizers, food additives, among others.

If we pay attention to the scheme of biorefinery (Figure I-1), it is clear that anaerobic digestion can be positioned as a central part since the microorganisms present in it are able to hydrolyze complex organic matter, produce various chemical substances and biogas that can be used as an energy source to keep the process running or others linked to the purification, transformation or transport of biorefinery products.

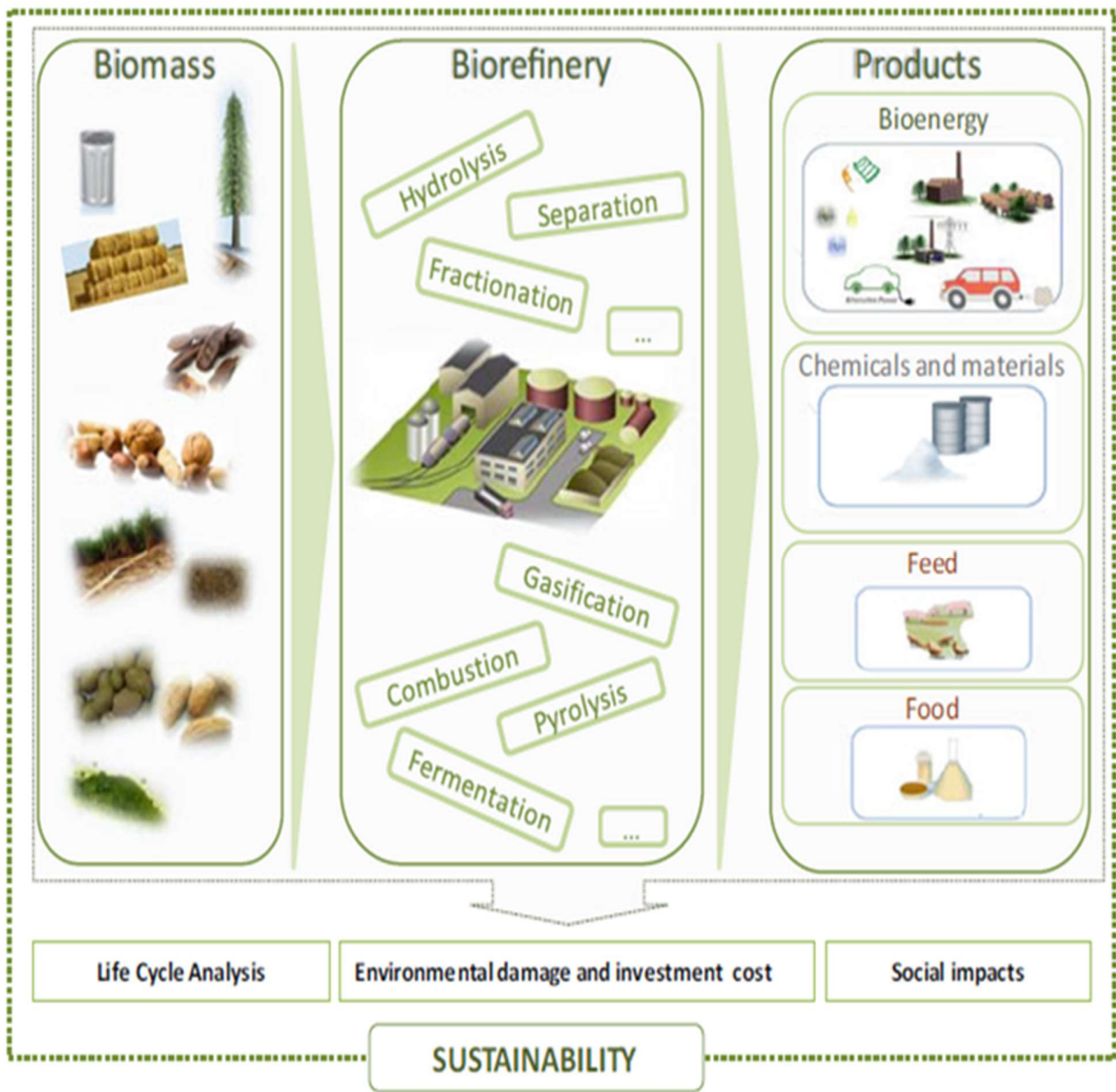


Figure I-1. Scheme of the biorefinery concept. Source: (Rabaçal et al., 2017).



## **1.3 Anaerobic digestion process**

Currently, anaerobic wastewater treatment systems have gained great importance because the space requirements and the costs of maintenance and operation are lower compared to the aerobic processes; in addition, anaerobic treatment offers the possibility of obtaining renewable energy and the recovery of useful nutrients for agriculture, thus promoting a sustainable economy that becomes a necessity every day due to the accelerated deterioration of the environment.

### **1.3.1 Principles of anaerobic digestion**

Anaerobic digestion is carried out by a set of microorganisms associated in complex trophic webs performing different functions that allow to transform the organic matter in stages, making the by-products of some the raw material of others as is schematized in Figure I-2. Anaerobic digestion is a complex process where the transformation reactions are catalyzed by both extracellular and intracellular enzymes from bacteria and archaea in the absence of oxygen (Appels et al., 2008). The stages of anaerobic digestion are essentially four (Ferrer Polo and Seco Torrecillas, 2008; Guo et al., 2015) namely:

1. Hydrolysis. Includes the decomposition of polymers and lipids in their basic structures, such as monosaccharides, amino acids and other related compounds through the action of extracellular enzymes. This process is primarily performed by heterotrophic acidogenic bacteria;
2. Fermentation. Encompasses the transformation of organic compounds, mainly dissolved, into short-chain volatile fatty acids such as acetic, propionic, butyric acid, as well as gases such as hydrogen and carbon dioxide;

3. Acetogenesis. This consists of the conversion of volatile acids and alcohols into acetate, hydrogen and carbon dioxide. It is carried out by a group of obligate hydrogen producing acetogenic bacteria;
4. Methanogenesis. At this stage, methanogens obtain energy by converting carbon dioxide, acetate and hydrogen into methane. According to the main substrate used, methanogens are divided into three large groups:
  - a. Acetoclastic. They consume acetate, alcohols and some amines.
  - b. Hydrogenotrophic. Microorganisms of this group transform hydrogen and CO<sub>2</sub>, as well as formic acid into methane.
  - c. Methylotrophic. This group of methanogens use methylated compounds, such as methanol, methylamines and methyl sulfides.

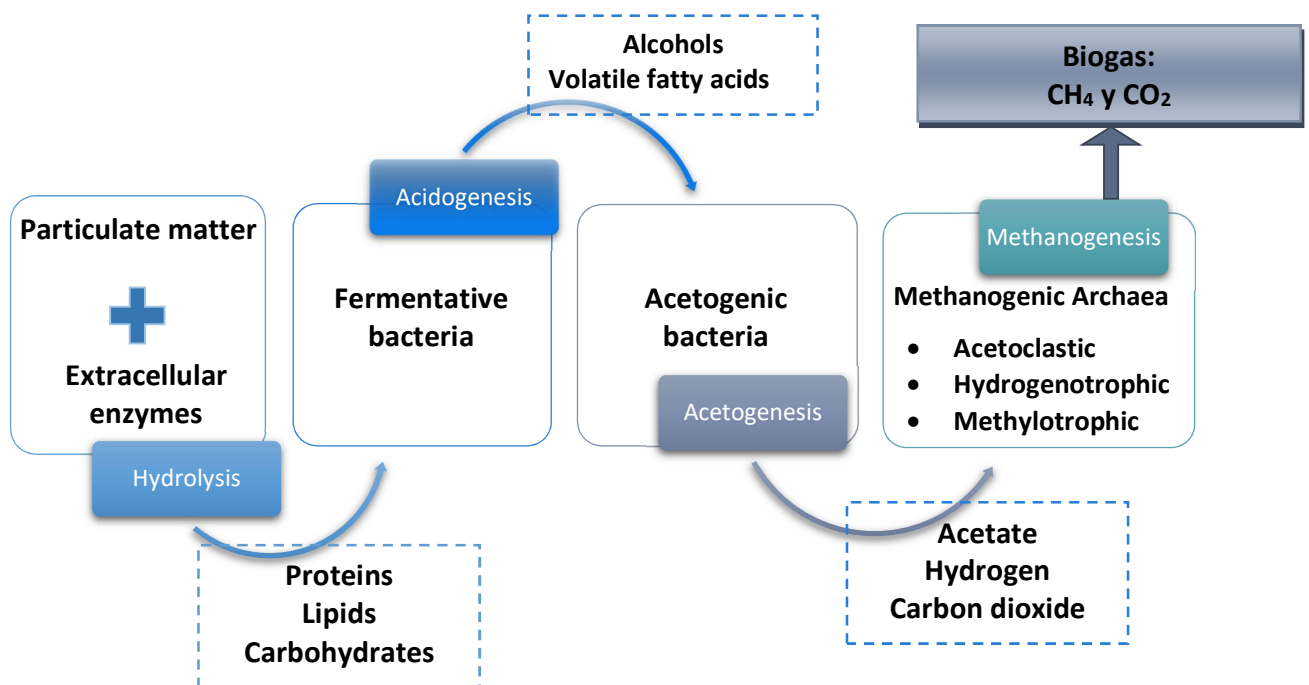


*Figure I-2. Stages of the anaerobic digestion.*



Recently a surprising discovery has shown that there are microorganisms capable of transferring electrons to the outside of the cell, which allows them to use solid materials as electron acceptors, either metals, humic substances and other microorganisms. Microorganisms such as the *Geobacter* species, can transfer the electrons through organic metallic-like conductive fibers called pili or through cytochromes on the outer surface of the cell.

When the electron acceptor is another microorganism, the process is called direct interspecies electron transfer (DIET). It is hypothesized that some methanogens can accept electrons and can form syntrophic associations with exoelectrogenic bacteria as outlined in Figure I-3 (Lovley, 2011). In addition, it has been reported that a variety of conductive materials have proven to improve DIET, including different types of carbonaceous materials such as activated carbon, graphene and different derivatives of the latter (Barua and Dhar, 2017; Lin et al., 2017a; Tian et al., 2017a; Xu et al., 2015). Microorganisms can replace the pili using conductive materials instead since it means an advantage by saving the energy required for the synthesis of pili (Zhao et al., 2015).

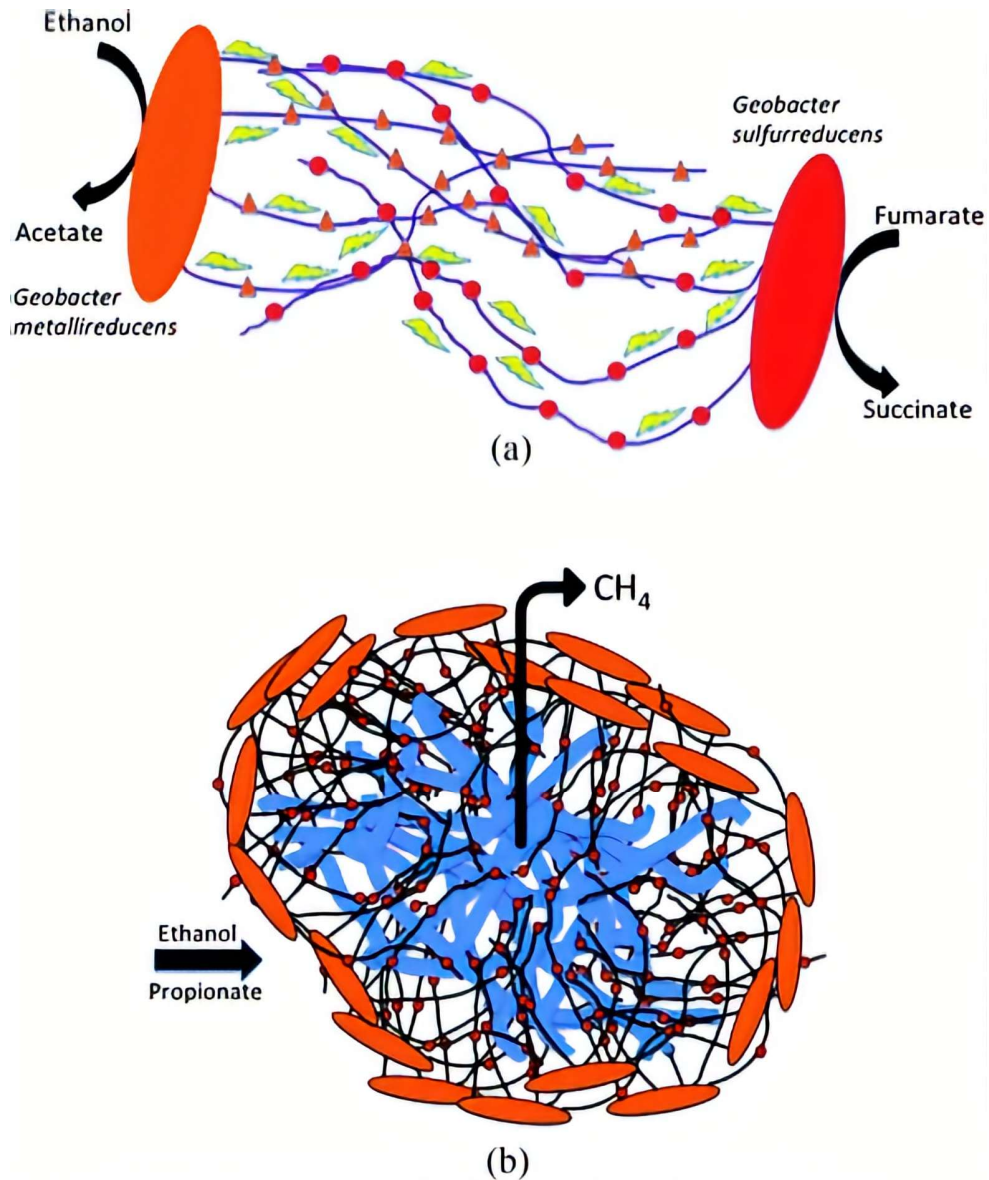


**Figure I-3.** Models for interspecies electron transfer. Interspecies electron transfer between *Geobacter* species. Multiple lines of experimental evidence suggest that *c*-type cytochrome (red circles) and pili (lines) are important for the electron exchange and thus *c*-type cytochrome is hypothesized to make electrical contacts with as yet unknown cytochromes (orange triangle) of *G. metallireducens* or conductive pili (a). Electron transfer in conductive methanogenic aggregates. *Geobacter* species (orange), and possibly other syntrophic bacteria, are hypothesized to contribute to aggregate conductivity with conductive pili, but the mechanisms by which methanogens (blue) can consume the electrons have yet to be determined (b). Source:(Lovley, 2011)



## **1.4 Graphene Oxide**

One of the most recently discovered nanomaterials is graphene, in 2004, which is a single graphitic sheet (carbon with  $sp^2$  hybridization) that has a two-dimensional structure. Graphene has attracted a lot of attention due to its exceptional mechanical, electrical, magnetic, optical and thermal properties. Currently the most viable way to obtain graphene in mass scale is through the oxidation of graphite, which is then subjected to an exfoliation to obtain graphene oxide (GO) and then reduced again to get graphene-like materials. Graphene oxide has the advantage of being dispersible in water and thus is easily handled and is an intermediary in obtaining other forms of modified graphene (Dreyer et al., 2010; Novoselov et al., 2012; Tiwari, 2013; Zhao et al., 2014).

### **1.4.1 Structure and chemistry**

There is no a precise defined model of the structure of GO (Figure 1-4) since the complexity of the material, that even show sample-to-sample variability due to its amorphous, and nonstoichiometric atomic composition. Characterization of this materials had revealed that the plane is decorated with hydroxyl and epoxy (1,2-ether) functional groups, while carbonyl groups are present, most likely as carboxylic acids along the sheet edge and as organic carbonyl defects within the sheet, in addition to other keto and quinone groups. More recently, studies proposed the presence of 5- and 6-membered lactols on the periphery. Various results support that epoxy and alcohol groups on the plane are dominant, while carboxylic acid groups are present in very low quantities.

These functional groups contribute significantly to the agglomeration behavior of GO sheets due to inter-sheet hydrogen bonding through the alcohols and epoxide as well as due to hydrogen bonding of water with oxygen of epoxides (Dreyer et al., 2010; Pei and Cheng, 2012).

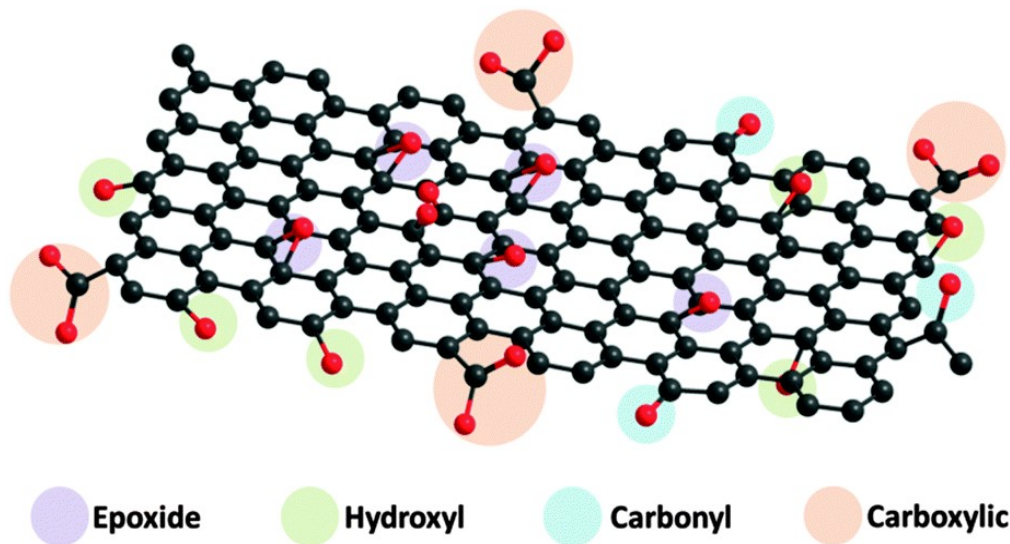


*Figure I-4. Functional groups of graphene oxide.*

#### **1.4.2 Reduced graphene oxide**

Graphene oxide (GO) is one of the main raw materials in the manufacture of graphene products because it is easy to reduce through different methods, such as thermal, laser irradiation, chemical, and electrochemical (Dreyer et al., 2010; Rogala et al., 2016), vitamins and saccharides (De Silva et al., 2017; Thakur and Karak, 2015) and also by microbial reduction (Salas et al., 2010; Wang et al., 2011). Reduced graphene oxide (rGO) is called this way since not all the oxygenated groups are removed in the reduction process. rGO is expected to be found in the environment or in wastewater treatment plants and the reduction degree could vary depending on the conditions of the manufacturing process and the management of the effluent.

The most used processes to obtain rGO are, firstly, thermal reduction, which consists in subjecting GO to high temperature in the absence of oxygen (Figure I-5) and secondly, the chemical reduction which uses a wide variety of substances. Meanwhile, biological reduction by bacterial respiration



(Figure I-6) is a new issue and still requires knowledge about the control of the reduction degree and the methods for purifying the resulting materials.

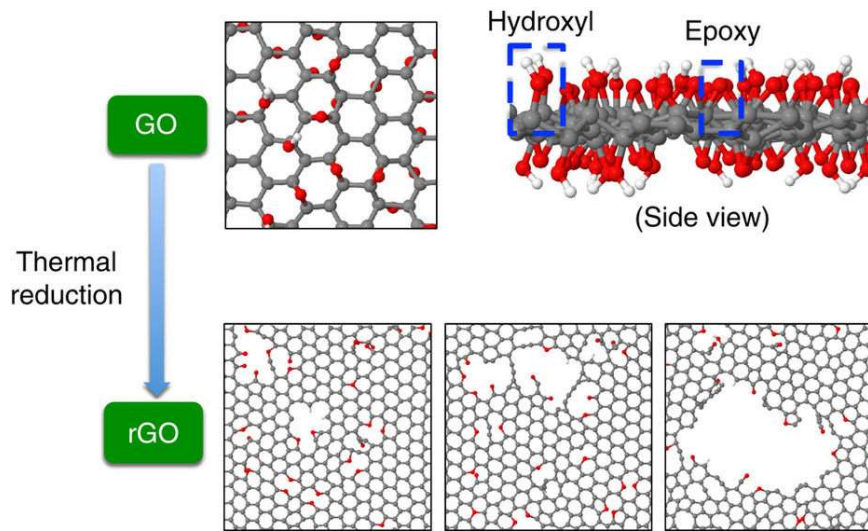


**Figure I-5.** Graphene oxide (GO) is used as a starting material for the preparation of reduced graphene oxide (rGO). Epoxy and hydroxyl functional groups are randomly distributed on both sides of the starting GO sheet. Via a thermal annealing process (that is, thermal reduction), some of atoms are removed, resulting in nanopores formed in rGO materials with a variety of sizes.

All structures are represented as ball and stick with carbon, oxygen and hydrogen atoms in grey, red and white color, respectively. Source: (Lin and Grossman, 2015).

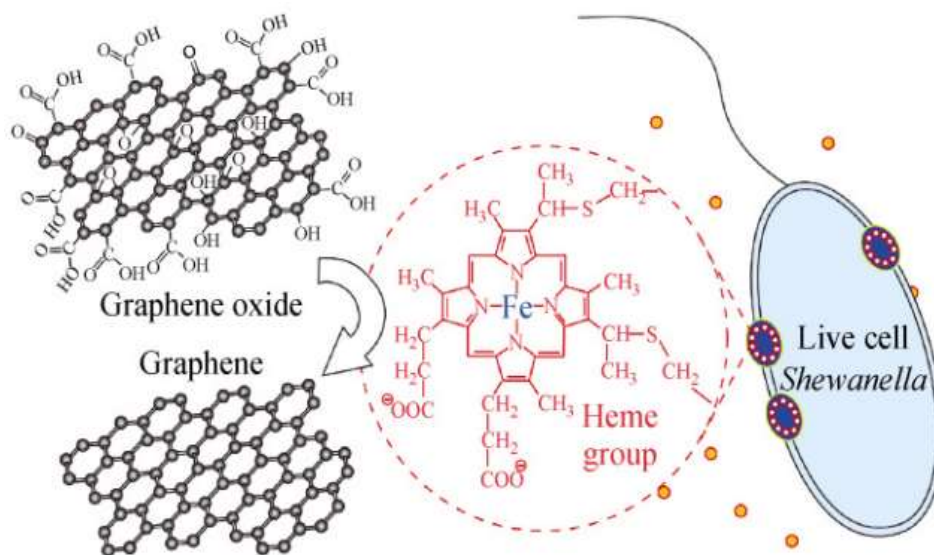


**Figure I-6.** Proposed mechanism of microbial reduction of graphene oxide. Orange dots represent self-secreted electron mediators; blue circles with white dots represent multiheme-containing outer-membrane c-type cytochromes; the molecular structure of the heme group is shown in the dashed circle. Source: (Wang et al., 2011).

## 1.5 Starch

### 1.5.1 Structure and chemistry

Starch is the way in which plants store energy and the second most abundant biopolymer; It is composed mainly of two types of polysaccharides, amylose and amylopectin that are organized in multilevel structures of increasing complexity as shown in Figure I-7 where the levels are: level 1, glucose unit to form the double helix; level 2 lamella; level 3 super helix; level 4 blocklets; level 5 growth rings; level 6 granule. Also, in this figure are shown observations from X-ray fiber diffraction pattern demonstrating a double helix structure (1a) compared with the model of the double helix structure (1b) and a transmission electron microscopy image on hydrolyzed starch, showing the shape of the crystalline lamellae (2a), which corresponds to the model of a crystalline lamella made of about 100 double helices (2b). Moreover, it shows the small angle X-ray scattering (SAXS) and Wide-angle X-ray scattering (WAXS) diffraction images indicating the occurrence



of a super-helix structure (3b) and the super-helix model, with a pitch of 9 nm and a diameter of 18 nm (3a); as well as the image by atomic force microscopy of a typical surface of a starch granule where the bumps seen on the surface show the presence of blocklets(4a) that are organized according to the a blocklets model (4b). Finally, the figure shows the image of starch granules observed by scanning electron microscopy and the pattern obtained under polarized light (6a), along with a set of microfocus X-ray diffraction patterns recorded on a starch granule showing the distribution and orientation of the crystalline domains in a starch granule (6b) and a schematic representation of starch granule section showing the radial orientation of the crystalline domains (lamellae) in a starch granule (6c) (Pérez and Bertoft, 2010).

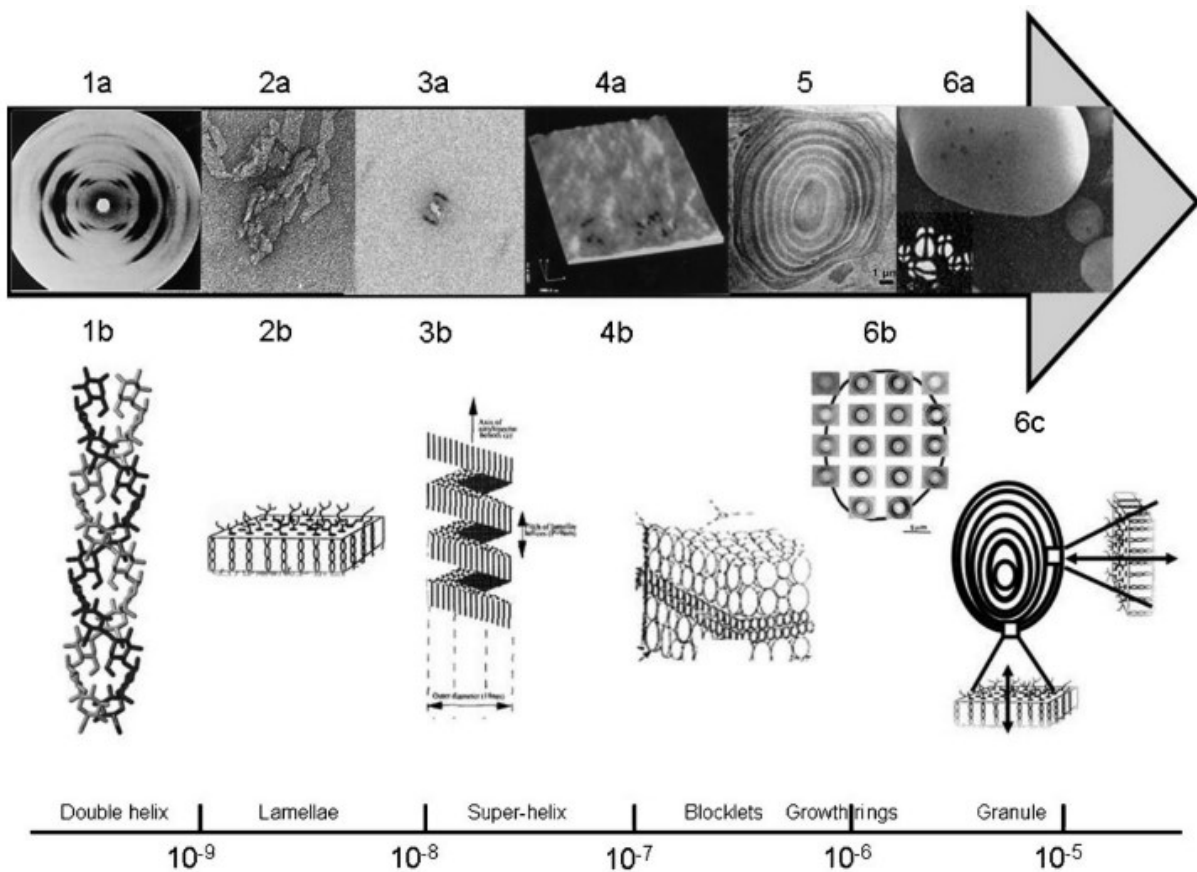


**Figure I-7.** Starch and the powers of ten. The different levels of structural organization spanning five orders of magnitude.

Source:(Pérez and Bertoft, 2010)



Starch granules are structures that vary in size (1-200  $\mu\text{m}$ ) and shape (ovals, spheres, polygons, etc.) depending on the botanical origin (Figure I-8) and display a concentric growth of rings defined by alternate layer of amorphous and semi-crystalline regions. (Hoover, 2001; Pérez and Bertoft, 2010; Vanier et al., 2017; Xie et al., 2013).

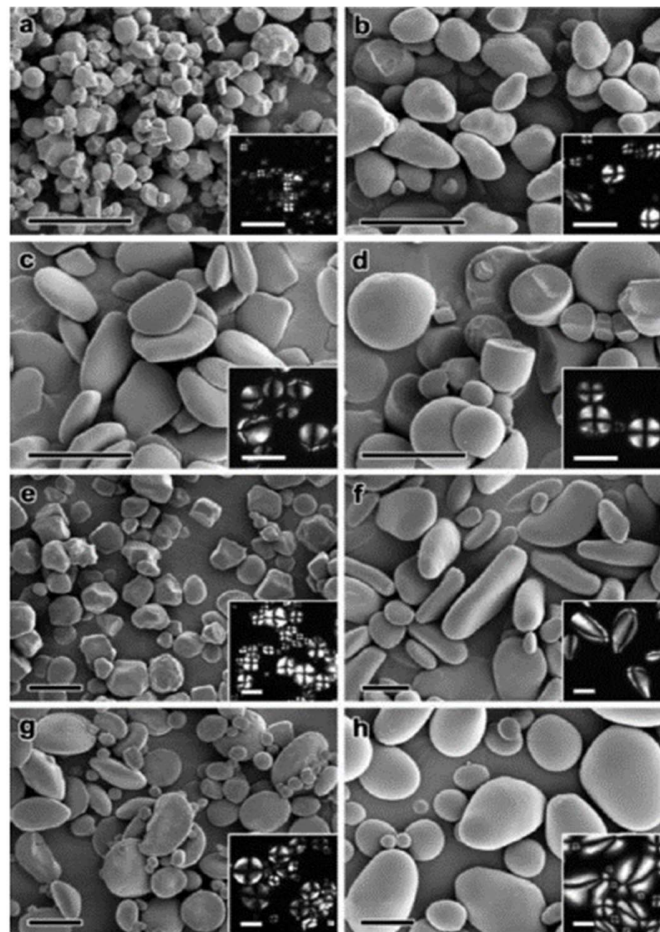


**Figure I-8.** Scanning electron microscopy (SEM) and polarized light optical microscopy (insets) images of native starch granules from various cultivars: (a) taro; (b) chest-nut; (c) ginger; (d) manioc; (e) corn; (f) green banana; (g) wheat and (h) potato. Scale bars in all images: 20  $\mu\text{m}$ . Source: (Pérez and Bertoft, 2010)



The crystallinity of the starch is classified according to the ramifications of amylopectin that cause a certain pattern of X-ray diffraction in:

- Type A.- Short chains and short link distances.
- Type B.- Long chains with long link distance.
- Type C.- it is believed to be a combination of types A and B.

A V- type that results from an amylose complex with substances, such as iodine, fatty acids, emulsifiers or butanol has also been identified. It is characterized by a right single helix. The hydrolysis of starch occurs in two stages: the first is rapid and occurs in the amorphous region and the second slow that develops in the crystalline region. Due to this sequential hydrolysis the starch nanocrystals present in the granules can be obtained (Le Corre et al., 2010).

Starch is of great importance within the food industry and is taking relevance every day in other industrial areas, such as the manufacture of biodegradable materials (Hoover, 2001; Pérez and Bertoft, 2010; Vanier et al., 2017; Xie et al., 2013), as well as, it is used in the synthesis of nanomaterials as a steric stabilizer (Pradeep and Anshup, 2009; Vasileva et al., 2011) and as a green reagent for its functionalization (Feng et al., 2013; Mohammadinejad et al., 2016). Hence, the interaction of the forms of starch with nanomaterials present in the processes of anaerobic digestion is a certainty.

## **1.6 Known effects of graphene materials on anaerobic digestion**

GO was employed as electron shuttle in a methanogenic system for the reduction of a recalcitrant pollutant (azo dye), but the concentration used was 5 mg/L due to toxic effects found at higher concentrations (Colunga et al., 2015). Also, it has been documented that (GO) has a toxic effect on bacteria in pure cultures depending on the size of the GO sheets and on their chemistry (Jastrzębska and Olszyna, 2015; Liu et al., 2012a).



The application of graphene in anaerobic digestion showed a stimulatory effect on methane production at concentrations between 30 and 120 mg/L, favoring specially acetoclastic methanogenesis. The results of this investigation considered a comparison against quinones and obtained that quinones fail to replicate graphene stimulation results, concluding that graphene did not function as electron shuttles in this kind of systems and gave the credit for the methane enhancement to the DIET (Tian et al., 2017a). A similar material to graphene is rGO, which is reported as an enhancer of degradation processes, but in this case attributed to the electron shuttle capacity of its remaining oxygenated functional groups as evidenced in chemical and biological experiments using rGO with different reduction degree used to reduce a halogenated organic drug. The results of these investigations point out that the higher reduction degree the higher reduction of pollutants is obtained, also, alluded to the enrichment of carbonyl groups as the explanation of the aforementioned enhancement (Toral-Sánchez et al., 2017, 2016).

## **1.7 Rationale**

The use of carbon-based materials, such as graphene, graphene oxide and its derivatives is very extensive and the tendency is to continue to increase due to the novel properties they present in applications, such as the miniaturization of electronic devices (Raveendran et al., 2013), optimization in storage, generation and use of energy (Mao et al., 2012; Raza, 2012), biomedical applications in nanomedicine (Besinis et al., 2015; Cheng et al., 2017), as well as applications in the treatment of effluents contaminated by industrial and domestic activities (Anjum et al., 2016; Wang et al., 2013). Knowledge about their impacts and interactions with environmental elements is scarce, to the point that there is no regulation (Eduok et al., 2013; Holden et al., 2016) that allows their detection, quantification and adequate control (Marcoux et al., 2013; Park et al., 2017). The presence of these materials can affect the efficiency of anaerobic processes during the treatment of wastewater. The present dissertation aims to investigate the effects of graphene oxide and



reduced graphene oxide in conjunction with starch, to assess if there is a toxic / inhibitory effect on the different stages of the anaerobic digestion process, since it has been reported that there is a certain selectivity of the inhibition of the stages of anaerobic digestion either independently of the trophic substrate (J. Ma et al., 2013) or dependent on it (Gonzalez-Estrella et al., 2013; Otero-González et al., 2014). Moreover, the results can identify changes occurring in graphene materials within anaerobic digestion. This information could clarify the potential role of graphene materials to enhance the efficiency of anaerobic treatment processes.

## **1.8 Hypotheses**

The functional groups of graphene oxide promote interactions with anaerobic microorganisms and starch granules affecting methane production.

Reduced graphene oxide enhances methane production in a reduction degree dependent manner due to the change in its capacity to conduct electrons that is related to the process of direct interspecies electron transfer.

The change in the physicochemical properties of the graphene oxide through the reduction process in turn causes each stage of the anaerobic digestion process to be affected differently.

## **1.9 Objectives**

### **1.9.1 General objective**

To elucidate the interactions between GO and rGO with a microbial consortium, and to assess the effects of these carbon-based materials on the methanogenic activity with complex (starch) and simple (glucose) substrates. In order to clarify the effects of these materials on the different steps



involved in anaerobic digestion, key intermediates will be monitored, and the carbon materials will be characterized before and after biological experiments to follow the changes that can be associated with the interaction mechanisms.

### **1.9.2 Specific objectives**

- To assess the effects of GO on the methanogenic activity of an anaerobic consortium, which was fed with a complex polymer (starch) or with a soluble readily fermentable substrate (glucose), to elucidate the effects of GO on anaerobic WWTS, which ultimately has relevance to achieve effective anaerobic treatment of industrial effluents to produce bioenergy.
- To study the acute effects of rGO, obtained from GO and reduced at different reductions times using ascorbic acid, on the methanogenic activity of an anaerobic consortium with two different substrates, one soluble (glucose) and other particulate (starch), in order to understand the interactions of rGO with different reduction degree within the methanogenic consortium.
- To study the effects of GO and partially rGO on the acetoclastic, hydrogenotrophic and methylotrophic methanogenic activity of an anaerobic consortium, to determine if there are specific effects (selectivity) on the methanogenic pathways and whether these effects depend on the reduction state and other physical and chemical characteristics of GO, to explain the mechanisms underlying the improvement or inhibition of methane production by carbonaceous materials.



# **Chapter II**

## **Graphene oxide triggers mass transfer limitations on the methanogenic activity of an anaerobic consortium with a particulate substrate\***



## Abstract

Graphene oxide (GO) is an emerging nanomaterial widely used in many manufacturing applications, which is frequently discharged in many industrial effluents eventually reaching biological wastewater treatment systems (WWTS). Anaerobic WWTS are promising technologies for renewable energy production through biogas generation; however, the effects of GO on anaerobic digestion are poorly understood. Thus, it is of paramount relevance to generate more knowledge on these issues to prevent that anaerobic WWTS lose their effectiveness for the removal of pollutants and for biogas production. The aim of this work was to assess the effects of GO on the methanogenic activity of an anaerobic consortium using a particulate biopolymer (starch) and a readily fermentable soluble substrate (glucose) as electron donors. The obtained results revealed that the methanogenic activity of the anaerobic consortium supplemented with starch decreased up to 23-fold in the presence of GO compared to the control incubated in the absence of GO. In contrast, we observed a modest improvement on methane production (>10 % compared to the control lacking GO) using 5mg of GO L<sup>-1</sup> in glucose amended incubations. The decrease in the methanogenic activity is mainly explained by wrapping of starch granules by GO, which caused mass transfer limitation during the incubation. It is suggested that wrapping is driven by electrostatic interactions between negatively charged oxygenated groups in GO and positively charged hydroxyl groups in starch. These results imply that GO could seriously hamper the removal of particulate organic matter, such as starch, as well as methane production in anaerobic WWTS.



## 2.1 Introduction

Nanotechnology is growing at vertiginous speed and everyday more goods containing nanomaterials are available in the market, from food to hi-tech applications (Vance et al., 2015). Unfortunately, the eventual negative effects of tailored nanoparticles on human health and on ecosystems are unknown. Moreover, there are some important knowledge gaps with regard to analytical methods for nanoparticles detection and also lack of legislation to establish guidelines and regulations to ensure the proper and safety management and disposal of nanomaterials-containing residues (Eduok et al., 2013). This is the outcome of poor understanding of the interactions between different nanomaterials and cellular constituents, both in engineered systems and in natural environments (He et al., 2014; Hu et al., 2016; Trujillo-Reyes et al., 2014).

Graphene and graphene oxide (GO) are two of the nanomaterials that have gained a lot of attention due to their interesting properties. GO is used as an intermediate to obtain graphene after its reduction (or reduced GO, rGO for short, since in most cases some oxygenated groups remain on graphitic sheets) (Bagri et al., 2010; Mattevi et al., 2009). Besides, GO contains a range of oxygenated functional groups that can be exploited as anchoring sites for functionalization and its production is inexpensive and easily scalable (Dreyer et al., 2010; Novoselov et al., 2012; Zhao et al., 2014), this is the reason why it is used in many processes and products.

Due to their widespread application, graphene and GO are frequently discharged in several industrial wastewaters, which ultimately reach biological WWTS. Anaerobic digestion is increasingly considered as the best option for wastewater treatment, but given the scenario in which nanomaterials are common components in industrial processes, the arrival of nanomaterials to WWTS is expected, where they will interact with organic matter and cells, eventually affecting the anaerobic digestion process (Yang et al., 2015; Zhao et al., 2014).

Starch is one of the most abundant biopolymers in the world and has been largely used in food industry for human and animal nutrition. Moreover, it is also employed in other applications, such as laundry services and the production of paper, pharmaceuticals, textiles, and biodegradable



products. This scenario has given rise to industries generating effluents with high levels of chemical oxygen demand (COD) due to the presence of residual starch (Lu et al., 2015; Şentürk et al., 2010; Vanier et al., 2017).

GO and its derivatives have also been intensively used in process treatments to remove pathogens, as well as organic and inorganic compounds from gaseous, aqueous and solid media (Shen et al., 2018; Trujillo-Reyes et al., 2014; Wang et al., 2013). They have also been explored as redox mediators in anaerobic systems to enhance the biotransformation of recalcitrant compounds (Colunga et al., 2015; Toral-Sánchez et al., 2017; Wang et al., 2014). Additionally, other studies report on the implementation of graphene as a conductive component in biological systems that facilitates direct interspecies electron transfer (DIET), resulting in enhanced methane production (Lin et al., 2017b; Lü et al., 2018; Tian et al., 2017b); and functionalized GO has even been used as growth stimulator for engineered bacteria (Luo et al., 2016). Therefore, it is conceivable that GO and starch coexist in several industrial discharges.

Nevertheless, recent literature related to the effects of GO on methanogenic activity by anaerobic consortia shows contradictory results and there are no data referring to the effect of combined systems, such as GO-starch, and their effects on anaerobic digestion, to the best of our knowledge. Hence, the objective of this work was to assess the effects of GO on the methanogenic activity of an anaerobic consortium, which was fed with a complex polymer (starch) or with a soluble readily fermentable substrate (glucose). This information contributes to elucidate the effects of GO on anaerobic WWTS, which ultimately has relevance to achieve effective anaerobic treatment of industrial effluents to produce bioenergy.



## 2.2 Materials and methods

### 2.2.1 Materials and chemical reagents

GO was purchased from Graphene Supermarket<sup>®</sup>, which has the following characteristics: concentration  $6.2 \text{ g L}^{-1}$  in aqueous dispersion, monolayer  $> 80 \%$ , nominal particle size between  $0.5$  and  $5 \mu\text{m}$ , C/O ratio 3.95. Starch, glucose and all the reagents used in this work were reactive grade from Sigma-Aldrich Company.

### 2.2.2 Solutions

The basal medium used during sludge activation was composed of ( $\text{mg L}^{-1}$ ):  $\text{NH}_4\text{Cl}$  (280),  $\text{K}_2\text{HPO}_4$  (250),  $\text{MgSO}_4 \cdot 7\text{H}_2\text{O}$  (100),  $\text{CaCl}_2 \cdot 2\text{H}_2\text{O}$  (10),  $\text{NaHCO}_3$  (5000) and 1 mL of trace elements solution composed of ( $\text{mg L}^{-1}$ ):  $\text{FeCl}_2 \cdot 4\text{H}_2\text{O}$  (2000),  $\text{H}_3\text{BO}_3$  (50),  $\text{ZnCl}_2$  (50),  $\text{CuCl}_2 \cdot 2\text{H}_2\text{O}$  (38),  $\text{MnCl}_2 \cdot 4\text{H}_2\text{O}$  (500),  $(\text{NH}_4)_6\text{Mo}_7\text{O}_{24} \cdot 4\text{H}_2\text{O}$  (50),  $\text{AlCl}_3 \cdot 6\text{H}_2\text{O}$  (90),  $\text{CoCl}_2 \cdot 6\text{H}_2\text{O}$  (2000),  $\text{NiCl}_2 \cdot 6\text{H}_2\text{O}$  (92),  $\text{Na}_2\text{SeO}_3 \cdot 6\text{H}_2\text{O}$  (162), EDTA (1000) and 1 mL HCl (36 %); pH was adjusted to  $7.0 \pm 0.2$  using NaOH or HCl 0.1 N if needed. In the case of batch assays,  $\text{NaHCO}_3$  ( $3.13 \text{ g L}^{-1}$ ) was used to get a pH of 7 in combination with a mixture of  $\text{N}_2/\text{CO}_2$  (80/20 v/v) used as headspace. Distilled water was used to prepare all solutions.

Using the basal medium described above, a starch stock of  $100 \text{ mg COD L}^{-1}$  was prepared by adding the proper amount of starch powder and mixing with magnetic stirring for 30 min. Using volumetric flasks of 100 mL, GO dispersions of 5, 25, 50, 152.5 and  $300 \text{ mg L}^{-1}$  were prepared, taking aliquots from the concentrated GO dispersion, adding to the volumetric flask and filling up to the 100 mL mark with the starch stock prepared before. The resulting mix was sonicated for 30 min prior to be placed into the incubation bottles.



### **2.2.3 Inoculum**

Anaerobic sludge from a full-scale up-flow anaerobic sludge blanket (UASB) reactor treating effluents from a candy factory (San Luis Potosí, Mexico) was used as inoculum in the batch experiments. The sludge was acclimated for three months in a lab-scale UASB reactor (1.5 L) under methanogenic conditions at a hydraulic residence time (HRT) of 1 day, with 1 g COD L<sup>-1</sup> of glucose as energy source at 25 °C. The efficiency of the reactor, in terms of COD removal, was up to 90 % under steady state conditions. Volatile suspended solids (VSS) content was 3.22 % respect to wet weight.

### **2.2.4 Characterization of materials**

#### **2.2.4.1 Spectroscopic characterization**

Identification of surface functional groups of materials was carried out using KBr pellets, prepared with a 99 %/1 % (w/w) KBr/material proportion, which were analyzed at 32 scans with a 4 cm<sup>-1</sup> resolution in a Thermo-Scientific Fourier Transform Infrared (FT-IR) spectrophotometer (Nicolet 6700) under ambient conditions. GO material was obtained by drying 500 µL of the concentrated dispersion, while GO-starch mixture was prepared using 2:1 (GO:Starch) ratio by mixing 322.6 µL of the concentrated GO dispersion and 1 mg of starch and then sonicated for 20 min. Both GO and GO-starch mixture were dried for 4 h at 45 °C and 1400 rpm under vacuum (Vacufuge plus Eppendorf). Raman spectra were recorded with RENISHAW Micro-Raman spectrometer with a laser frequency of 633 nm at a potency of 10 % through a 50× objective. Elemental composition, oxidation states of the elements and information about the structure of GO surface were obtained through X-ray photoelectron spectroscopy (XPS) analysis. Sample preparation consisted of a GO dripping deposition on a silicon wafer, dried at room temperature for 12 h and the resulting film was analyzed using a PHI 5000 VersaProbe II equipment with a monochromatic X-ray beam source at 1486.6 eV and 15 kV. The obtained spectra were deconvoluted with help of Aalyzer software v1.27, and the elemental composition was acquired with CasaXPS software v2.3.18PR1.0.



#### **2.2.4.2 Particle charge and size distribution**

Size distribution and zeta potential ( $\zeta$ ) of GO and starch were obtained using a MICROTRAC Zetatrac NPA152-31A equipment. Each sample was sonicated for 10 s before zeta potential measurement. For size distribution, starch was suspended in deionized water at 500 mg L<sup>-1</sup> and mixed for 30 min before measurement, while a dispersion of 150 mg L<sup>-1</sup> in deionized water was used for GO.

Zeta potential was obtained using deionized water and basal medium as dispersants, considering a pH range from 6 to 8 obtained by adding NaOH or HCl 0.1 N as needed. Mixtures of GO (5 mg L<sup>-1</sup>) and starch (150 mg L<sup>-1</sup>) in deionized water and basal medium were prepared following the same procedure described above for starch, and then GO was added. The resulting mixture was sonicated for 10 min before being placed into polypropylene tubes to adjust pH to the desired values.

Dissociation constants (pKa) of GO functional groups were determined by potentiometric titration (METTLER TOLEDO T70), employing mixtures of 5 mg of GO in 20 mL of NaCl 0.01 N solution. The mixtures obtained were left for 12 h at room temperature under mixing at 130 rpm. After this time, pH was adjusted to 3 by adding HCl 0.1 N and then titrated using NaOH 0.1 N until the solution reached a pH value of 12. The resulting titration data were analyzed using SAEIU-pK-Dist© software to get the pKa distribution (Jagiello et al., 1995).

#### **2.2.4.3 Scanning electron microscopy (SEM)**

Micrographs of GO, starch, sludge and their mixtures were obtained with a FEI Helios Nanolab 600 Dual Beam Scanning Electron Microscope, operated at 5.00 kV and 86 pA. Samples were mounted on aluminum pins by dripping deposition. In the case of GO and the sludge, deionized water and basal medium were used as dispersant, respectively, while two different samples were prepared for starch: (1) powder was placed on carbon tape; and (2) a few drops of starch dispersed in deionized water. All samples were dried at atmospheric conditions overnight before being observed and studied under the microscope.



### **2.2.5 Methanogenic activity tests**

Methane production inhibition was evaluated in batch experiments by duplicate, using 120-mL glass serum bottles in which 600 mg VSS L<sup>-1</sup> were inoculated into 50 mL GO-starch dispersion. In these experiments, starch was the substrate for microbial growth, while to assess the impact of the type of substrate and study the influence of possible GO-starch interactions, a set of experiments were carried out using glucose as substrate. Both substrates were supplied at a concentration of 100 mg COD L<sup>-1</sup>. Glucose was added just before incubation to prevent GO reduction (T. Ma et al., 2013). Control experiments without GO were performed to define the effect of GO itself on methanogenesis. Anaerobic conditions were kept along the inoculation process under N<sub>2</sub>/CO<sub>2</sub> (80/20 v/v) atmosphere and incubation was performed in the dark at 25 °C. Cumulative methane production was measured by gas chromatography using an Agilent equipment model 6890N, under previously reported conditions (Valenzuela et al., 2017), sampling gas phase every 5 h in the case of glucose and every 10 h for starch. Liquid samples were taken every 10 h to measure volatile fatty acids (VFAs) by capillary electrophoresis (Agilent 1600A equipment), as described elsewhere (Arriaga et al., 2011). All samples were previously centrifuged and filtered through 0.22 µm nitrocellulose membranes.

## **2.3 Results and discussion**

### **2.3.1 Effects of GO on methanogenic sludge**

In order to elucidate the limiting steps affected by GO on anaerobic digestion, two different substrates were considered in the assessments: a soluble readily fermentable substrate (glucose) and a particulate complex polymer (starch) that depends on its hydrolysis to be converted during methanogenesis. Methane quantification (Figure II-1) revealed that conversion of starch into methane occurred at a lower rate as compared to that observed with glucose (6.8 and 10 mmol h-

1, respectively). In addition, the results of methane production also indicated a negative effect with the increase in GO concentration in both cases. In fact, incubations performed with starch were more affected by GO on the methanogenic activity compared to incubations supplied with glucose as electron donor. Interestingly, the lowest tested concentration of GO (5 mg L<sup>-1</sup>) showed a positive effect on methane production (>10 % increase compared to the control incubated without GO) when glucose was supplied as an electron donor. This improvement could be due to the conductivity of the rGO sheets that promote DIET by syntrophic associations between bacteria and methanogens or due to GO redox-mediating capacity (Colunga et al., 2015; Feng et al., 2013; T. Ma et al., 2013; Salas et al., 2010; Salvador et al., 2017; Wang et al., 2011; Xu et al., 2015).

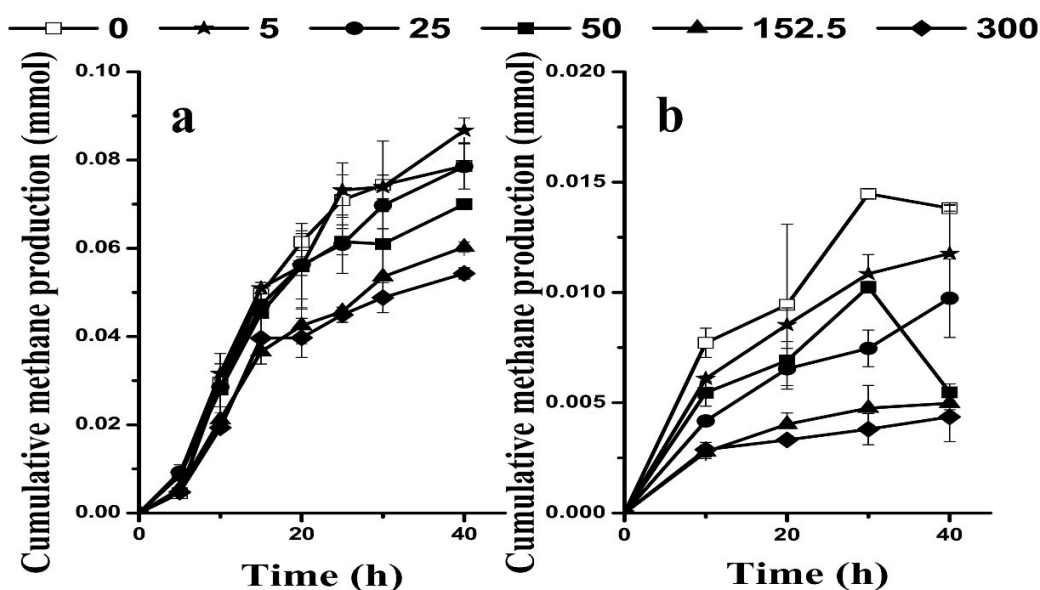
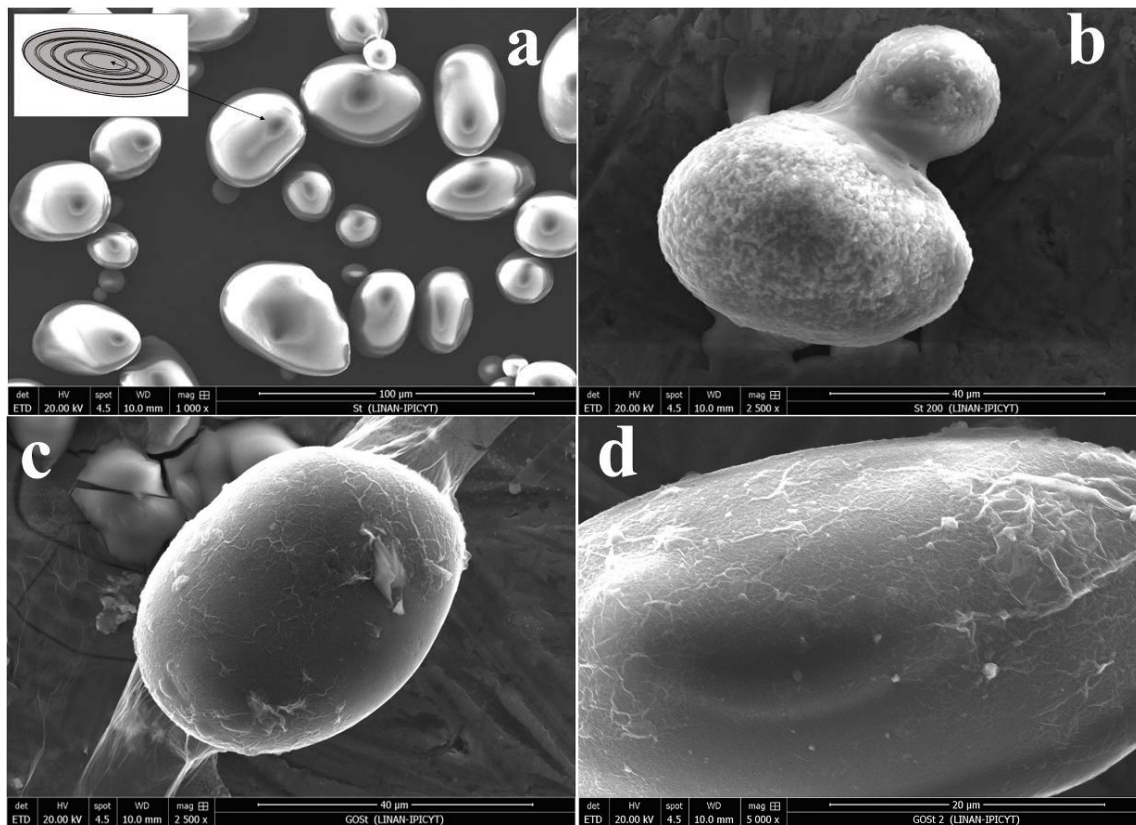


Figure II-1. Cumulative methane production by anaerobic sludge supplied with glucose (a) and starch (b) as substrates at different GO concentrations (numbers displayed in series represent GO concentrations in mg/L).



SEM images show that starch granules in powder form have smooth appearance (Figure II-2a), while those dispersed in water have rugged surface (Figure II-2b), which indicates that starch granules partially dissolve in the medium. In Figure II-2c and Figure II-2d, it is clearly visible a homogeneous coverage of starch granules by GO sheets. Most GO sheets have a size around 687 nm, while prevalent size of starch is around 102.2 nm (Figure II-3). This last value agrees with the size of the hierarchical structures that form starch granules (Figure II-1a), called blocklets (Figure II-4a inset) (Pérez and Bertoft, 2010), suggesting that, in the absence of GO, starch granules in suspension are separated into blocklets during sonication. While starch granules might have had larger size when dispersed in the basal medium used in sludge incubations, they were clearly covered by multiple GO sheets (Figure II-2). The wrapping of starch granules by GO observed here could prevent starch hydrolysis and limit substrate available to cells, consequently leaving only the soluble starch fraction for methanogenesis, explaining the low methane values observed when starch was employed as electron donor.



*Figure II-2. SEM images of starch granules in dry powder (a) and the schematic growth rings around the hilum identified by the arrow (a inset); granules dispersed in water and dried before observation (b); and starch granules covered with GO sheets (c, d).*

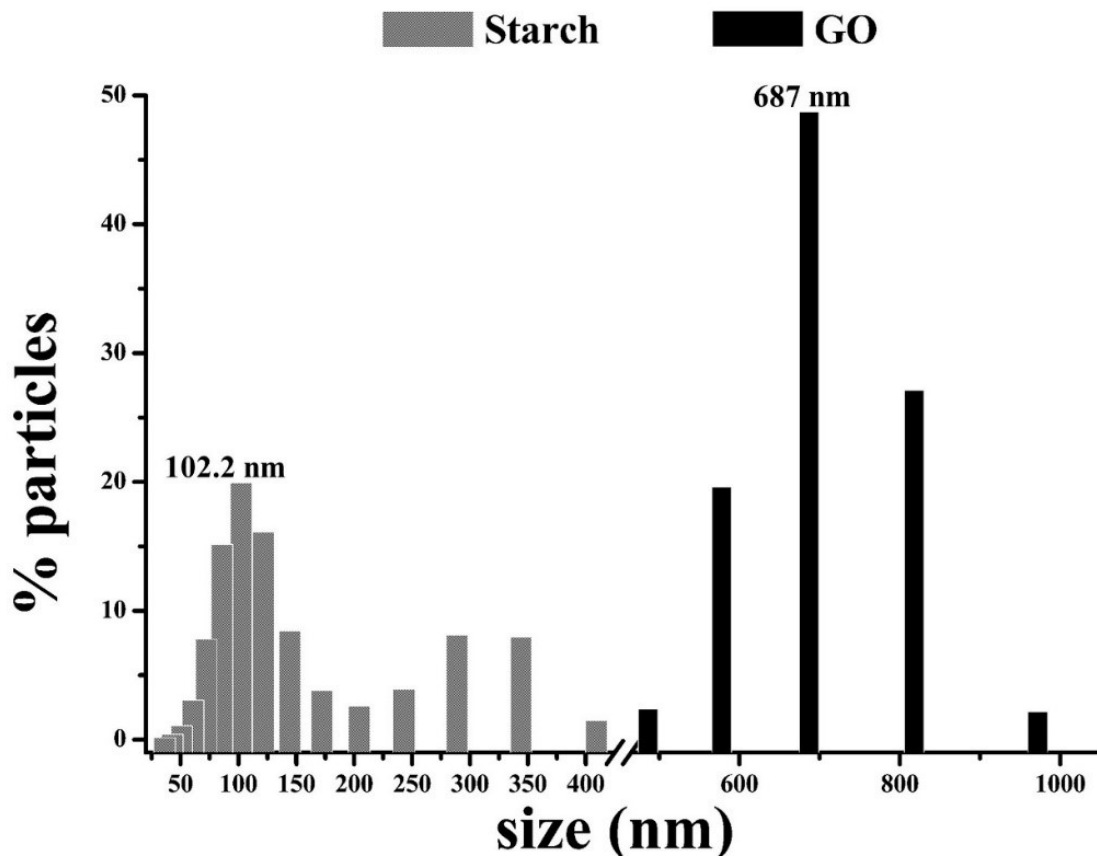


*Figure II-3. Size distribution obtained by dynamic light scattering of starch (gray) and GO (black) at pH 7 using deionized water as dispersant.*

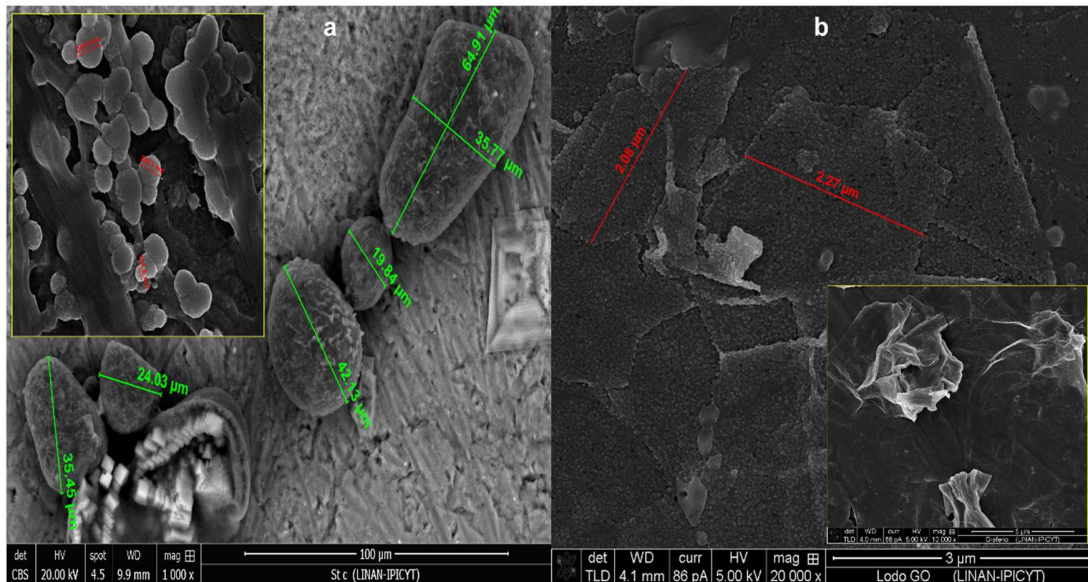


**Figure II-4.** SEM images showing size of starch granules previously dispersed in water (a), size of some blocklets from 103.5 nm to 257 nm (a inset), GO sheets from incubation with glucose (b) and GO without treatment dried at room temperature over 12 h before observation (b inset).

Besides methane measurements, VFAs were also quantified during the incubations (data not shown); nevertheless, results showed concentrations under the detection limit for all VFAs monitored, including acetate, propionate, lactate and butyrate, in all samples taken throughout the incubation period. These results imply that VFAs were readily used as soon as they were produced either from glucose fermentation or from starch hydrolysis, which suggests that methanogenesis was probably not inhibited by GO during the incubation.

Mass transfer limitation imposed by GO coating on starch granules might have not been the only mechanism responsible for the low of methane production observed, since it is also expected a wrapping of cells because peptidoglycan, pseudo-peptidoglycan (for archaea (Bullock, 2000)) and other cell components have functional groups that could interact via hydrogen bonding,  $\pi$ - $\pi$  interactions and electrostatic adsorption with GO (Zou et al., 2016). These interactions might have decreased methane production in experiments amended with glucose, which was completely solubilized and thus the sequestering effect of substrate can be discarded. These suggestions are supported by reports, which demonstrated cells coverage by GO and correlated its inactivation



capacity to its lateral dimension, that is, bigger GO sheets are more effective inactivating cells in a short time due to cell isolation (Liu et al., 2012a) while small particles can enter the cytoplasm, especially those with positive charge, causing oxidative stress (Hu et al., 2017; Hu and Zhou, 2013).

In addition, the presence of cations in the basal medium has to be considered; it has been reported that GO, in the presence of organic matter or bacteria and low concentrations of divalent cations, forms flocs due to bridging effect between cations and GO functional groups (Chowdhury et al., 2015; Zhang et al., 2013).

Wrapping of cells by rGO could also be plausible, considering that GO can be reduced by glucose (T. Ma et al., 2013), starch (Feng et al., 2013) and bacteria (De Silva et al., 2017; Salas et al., 2010), causing aggregation of graphene and trapping bacteria within the aggregated sheets in the process (Akhavan et al., 2011). SEM images show cells and sludge flocs covered by GO (Figure II-5); however, further studies are needed to clarify the interactions between GO and anaerobic microorganisms present in methanogenic consortia.

### **2.3.2 Interactions between GO and starch affecting anaerobic digestion**

According to  $\zeta$  results obtained with deionized water, the expected interaction is electrostatic attraction due to positive charges of starch and negative ones on GO in the pH range of interest. It is possible to find a change of charge when the mixture GO-starch goes from pH = 6 to pH = 7, from 24.5 mV to 2.46 mV, respectively (Figure II-6). This charge drop agrees with the pKa of ~6.6 found in GO characterization (Figure II-7), corresponding to deprotonation of carboxylic groups and it results in charge neutralization with the positive charge of hydroxyl groups of starch that stay with positive charge at those pH values. Even though C1s XPS results (Figure II-8) indicate that carboxylic groups (at 289.3 eV) are just a fraction of the total GO functional groups, they could be the main responsible for built up negative charges (Konkena and Vasudevan, 2012), favoring the attraction of starch and then triggering the interaction with other GO groups. Other



groups found through C1s XPS are C=C (284.5 eV) and their associated  $\pi$ - $\pi^*$  shake-up of the aromatic system (291.4 eV), as well as C=O (288.3 eV) and C-O (287.4) (Castro et al., 2016), which have higher intensities than carboxylic groups.

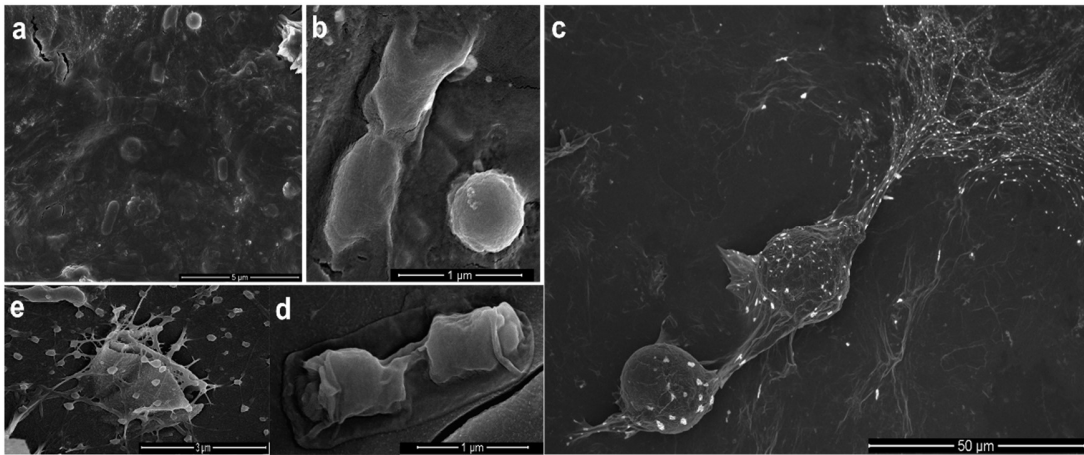


**Figure II-5.** SEM images of sludge obtained from the UASB reactor without treatment (a), where bacilli and cocci are the most abundant and with scarce presence of exopolysaccharides (b). Sludge floccules were covered by GO in the treatment with glucose and salt crystals show affinity for GO (c). Similarly, cells in the treatment with starch show a GO wrapping that remains after cell dehydration (d). Image of sample taken from the treatment with starch and GO showing starch blocklets and GO sheets tangled up in exopolysaccharides threads (e).

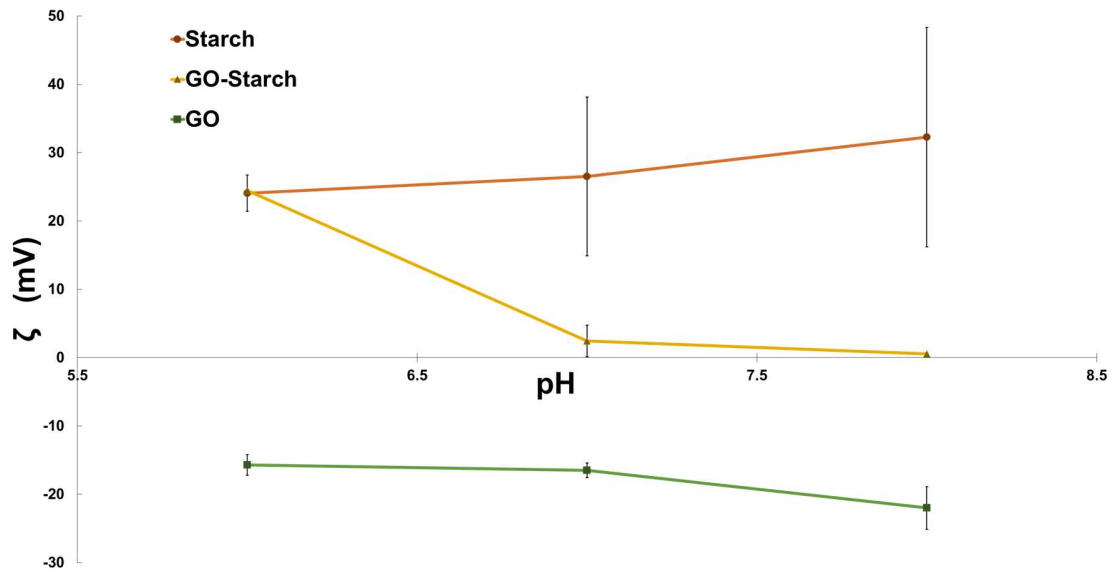


Figure II-6. Zeta potential of starch, GO-starch mixture and GO with respect to pH. Deionized water was the dispersant.

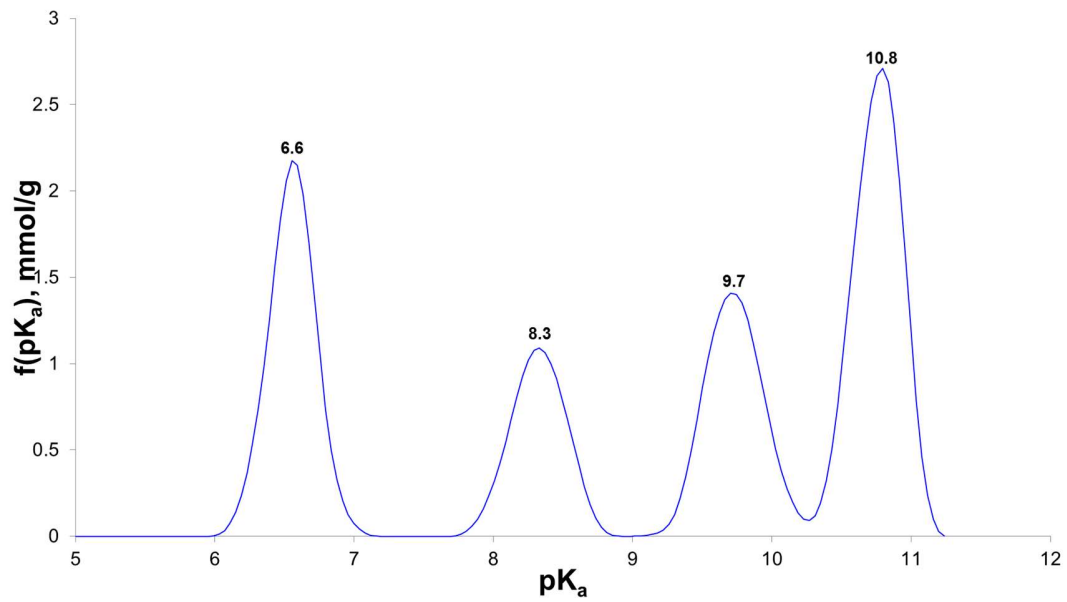
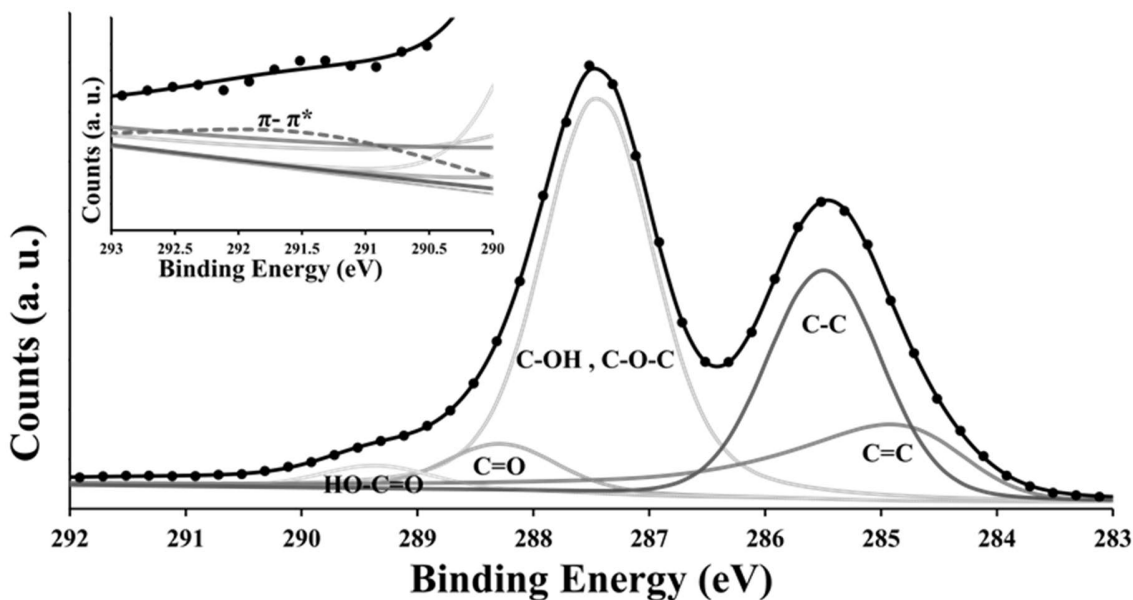


Figure II-7. Dissociation potential (pKa) distribution of GO using deionized water as dispersant.



*Figure II-8. High-resolution C1s X-ray photoelectron spectrum of GO. Dots represent experimental data; solid lines are fitted peaks that identify the different bond types of carbon, and dashed line shows  $\pi$ - $\pi^*$  transitions in aromatic rings (inset).*

In O1s XPS spectrum (Figure II-9), the peak with the largest area at  $\sim 533.1$  eV can be assigned to the combined effects of singly bonded oxygen, followed in decreasing order, by a peak at 532.5 eV assigned to C=O in carbonyl and/or carboxyl groups and finally by the peak at 533.8 eV corresponding to hydroxyl groups (mainly in phenolic compounds) (Hantsche, 1993; Levi et al., 2015; Puziy et al., 2008). In both C1s and O1s XPS spectra, single bonds between carbon and oxygen are predominant. In addition, the concentration of oxygen-containing groups (phenolic, carbonyl and carboxylic) obtained by Boehm titration (Table II-1), agrees with that reported by XPS analysis.

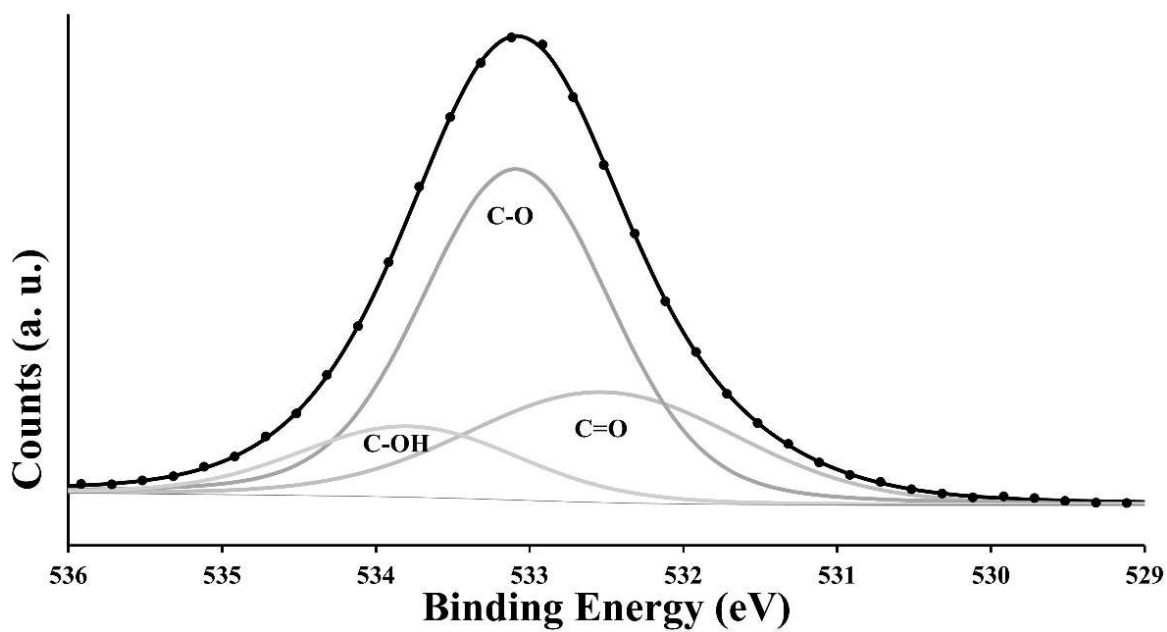


Figure II-9. High-resolution O1s X-ray photoelectron spectrum of GO. Grey scale solid lines represent deconvoluted peaks, while dots are the experimental data.

Table II-1. Concentration of acidic oxygenated functional groups (in milli-electron equivalents per g (meq/g)) in GO quantified by Boehm titration.

| <i>Group</i>      | <i>meq/g</i> |
|-------------------|--------------|
| <i>Phenolic</i>   | 3.14         |
| <i>Carbonyl</i>   | 2.65         |
| <i>Carboxylic</i> | 2.01         |
| <i>Total</i>      | 7.8          |



Interaction between GO and starch functional groups were studied by FT-IR (Figure II-10), finding out a shift in peaks at 1730 cm<sup>-1</sup>, 1570 cm<sup>-1</sup>, 1200 cm<sup>-1</sup>, 1100 cm<sup>-1</sup> and 600 cm<sup>-1</sup> to 1646 cm<sup>-1</sup>, 1414 cm<sup>-1</sup>, 1169 cm<sup>-1</sup>, 998 cm<sup>-1</sup> and 570 cm<sup>-1</sup>; related with C=O, C=C, C-O-C (epoxide), C-O and phenolic groups, respectively. These shifts have been attributed to hydrogen bonding, in the case of the oxygenated groups (Li et al., 2011; Socrates, 2004; Xu et al., 2016), and to Lewis acid-base interaction for C=C in aromatic rings (Zhao et al., 2014). These results and those from ζ data suggest that the wrapping observed by SEM images is due to interactions that possibly include hydrogen bonding, which implies that the GO coating is tightly bound and as a result interferes with the hydrolysis of the starch, as indicated in the previous section.

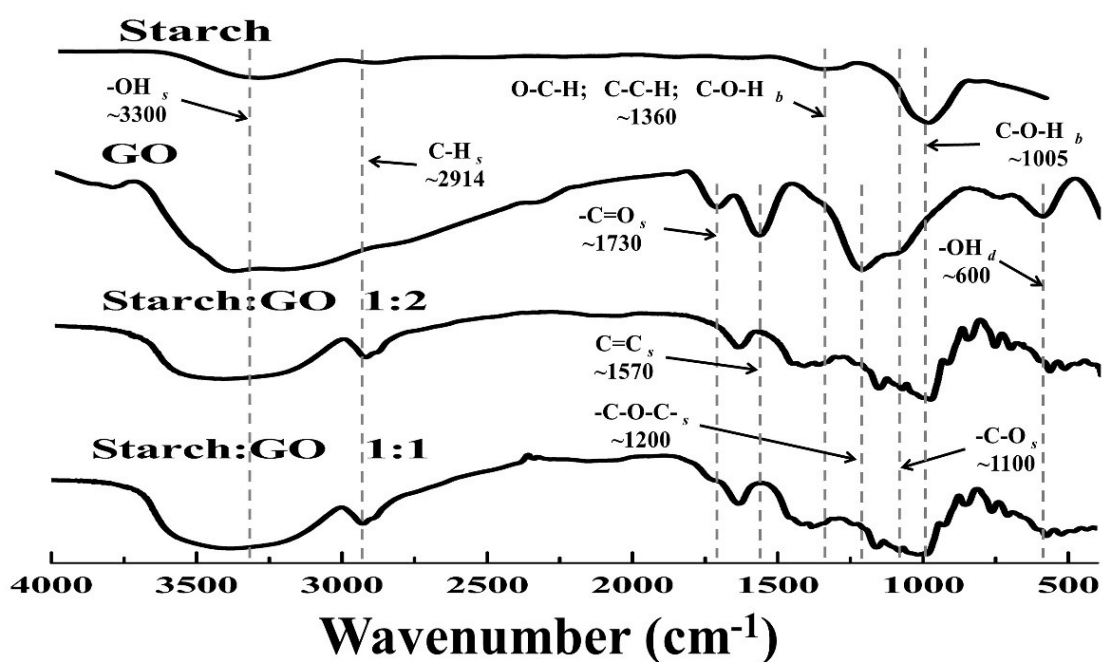


Figure II-10. FT-IR spectra of starch, graphene oxide (GO) and starch-GO mixtures with 1:2 and 1:1 ratio, respectively.



FT-IR of GO-starch mixtures show a narrowing and improvement in definition of band at  $\sim 3300$   $\text{cm}^{-1}$  assigned to  $-\text{OH}$ . This band is broader in the spectrum of GO alone (Figure II-10); A broader band shape has been associated with the presence of water either intercalated among stacks of GO or physisorbed on GO sheets (Acik et al., 2011), so the narrower band of GO-starch mixtures suggests a decrease in water amount due to a conformation of stacks with fewer layers on the surface of starch granules. The relevance of the above lies on the possible development of “blade like edge” that can damage cell membrane (Cai et al., 2011); however, no evidence of this phenomenon was found; even when GO appears to have single or few sheets in the incubations with glucose ( Fig 2.4b) or starch. It is important to note that stacks of some sheets were seen when GO was dried without being in contact with starch or sludge (Figure II-4b inset).

### **2.3.3 Environmental relevance**

The results presented in this study showed that starch granules can be wrapped by GO sheets preventing their hydrolysis, which is the initial step for their conversion to methane under anaerobic conditions, leading to poor methane production. This scenario represents a challenge to anaerobic wastewater treatment systems, as removal of pollutants from industrial effluents to produce renewable energy (as biogas) can be seriously hampered, especially in the case of effluents of food and other industrial sectors containing starch as the main COD fraction.

In natural ecosystems, the wrapping of particulate organic matter (POM) by GO could affect the availability of nutrients for heterotrophic organisms, thus altering the trophic web or cause a disruption of the dynamic interchange between POM and dissolved organic matter (DOM), that may result in major disequilibrium of ecosystems since both DOM and POM are involved in complex biogeochemical cycles.



## **2.4 Conclusions**

This study elucidates, for the first time, mass transfer limitation imposed by GO on the methanogenic activity by an anaerobic consortium. Collected evidence indicated that wrapping of starch granules was the main mechanism involved. The results also reveal that low concentration of GO may enhance the methanogenic activity of the anaerobic consortium studied, presumably driven by DIET, during glucose fermentation. This information contributes to shed light on the effects of GO on anaerobic WWTS.



# Chapter III

## **Enhanced methane production promoted by reduced graphene oxide in an anaerobic consortium supplied with particulate and soluble substrates\***



## **Abstract**

Reduced graphene oxide (rGO) is expected to be present in wastewater treatment systems as the use of graphene oxide (GO) increases and it can be reduced to rGO by physical, chemical and biological processes prevailing in these engineered systems. This paper provides information on the acute effects of GO with three different degrees of reduction (rGO) on the methane production of an anaerobic consortium. In general, obtained results showed that rGO materials had a stimulatory effect increasing the maximum methanogenic activity (MMA) up to 14 % and 114 % when glucose and starch were provided as substrates, respectively, as compared to the MMA achieved in control incubations performed in the absence of rGO. Also, this work showed that the reduction degree of rGO is an important factor driving its interaction with the provided substrates. Particularly, rGO promoted starch disintegration into its components, thus accelerating its hydrolysis. This study provides valuable information to elucidate the effects of rGO in methanogenic consortia.

### **3.1 Introduction**

Several carbonaceous materials have been used to improve the biotransformation of a wide variety of pollutants as well as the methanogenic activity of anaerobic consortia. One of those materials is activated carbon, which showed an enhancement on methane yield, especially when it was supplied as a fine powder. Activated carbon increases methane production due to the porosity of its particles, which serve as a proper niche to support microbial growth. Additionally, the conductivity of activated carbon favors direct interspecies electron transfer (DIET) (Xu et al., 2015). Carbon nanofibers have also been reported to enhance the anaerobic biotransformation of nitroaromatic compounds; moreover, chemical surface modification played a relevant role, indicating that functional groups able to accept and donate electrons, such as quinone groups, take part as redox mediators (Amezquita-Garcia et al., 2016). In the field of carbon nanomaterials, GO was also applied as electron shuttle for the reduction of recalcitrant pollutants by methanogenic



sludge, but the concentration used was 5 mg/L due to toxic effects found at higher concentrations (Colunga et al., 2015). In opposition to the toxic effect of GO, the use of carbon nanotubes, in concentrations in the range of grams, showed an increase in methane production in a dose-dependent manner, but these experiments suggested that DIET is not the driving factor for methane improvement and probably other factors, such as the adsorption capacity may contribute to these results (Salvador et al., 2017).

Application of graphene in anaerobic digestion processes, at concentrations between 30 and 120 mg/L, showed a stimulation effect on methane production, specially favoring acetoclastic methanogenesis. These studies include a comparison with quinones and revealed that these moieties failed to replicate graphene stimulation, concluding that graphene did not function as electron shuttle in this kind of systems and support DIET as the mechanism for the observed methane enhancement (Tian et al., 2017b). rGO has also been reported to increase degradation processes, which was attributed to the electron shuttling capacity of its remaining oxygenated functional groups as evidenced by chemical and biological experiments using rGO with different reduction degree. Moreover, the results pointed out that the higher the reduction degree of rGO, the higher the reduction rate observed in the studied pollutants and suggested that the enrichment of carbonyl groups in rGO might be responsible for the enhanced degradation observed (Torales-Sánchez et al., 2017, 2016). In all the previously discussed cases, the contaminants, as well as the substrates, are soluble. Therefore, it is necessary to investigate what happens when particulate matter serves as substrate since previous results have indicated that GO wraps starch granules and therefore prevents its hydrolysis. In fact, the envelope of starch granules is given by the interaction of the oxygenated groups of GO, which have negative charge, and the hydroxyl groups in starch, which have positive charge (Bueno-López et al., 2018). The above opens the questions on what interactions between rGO and starch occur and what will be the effects when all these components are present in anaerobic digestion processes.

Starch is an energy reserve in plants and the second most abundant biopolymer on Earth. It is mainly composed of two types of polysaccharides, amylose and amylopectin, which are organized in multilevel structures of increasing complexity. Starch granules are structures that vary in size



(1-200  $\mu\text{m}$ ) and shape (ovals, spheres, polygons, etc.) depending on the botanical origin. Starch is of great importance within the food industry and is taking relevance every day in other industrial areas, such as the manufacture of biodegradable materials (Hoover, 2001; Pérez and Bertoft, 2010; Vanier et al., 2017; Xie et al., 2013).

The aim of the present work was to study the acute effects of rGO on the methanogenic activity of an anaerobic consortium with two different substrates: glucose as a soluble model substrate and starch as a particulate model substrate. The goal of the study is to provide evidence to understand the interactions of rGO, with different reduction degrees, within the methanogenic consortium.

## **3.2 Materials and methods**

### **3.2.1 Materials and chemical reagents**

GO was purchased from Graphene Supermarket<sup>®</sup> and has the following characteristics: concentration 6.2 g/L in aqueous dispersion, monolayer > 80 %, nominal particle size between 0.5 and 5  $\mu\text{m}$ , C/O ratio 3.95. Ascorbic acid (L-AA, ACS grade) was obtained from GOLDEN BELL<sup>®</sup> (Mexico City, Mexico), while starch, glucose and all other reagents used in this work were reactive grade from either Sigma-Aldrich Company or Merck.

### **3.2.2 Solutions**

The basal medium used during sludge activation was composed of (mg/L):  $\text{NH}_4\text{Cl}$  (280),  $\text{K}_2\text{HPO}_4$  (250),  $\text{MgSO}_4 \cdot 7\text{H}_2\text{O}$  (100),  $\text{CaCl}_2 \cdot 2\text{H}_2\text{O}$  (10),  $\text{NaHCO}_3$  (5000) and 1 mL/L of trace elements solution composed of (mg/L):  $\text{FeCl}_2 \cdot 4\text{H}_2\text{O}$  (2000),  $\text{H}_3\text{BO}_3$  (50),  $\text{ZnCl}_2$  (50),  $\text{CuCl}_2 \cdot 2\text{H}_2\text{O}$  (38),  $\text{MnCl}_2 \cdot 4\text{H}_2\text{O}$  (500),  $(\text{NH}_4)_6\text{Mo}_7\text{O}_{24} \cdot 4\text{H}_2\text{O}$  (50),  $\text{AlCl}_3 \cdot 6\text{H}_2\text{O}$  (90),  $\text{CoCl}_2 \cdot 6\text{H}_2\text{O}$  (2000),  $\text{NiCl}_2 \cdot 6\text{H}_2\text{O}$  (92),  $\text{Na}_2\text{SeO}_3 \cdot 6\text{H}_2\text{O}$  (162), EDTA (1000) and 1 mL HCl (36 %); pH was adjusted to  $7.0 \pm 0.2$  using NaOH or HCl 0.1 N if needed. In the case of batch assays  $\text{NaHCO}_3$  (3.13 g/L) was



used in order to get a pH of 7 in combination with a mixture of N<sub>2</sub>/CO<sub>2</sub> (80 %/20 %, v/v) used as headspace. Distilled water was used to prepare all solutions.

### **3.2.3 Chemical reduction of GO**

Reduction of GO was carried out according to Toral-Sánchez et al., 2016, with the following amendments: reaction times of 1, 2 and 4 hours; after the reaction time, rGO was centrifuged for 20 min at 10,000 rpm in an Avanti J-30I equipment and washed three times using deionized water in cycles of centrifugation and re-dispersion. Finally, washed rGO was dispersed in deionized water and sonicated for 30 min. rGO materials obtained from 1, 2 and 4 hours of reaction are referred to as rGO1, rGO2 and rGO4, respectively, in the present study.

The concentration of the three rGO dispersions was measured by a gravimetric method, which implied drying 1 mL of the dispersions in vials at constant weight at 45 °C under vacuum and 1400 rpm for 6 hours using Vacufuge plus Eppendorf concentrator equipment.

### **3.2.4 Characterization of materials**

#### **3.2.4.1 Spectroscopic characterization**

Functional groups of rGO1, rGO2 and rGO4 were identified by Fourier transform infrared spectroscopy (FTIR) using a Thermo-Nicolet 6700 FT-IR equipment. Samples were prepared using dried materials for 4 hours into a Vacufuge plus Eppendorf concentrator equipment at 45 °C under vacuum and 1400 rpm, mixed with KBr in a 1:1000 ratio, respectively, and compressed to form pellets. The pellets were analyzed by transmission under conditions of 128 scans, resolution of 4 cm<sup>-1</sup>, CO<sub>2</sub> and H<sub>2</sub>O automatic correction.

The reduction degree of the materials, rGO1, rGO2 and rGO4, was also studied by Raman spectroscopy using a RENISHAW Micro-Raman Invia spectrometer with laser frequency of 532 nm as excitation source through a 50× objective. The sample preparation consisted in the formation



of films on aluminum foil by dripping deposition of each material dispersions, and then allowed to dry for 12 h prior to analysis.

#### **3.2.4.2 Particle charge and size distribution**

Zeta potential ( $\zeta$ ) measurements were performed in aqueous solution for rGO1, rGO2 and rGO4 at pH of 7, which is the pH value of the biological experiments performed. For this purpose, dispersions of 150 mg/L of each rGO material were adjusted to the desired pH value using NaOH or HCl 0.1 N as needed until the variation of pH values was less than 0.5 in separated measurements spaced for 5 hours. After pH stabilization, 1 mL of the sample was sonicated using a Branson model B2510-DTH equipment at 40 kHz for 10 s and immediately placed into the MICROTRAC Zetatrac NPA152-31A cell.

Size distribution was measured by Dynamic Light Scattering, using the same equipment described above, at pH 7 and with the same sample preparation mentioned before.

#### **3.2.4.3 Scanning electron microscopy (SEM)**

Micrographs of rGO materials and starch were obtained with a FEI Helios Nanolab 600 Dual Beam Scanning Electron Microscope, operated at 5.00 kV and 86 pA, and elemental analyses were carried out by energy dispersive spectrometer (EDS) with the same equipment. Samples were prepared on silicon wafers by dripping deposition and were dried at atmospheric conditions over night before microscope observation. rGO materials and starch mixtures were prepared using the same procedure followed for the acute exposure biological batch assays. Biological samples were prepared using the procedure described by Patrón-Soberano et al. (2017) and examined using an FEI model Quanta 250 SEM, adjusted to 25 kV, spot size 4.5 and WD 10 mm, recording the micrographs using an Everhart Thornley Detector.



### **3.2.5 Biological assays**

#### **3.2.5.1 Inoculum**

Methanogenic granular sludge was obtained from a full-scale up-flow anaerobic sludge bed reactor treating brewery wastewater (Mahou, Guadalajara, Spain). The sludge was stored at 4 °C and it was washed and crushed using a needle gauge 22 G before its use in the incubations. The content of volatile solids (VS) of the sludge was 6.96 % of wet weight.

#### **3.2.5.2 Sludge incubations with rGO**

Batch assays were conducted in triplicates using serological bottles of 60 mL of volume. In these experiments, 9 mL of basal medium containing starch or glucose (final concentration of 2 g chemical oxygen demand (COD)/L) and 1.5 g VS/L of sludge were added to each bottle and then flushed with a gas mixture of N<sub>2</sub>/CO<sub>2</sub> (80:20, v/v) for 3 min. Subsequently, bottles were sealed, and the headspace was further flushed using the same gas mixture for 3 min. The bottles were incubated overnight at 30 °C in an orbital shaker at 120 rpm. After this period, 1 mL of deionized water was added to the control bottles and 1 mL from the corresponding stock solution of rGO material to amended cultures (10 mL as total volume in all cases) in order to get a concentration of 300 mg/L of each GO material. Once the GO materials were added, the headspace of all bottles was flushed again with the N<sub>2</sub>/CO<sub>2</sub> gas mixture for 3 min and incubated at 30 °C in an orbital shaker at 120 rpm. Gas samples (100 µL) were periodically taken for methane measurement by gas chromatography. Methane concentration was plotted against time to obtain the maximum slope by linear regression from at least three points throughout the incubation period and the maximum methanogenic activity (MMA) was then calculated.



### **3.3 Results and discussion**

#### **3.3.1 Physical characterization**

Zeta potential values for rGO1, rGO2 and rGO4 were 0.284 mV, 0.565 mV and 4.453 mV, respectively. These data indicate a clear trend to higher values linked to the increase in reduction time, which was related with the loss of oxygenated functional groups conferring negative charge to GO, which showed a zeta potential of -16.5 mV. These results agreed with FTIR analysis, which revealed the loss of some oxygenated functional groups through the reduction process and indicated the persistence of hydroxyl groups, which possess partial positive charge at pH 7.

The reduction process turned GO sheets more hydrophobic, so that they tended to stack among them due to  $\pi$  interactions of the aromatic rings. Consequently, size distribution moved to larger sizes of particles consistent with the increase in reduction time. Besides, low values in  $\zeta$  mean instability of colloidal dispersion, thus rGO sheets agglomerate easily. Taking all these aspects into account Figure III-1 makes sense since most rGO1 particles showed a size of 687 nm, while rGO2 particles were divided between sizes of 687 nm (37.4 %) and 818 nm (34.7 %). Finally, rGO4 particles predominated with a size of 818 nm.

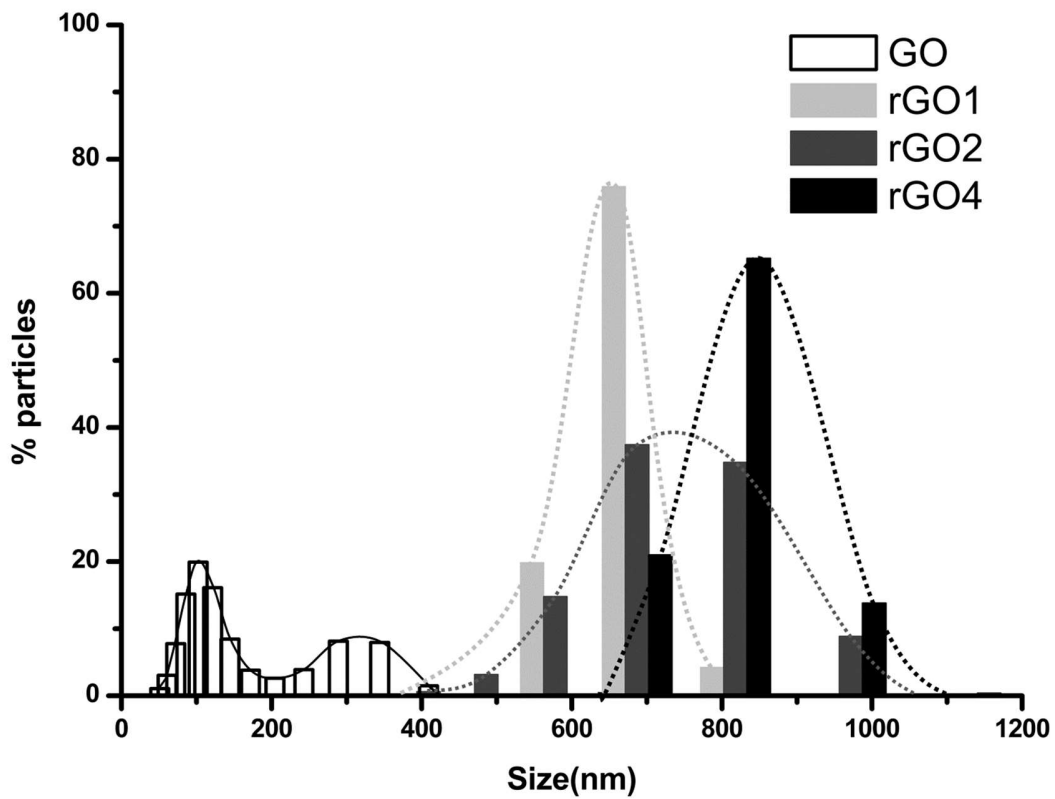


*Figure III-1. Size distribution of GO and rGO materials, bars represent the percentage of particles of a given size, while curves were added to make clearer the pattern of size distribution due to the reduction process*

The morphology of GO and rGO materials was studied by SEM. Obtained images revealed that GO is thinner, shows cracks and tends to fold over itself, while rGO materials have thicker lamellae, due to the stacking of rGO sheets caused by the reduction treatment. Furthermore, the extended sections found in the samples presented changes in transparency and the way they fold; for example, lamellae of rGO2 and rGO4 were smoother and apparently more rigid/denser, while rGO1 still presented fine sheets (see Figure III-2).

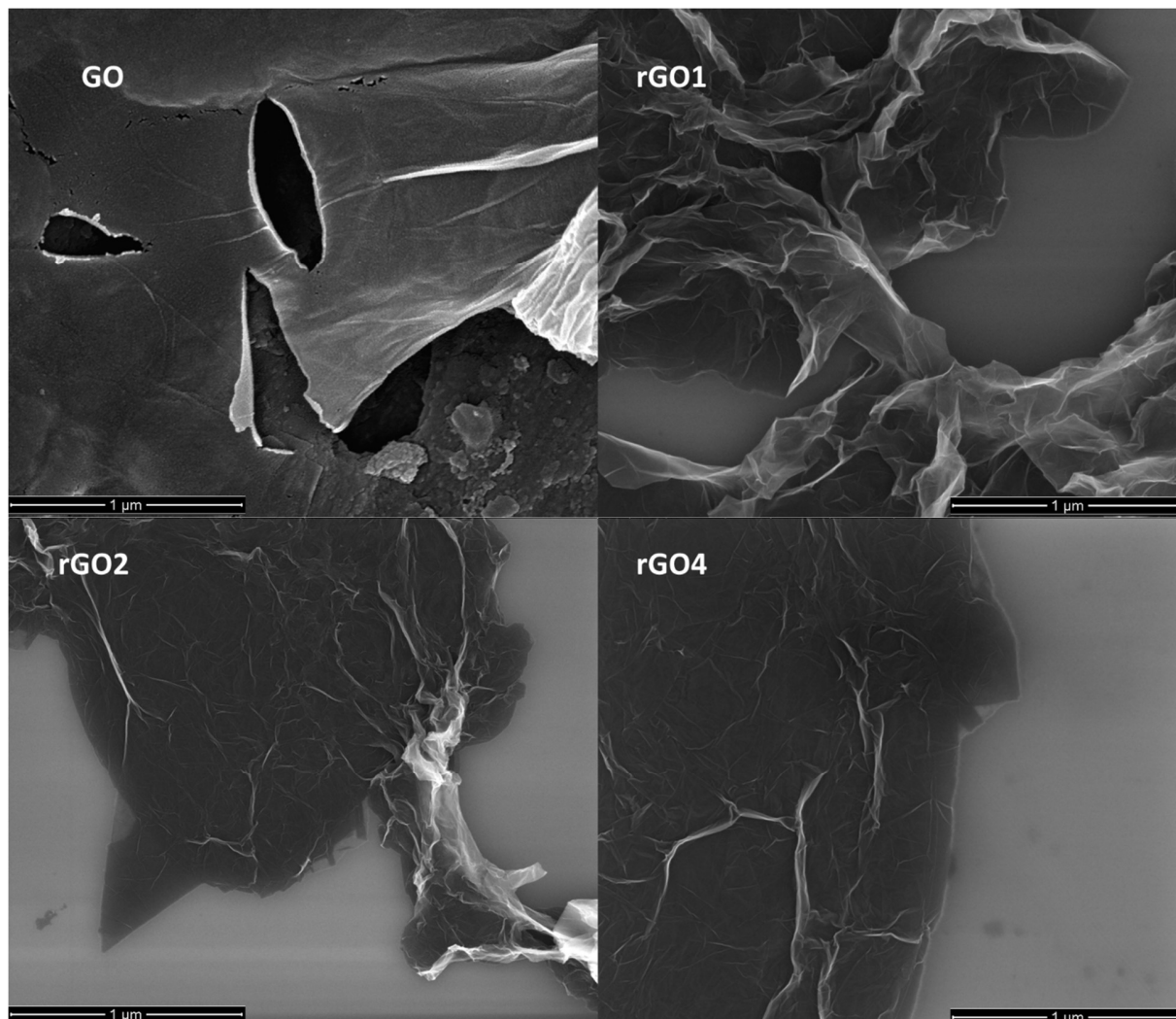


*Figure III-2. SEM images of untreated GO and the reduced materials obtained at increasing reduction time (rGO1, rGO2 and rGO4).*

In the case of the graphene materials mixed with starch, SEM images (Figure III-3) show that GO perfectly wraps starch granules (Figure III-3b), even following the shape of those that were broken by the preparation procedure. Granules were easily found in the sample, but when the mixture contained any of the rGO materials, starch granules were not detected in the samples, instead much smaller clusters were found (rGO4 used for Figure III-3c). These clusters are essentially crystals



from the basal medium, rGO sheets, and particles with spherical/polyhedral and rod-like shapes (Figure III-3d). The observed clusters agree with the hierarchical structures integrating starch granules, being consistent with blocklets and super helical structures, which seemed to be composed of a mixture of A-type and B-type crystalline polymorphs that give them that “Cheetos-type” shape (Bras and Dufresne, 2010; Pérez and Bertoft, 2010). These findings indicate that rGO materials did not cover starch granules but broke them into smaller sub-structures. The latter suggests that rGO materials promoted the disintegration of starch granules, possibly due to catalytic activity of remaining carboxylic groups and/or defects at edges of rGO sheets with unpaired electrons (Song et al., 2010; Su et al., 2012). However, further research is needed to clarify what are the mechanisms that give rise to the observed results.

When collected samples were observed, it was possible to find starch granules attached to exopolysaccharides, bacteria and rGO sheets. Nevertheless, rGO sheets never wrapped starch granules (rGO4 was used for Figure III-3e), so that they were always interacting with cells and exopolysaccharides (Figure III-3f). These results show that rGO preferentially adheres to bacteria, which have a negative surface charge, while, as was shown by the results of  $\zeta$  values, rGO had a greater positive charge by increasing the reduction time. Nonetheless, it must be considered that bacteria can adhere to rGO sheets, because they serve as conductive material favoring DIET and facilitating bacterial growth.

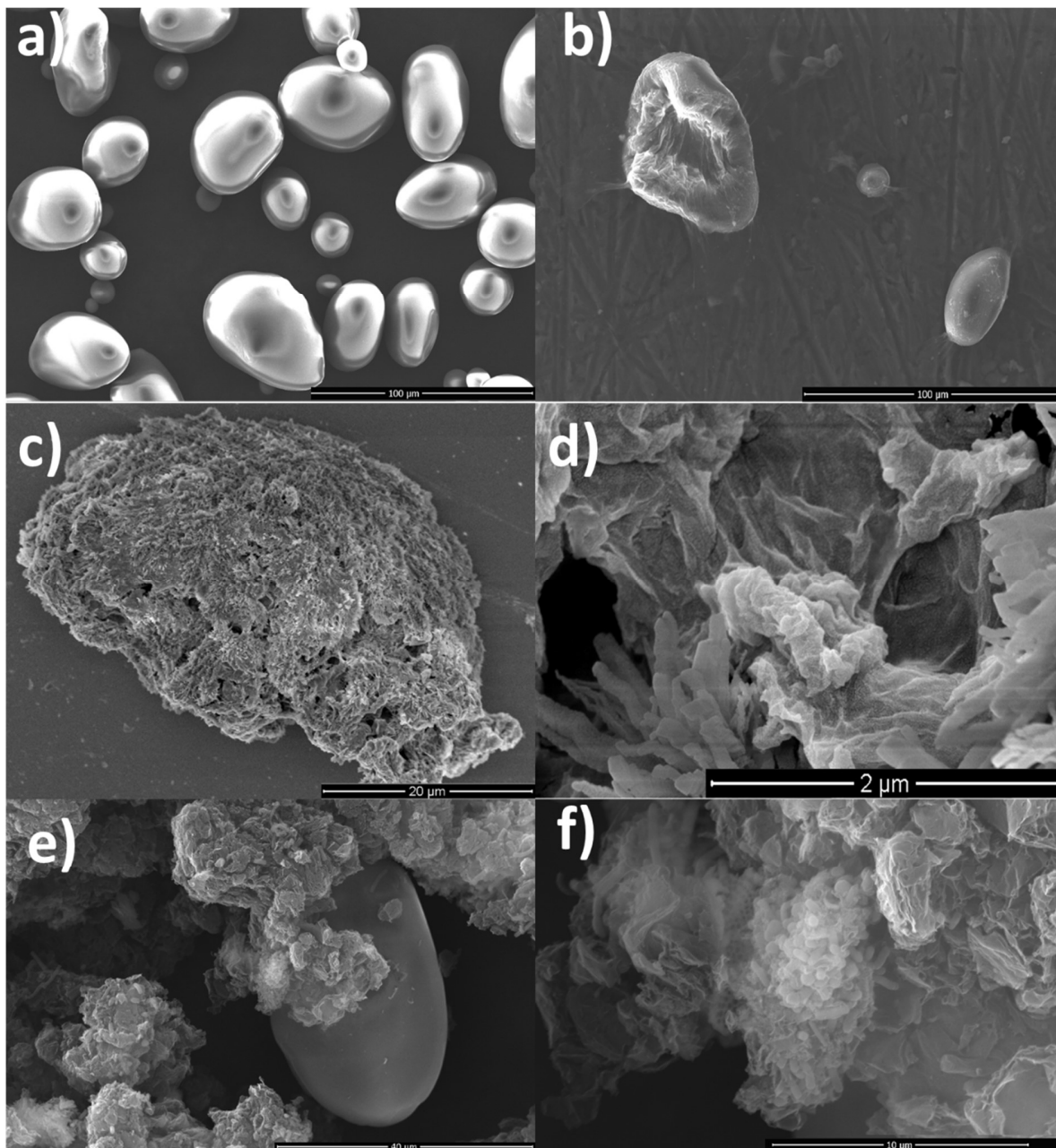


**Figure III-3.** SEM images of pristine starch granules (a), mixture of starch and GO (b), clusters found in samples with rGO4 (c), structures inside the clusters (d) and a sample of the bioassays using starch and rGO4 at low (e) and high magnification (f).



### 3.3.2 Spectroscopic characterization

Raman spectra (Figure III-4) of reduced materials and GO displayed the characteristic D and G bands of carbon at  $\sim 1350\text{ cm}^{-1}$  and  $\sim 1600\text{ cm}^{-1}$ , respectively. D band is associated with disorder-induced symmetry-breaking effects of  $\text{sp}^2$  network, while G band is related with the ordered structure of graphene hexagons and graphite crystallinity. Additionally, Raman spectra show the 2D band at  $\sim 2676\text{ cm}^{-1}$ , which is sensitive to the  $\pi$  bond in the graphitic electronic structure and the number of layer; and D+G band at  $\sim 2950\text{ cm}^{-1}$ , which is the combination of band D and G induced by disorder (Ferrari, 2007).

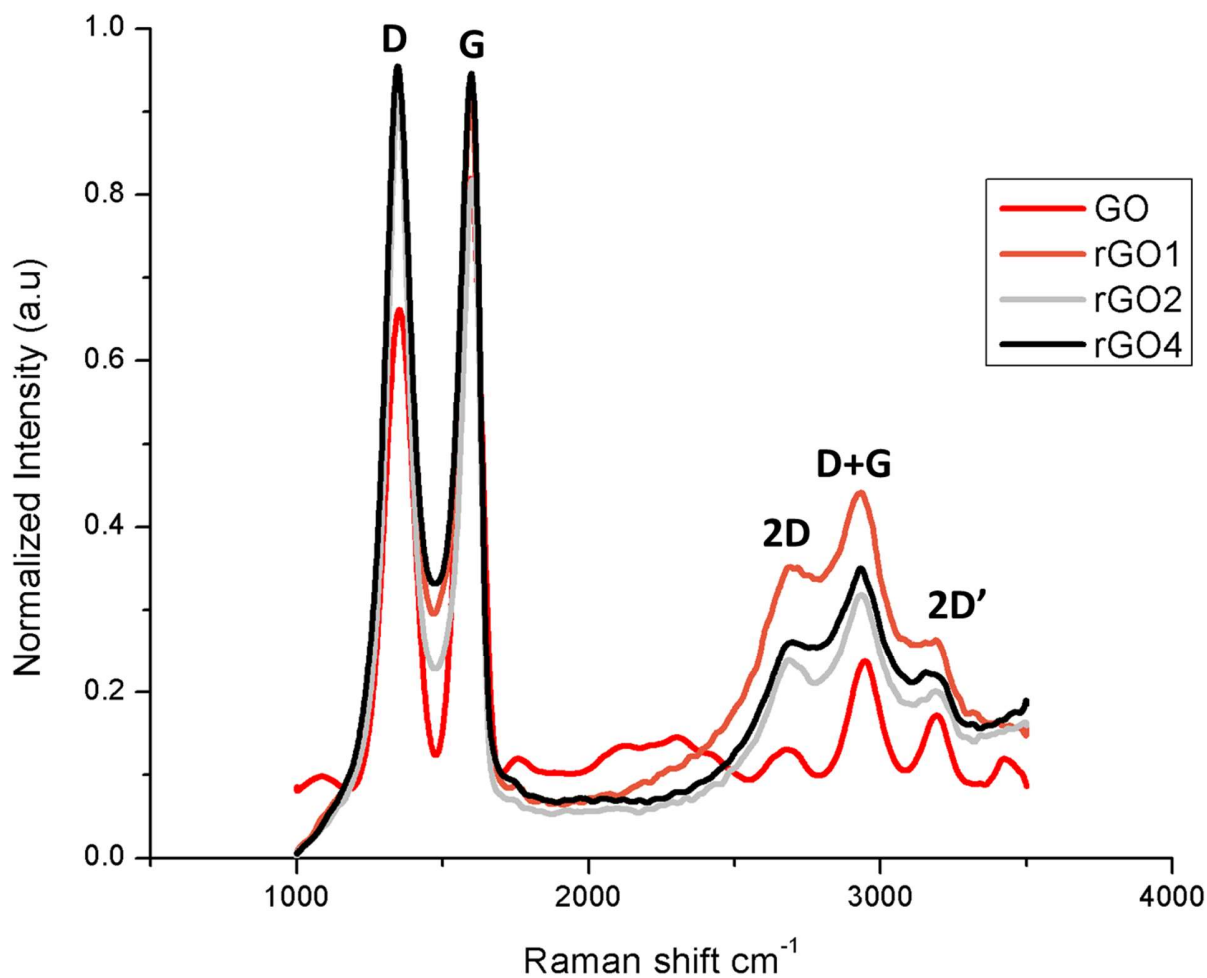


*Figure III-4. Raman spectra of reduced and unreduced GO materials showing the main bands of carbonaceous materials.*

The ratio  $I_D/I_G$  provides information of the amount of disorder linked to the oxidation process, but in the case of the reduction process, the  $I_D/I_G$  ratio has been reported to show increase by increasing the reduction degree in the case of GO. This could be corroborated by the results obtained for  $I_D/I_G$  ratios of GO, rGO1, rGO2 and rGO4, which correspond to 0.809, 1.011, 1.124 and 1.011, respectively. The previous values show small difference among the reduced materials; thus,  $I_{2D}/I_G$  ratio was calculated since it has relationship with the measurement of  $sp^2$  regions and with electron mobility (Raza, 2012). The values of the  $I_{2D}/I_G$  ratio for GO, rGO1, rGO2 and rGO4 are 0.164, 0.386, 0.295 and 0.278, respectively, and indicate larger graphitic domains and consequently



higher electron mobility in the reduced materials. Nevertheless, the observed trend for  $I_D/I_G$  and  $I_{2D}/I_G$  ratios disagree with the expected raise in graphitization according to the increment in reduction time, which trend seems to point out that the reduction process is also creating defects, something that is commonly seen in thermal reduction (Lin and Grossman, 2015). Additionally, the shape of the 2D band indicates the presence of multilayer rGO (Ferrari, 2007), which agrees with observations collected by SEM images.

FTIR spectra in Figure III-5 show the presence of oxygenated functional groups in GO at  $3300\text{ cm}^{-1}$ ,  $1730\text{ cm}^{-1}$ ,  $1200\text{ cm}^{-1}$  and  $1100\text{ cm}^{-1}$  associated with  $-\text{OH}$ ,  $-\text{C}=\text{O}$ ,  $-\text{C}-\text{O}-\text{C}$  and  $-\text{C}-\text{O}$ , respectively. The reduction time triggered a decrease on the intensity of the bands related with  $-\text{C}=\text{O}$ ,  $-\text{C}-\text{O}-\text{C}$  and  $-\text{C}-\text{O}$ , indicating that these groups were removed from GO by reacting with ascorbic acid. According to longer reaction times, the intensity of those groups decreased, being rGO4 the material with minimal groups. In contrast,  $\text{C}=\text{C}$  band prevailed independently of the reduction time since these groups did not react with ascorbic acid. Interestingly, only the spectrum corresponding to rGO1 displays a band at  $2900\text{ cm}^{-1}$  that is attributed to  $\text{C}-\text{H}$  groups together with a drastic decrease in the intensity of the band associated with the epoxy groups.

However, the band of  $-\text{OH}$  showed a narrowing, while its intensity seemed to be the same. This phenomenon could be explained considering that hydrophobicity increase with the reduction degree of GO sheets, so water physisorbed or intercalated among stacks of rGO sheets will be minor (Acik et al., 2011). Moreover, the prevalence of the band related to  $-\text{OH}$  groups agree with reports about the stability of these groups as compared to epoxy groups ( $-\text{C}-\text{O}-\text{C}$ ) under the conditions prevailing in the reduction process. As well, FTIR spectra agree with information that points out that epoxy groups are the most abundant and the most reactive (Dreyer et al., 2010), since they displayed a band with high intensity in the GO spectrum and the intensity decreased after the reduction reaction .

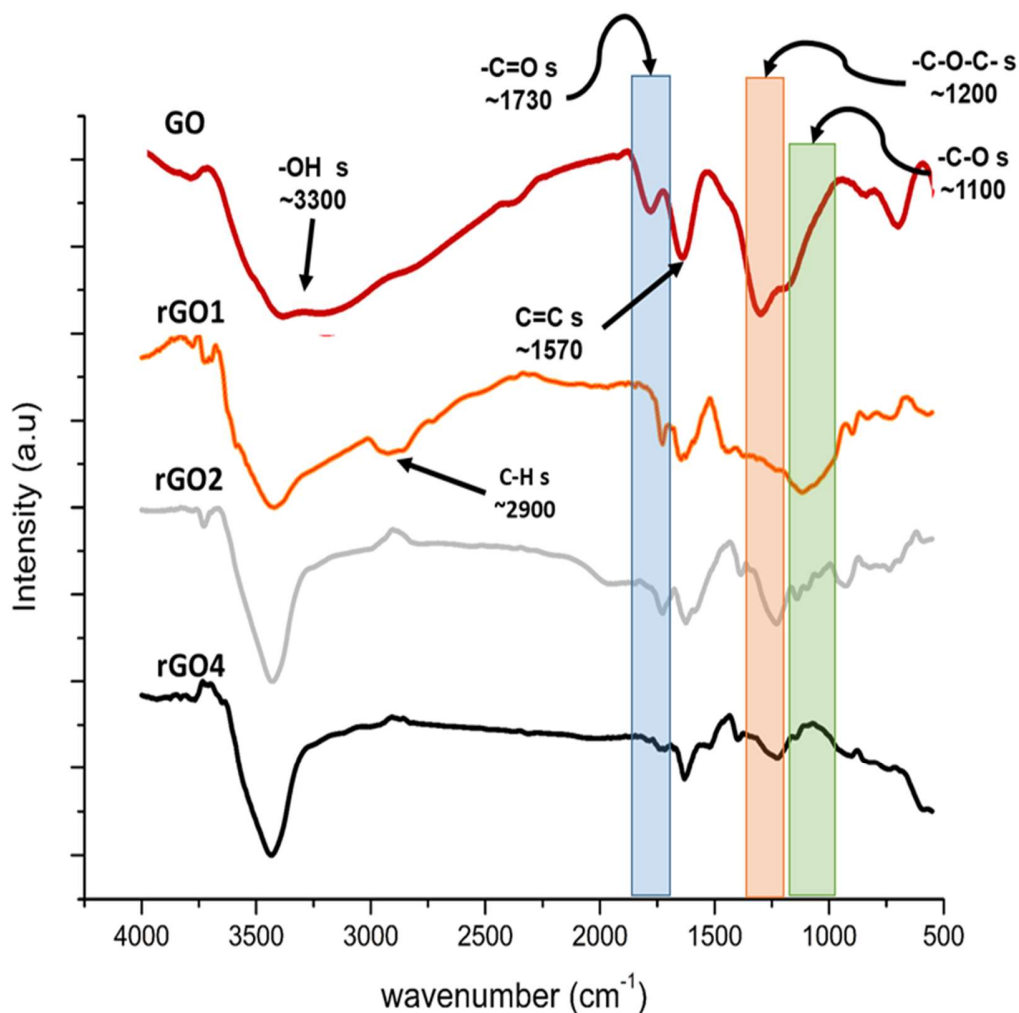


*Figure III-5. FTIR spectra of reduced and unreduced materials. Shaded areas indicate the regions of the oxygenated functional groups that underwent changes throughout the reduction process.*

### 3.3.3 Acute effects of rGO materials on methanogenesis

Sludge exposed to rGO with different extent of reduction revealed a positive effect on methanogenesis with both glucose (Figure III-6a) and starch (Figure III-6c) as substrates. This positive effect improved the amount of methane produced as well as the MMA. The most relevant



increase occurred in sludge incubations performed with starch, in which the difference between the treatments with rGO and the control incubated without rGO is highly evident. MMA could be calculated from the kinetic data (Table III-1). For experiments performed with glucose, it was observed that rGO1 increased 4.7 % the MMA, while rGO2 and rGO4 promoted an enhancement of 13.8 % and 8.9 %, respectively, with respect to the control incubated in the absence of rGO materials (Figure III-6b). Furthermore, rGO materials greatly enhanced methane production in sludge incubations conducted with starch, especially with rGO1, which triggered an improvement of 114 % on the MMA as compared to the control treatment prepared without rGO materials. Meanwhile, materials rGO4 and rGO2 increased the MMA by 86.4 % and 70.6 %, respectively, with respect to the control when starch was provided as electron donor (Figure III-6d). These results suggest that rGO materials did not cover starch granules, which was shown to occur in the case of sludge incubations conducted with GO (Bueno-López et al., 2018). Wrapping of starch granules by GO sheets caused mass transfer limitations negatively affecting the methanogenic activity of anaerobic sludge (Bueno-López et al., 2018).

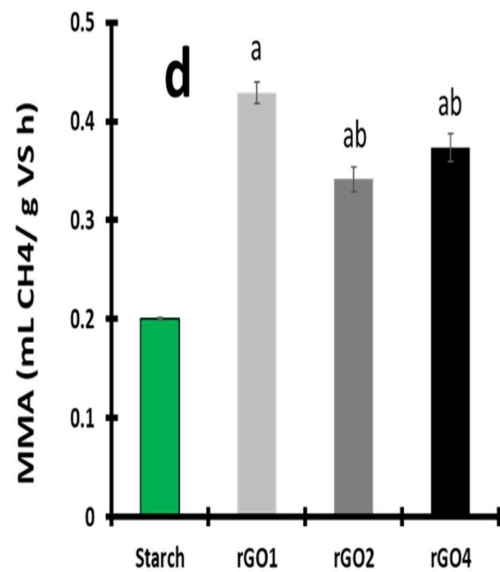
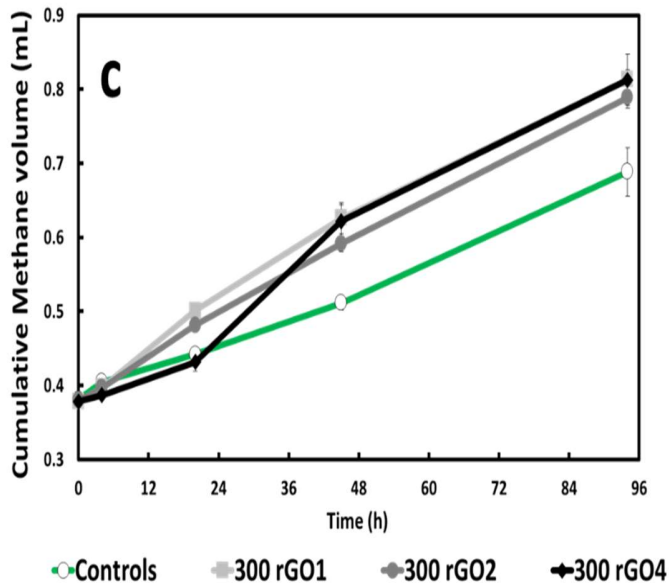
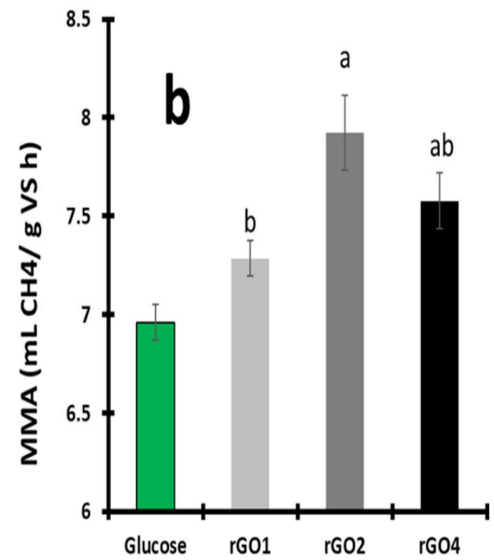
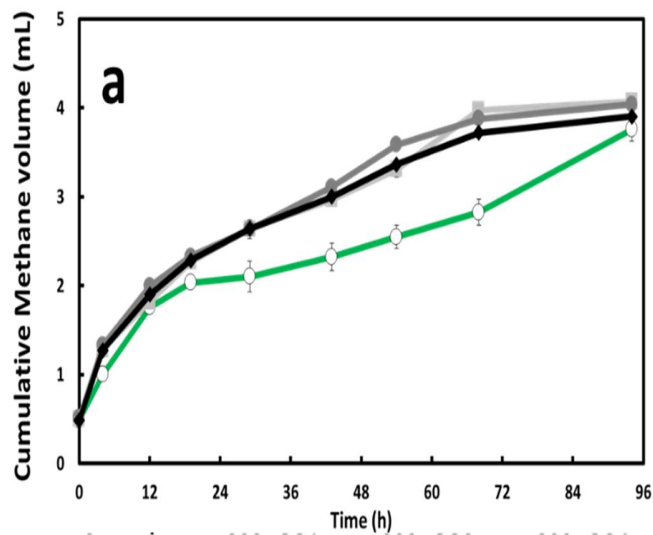


**Figure III-6.** Cumulative methane concentration using glucose (a) or starch (b) and their corresponding maximum methanogenic activity (MMA; b and d) Number displayed in the series legend indicate de concentration (mg/L) of rGO materials reduced 1, 2 and 4 hours, respectively, rGO1, rGO2 and rGO4. Letters on top of bars show statistical difference ( $p < 0.05$ ) respect to the control without rGO materials (letter a) and between treatments (letter b). Same set of letters means no statistically difference.



**Table III-1.** Maximum methanogenic activity (MMA) obtained for experiments using glucose or starch and rGO with different reduction degrees

| Treatment | Glucose               |                                   | Starch                |                                   |
|-----------|-----------------------|-----------------------------------|-----------------------|-----------------------------------|
|           | MMA <sup>a</sup> ± SD | Treatment effect <sup>b</sup> (%) | MMA <sup>a</sup> ± SD | Treatment effect <sup>b</sup> (%) |
| Ctrl      | 7.0 ± 0.1             | -                                 | 0.20 ± 0.00           | -                                 |
| rGO1      | 7.3 ± 0.1             | 4.7                               | 0.43 ± 0.01           | 114.1                             |
| rGO2      | 7.9 ± 0.2             | 13.8                              | 0.34 ± 0.01           | 70.6                              |
| rGO4      | 7.6 ± 0.1             | 8.9                               | 0.37 ± 0.01           | 86.4                              |

<sup>a</sup>Maximum methanogenic activity calculated from 3 points of the kinetic curves by linear regression (mL CH<sub>4</sub> /g VS h). <sup>b</sup>Treatment effects are the difference on MMA using rGO (300 mg/L) compared to control treatments (Ctrl) without rGO.

In experiments performed with starch, it was observed that the highest methane production was obtained with rGO1, which makes sense when considering the smaller particle size of this conductive material as compared to the other reduced materials. Namely, rGO1 has a greater exposed surface area than rGO2 and rGO4 and therefore greater interaction with starch granules. However, contrary to what was observed in experiments conducted with GO (Bueno-López et al., 2018), the interactions with rGO1 promoted the disintegration of starch granules. This may be due to the removal of epoxy groups through the reducing process of GO to rGO since these functional groups were responsible for the wrapping of starch granules by GO (Bueno-López et al., 2018). Moreover, carbonyl functional groups, which prevail mainly at the edges of graphene sheets (Pei and Cheng, 2012) can interact with the hydroxyl groups of the polysaccharide chains by hydrogen bonding, thus fragmenting starch granules and producing the structures observed in Figure III-3d. In addition to the disintegration of the starch granules, according to collected Raman spectra, rGO1 also showed a great mobility of electrons, which can favor DIET. On the other hand, the lower MMA observed in sludge incubations amended with rGO2 or rGO4 as compared to those performed with rGO1 could be due to agglomeration of rGO sheets in rGO2 and rGO4, with the resulting decrease in surface area. Additionally, a decrease in carbonyl groups in rGO2 and rGO4



(Figure III-5) could also explained the worse catalytic effect stimulated by these materials on methane production.

The positive effects of rGO on anaerobic digestion reported herein could be explained by different aspects. In the case of micro-structures, they provide available surface and porosity, which may protect microorganisms by creating a micro-environment. Additionally, functional groups on the materials surface could serve as electron shuttles and their conductivity could be involved in DIET. Moreover, large surface area promotes adsorption of substrates, which are easily accessible to microorganisms attached to the materials. Furthermore, rGO could also play a buffering roll against abrupt changes in concentration of inhibitors and it promotes disintegration of particulate organic matter improving the hydrolysis stage.

### **3.4 Conclusions**

The effects of GO with different degree of reduction were studied and the results indicate that rGO promotes the methanogenic activity of an anaerobic consortium provided with a soluble (glucose) or a particulate (starch) substrate. Interactions of rGO with starch granules appeared especially important depending on the degree of reduction of GO, which directly affects the disintegration of starch granules. Oxygenated groups present in the surface of rGO interacted with the hydroxyl groups of starch polysaccharides promoting disintegration of the granules into smaller elements, which increases the specific area and thus enhanced the hydrolysis step. The knowledge generated by this study allows to predict the effects of the different materials derived from GO when applied to anaerobic digestion processes.



# Chapter IV

## Effects of graphene oxide and reduced graphene oxide on acetoclastic, hydrogenotrophic and methylotrophic methanogenesis\*



## **Abstract**

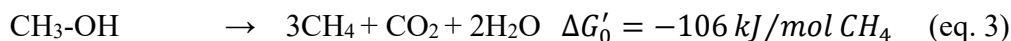
This study describes the effects of graphene oxide (GO) and reduced graphene oxide (rGO) on the acetoclastic, hydrogenotrophic and methylotrophic pathways of methanogenesis by an anaerobic consortium. The results showed that GO negatively affected the hydrogenotrophic and acetoclastic pathways at a concentration of 300 mg/L, causing a decrease of ~38 % on the maximum specific methanogenic activity (MMA) with respect to the controls lacking GO. However, the presence of rGO (300 mg/L) promoted an improvement of the MMA (>45 %) achieved with all substrates, except for the hydrogenotrophic pathway, which was relatively insensitive to rGO. The presence of either rGO or GO enhanced the methylotrophic pathway and resulted in an increase of the MMA of up to 55 %. X-ray photoelectron spectroscopy (XPS) analysis revealed that GO underwent microbial reduction during the incubation period. Electrons derived from substrates oxidation were deviated from methanogenesis towards the reduction of GO, which may explain the MMA decreased observed in the presence of GO. Furthermore, XPS evidence indicated that the extent of GO reduction depended on the metabolic pathway triggered by a given substrate.

## **4.1 Introduction**

Anaerobic digestion (AD) has emerged as an alternative to obtain renewable energy and to recover nutrients from wastewaters. AD is a complex process involving different types of microorganisms that occupy a niche in the trophic web. AD is divided into four stages; the first one is hydrolysis in which the decomposition of polymers and lipids occurs in their basic structures through the action of extracellular enzymes. This process is mainly carried out by heterotrophic acidogenic bacteria. The second step is fermentation, in which organic compounds are converted into short-chain volatile fatty acids (VFA), such as acetic, propionic, and butyric acid, as well as gases, such



as hydrogen and carbon dioxide (CO<sub>2</sub>). The third step of AD is acetogenesis, which involves the conversion of VFA and alcohols into acetate, hydrogen and CO<sub>2</sub>. Acetogenesis is carried out by a group of obligate hydrogen-producing, acetogenic bacteria. The fourth and final step is methanogenesis, a process in which methanogens obtain energy through the conversion of simple substrates into methane. Methanogens use three different pathways to produce methane: (1) hydrogenotrophic pathway, also known as CO<sub>2</sub> reduction pathway, in which archaea produce methane by reducing CO<sub>2</sub> using H<sub>2</sub> or formate; (2) acetoclastic pathway, which involves the production of methane and CO<sub>2</sub> from acetate, and (3) methylotrophic pathway that converts methyl groups of methanol, methylamines and methyl sulfides to methane and CO<sub>2</sub>. The stoichiometry of these pathways is expressed by the following equations (Caruana and Olsen, 2016; Cervantes and Dos Santos, 2011; Costa and Leigh, 2014; Deppenmeier, 2002):



In the search to enhance the efficiency of microbial methane production, a variety of conductive materials have been investigated to improve direct interspecies electron transfer (DIET) between syntrophic bacteria and methanogens. Those include different types of carbonaceous materials, such as activated carbon, biochar, graphene and their derivatives (Barua and Dhar, 2017; Lin et al., 2017a; Tian et al., 2017a; Xu et al., 2015). Graphene is a material composed of a single molecular layer of graphite, which exhibits very interesting mechanical, optical and electrical properties. However, graphene is difficult to produce at industrial scale; thus, graphene oxide (GO) is preferred in many applications since its production is easily scalable. GO has several oxygenated functional groups, such as epoxy, carbonyl, carboxyl and hydroxyl moieties, which allow its dispersion in water (Bagri et al., 2010; Dreyer et al., 2010). Contrary to graphene, GO has shown negative effects on bacteria promoted by wrapping of cells, production of reactive oxygen species



or disruption of cell membranes. These effects depend on the properties of GO sheets (size and surface chemistry), which drive interactions with cells (Jastrzębska and Olszyna, 2015; Liu et al., 2012a) and substrates (Bueno-López et al., 2018). Interestingly, a few recent studies have reported that bacterial respiration can modify the chemistry of GO through the removal of oxygenated groups, producing partially reduced GO (rGO) (Chen et al., 2017; Guo et al., 2017; Salas et al., 2010). However, these reports only consider pure cultures and, therefore, there is a lack of information regarding GO modifications driven by complex microbial communities, such as anaerobic consortia. Additionally, physical and chemical agents, such as ultraviolet light, vitamins and saccharides, among others (De Silva et al., 2017; Thakur and Karak, 2015), can promote the reduction of GO. Hence, wastewater and natural water samples are more likely to contain rGO than GO, depending on the environmental conditions prevailing.

The mechanisms responsible for the beneficial effects of conductive carbonaceous materials (e.g., coal, charcoal, activated carbon, carbon fiber, graphene, GO, etc.) on methane production are poorly understood. Most reports attribute the observed methanogenic activity enhancement to improved DIET between syntrophic bacteria and methanogens. Nevertheless, results using materials with different conductivities have not shown a clear correlation between methane production and conductivity (Martins et al., 2018; Park et al., 2018). Therefore, other factors can also play an important role. For example, in the case of activated carbon, it is well known that this highly porous and heterogeneous material is able to adsorb AD inhibitors and serve as shelter where microorganisms can be immobilized, creating a suitable microenvironment to grow (Capson-Tojo et al., 2018). Therefore, the influence of GO and rGO on methanogenic pathways requires further investigation to identify the underlying mechanisms responsible for the methanogenic activity improvement or inhibition reported so far, since these materials possess a diversity of functional groups capable of participating in various reactions, as well as electrical conductivity that varies depending on the graphitic structure.

The aim of the present work was to study the effects of GO and partially reduced GO on the acetoclastic, hydrogenotrophic and methylotrophic methanogenic activity of an anaerobic microbial consortium. This study will contribute to determine if there are specific effects



(selectivity) on the methanogenic pathways and whether these effects depend on the reduction state and other physical and chemical characteristics of GO. In addition, the results contribute to explain the underlying mechanisms of improvement or inhibition of methane production associated with conductive carbonaceous materials.

## **4.2 Materials and methods**

### **4.2.1 Chemicals**

GO was purchased from Graphene Supermarket<sup>®</sup> and had the following characteristics: concentration 6.2 g/L in aqueous dispersion, monolayer > 80 %, nominal particle size between 0.5 and 5  $\mu\text{m}$ , C/O ratio 3.95. Ascorbic acid (ACS grade) was from Golden Bell (Mexico City, Mexico). All other reagents used in this work were reactive grade and they were obtained from either Sigma-Aldrich Company or Merck.

### **4.2.2 Solutions**

The basal medium used in all bioassays was composed of (mg/L):  $\text{NH}_4\text{Cl}$  (280),  $\text{K}_2\text{HPO}_4$  (250),  $\text{MgSO}_4 \cdot 7\text{H}_2\text{O}$  (100),  $\text{CaCl}_2 \cdot 2\text{H}_2\text{O}$  (10),  $\text{MgCl}_2 \cdot 6\text{H}_2\text{O}$  (100), yeast extract (100),  $\text{NaHCO}_3$  (3000) and 1 mL of trace elements solution composed of (mg/L):  $\text{FeCl}_2 \cdot 4\text{H}_2\text{O}$  (2000),  $\text{H}_3\text{BO}_3$  (50),  $\text{ZnCl}_2$  (50),  $\text{CuCl}_2 \cdot 2\text{H}_2\text{O}$  (30),  $\text{MnCl}_2 \cdot 4\text{H}_2\text{O}$  (50),  $(\text{NH}_4)_6\text{Mo}_7\text{O}_{24} \cdot 4\text{H}_2\text{O}$  (50),  $\text{AlCl}_3 \cdot 6\text{H}_2\text{O}$  (90),  $\text{CoCl}_2 \cdot 6\text{H}_2\text{O}$  (2000),  $\text{NiCl}_2 \cdot 6\text{H}_2\text{O}$  (50),  $\text{Na}_2\text{SeO}_3 \cdot 6\text{H}_2\text{O}$  (100), EDTA (1000), resazurin (200), and 1 mL HCl (36 %). The pH of the medium was adjusted to  $7.0 \pm 0.2$  using NaOH or HCl 0.1 N if needed. Deionized (DI) water was used to prepare all solutions.



### 4.2.3 Chemical reduction of graphene oxide

Reduction of GO was carried out according to the procedure described elsewhere (Toral-Sánchez et al., 2016) with a reaction time of 4 hours. Briefly, a solution with ascorbic acid and GO was prepared in a beaker with a magnetic stirrer, at high speed under ambient conditions. After the reaction time, rGO was centrifuged for 20 min at 10,000 rpm in an Avanti J-30I equipment and washed three times using deionized water in cycles of centrifugation and dispersion. Finally, washed rGO was dispersed in deionized water and sonicated (Bransonic model B2510-DTH, 40 kHz) for 30 min at room temperature.

### 4.2.4 Spectroscopic characterization of materials

Fourier transform infrared spectroscopy (FTIR) analyses were performed using a Thermo-Nicolet 6700 FT-IR equipment in transmission mode at 128 scans, resolution of  $4\text{ cm}^{-1}$  and  $\text{CO}_2$  and  $\text{H}_2\text{O}$  automatic correction. The pellets examined were made with freeze-dried GO materials and KBr in a 1:1000 ratio, respectively.

X-ray photoelectron spectroscopy (XPS; SPECS Phoibos 150) spectra of the freeze-dried materials were collected and peak fitting was done using the “Aanalyzer” software v1.36.

Raman spectra of GO and rGO were obtained using a RENISHAW InVia Confocal Raman spectrometer with laser frequency of 514 nm as excitation source through a 50× objective. Sample preparation implied the formation of films on aluminum foil by dripping deposition and subsequent drying for 12 h prior to analysis.

Elemental analyses were carried out by energy dispersive spectrometry (EDS) using a FEI Helios Nanolab 600 dual beam field emission scanning electron microscope (FE-SEM) operated at 5.00 kV and 86 pA. At least three different spots of the sample were imaged, and the results were expressed as the average value of the measurements. Samples were prepared on silicon wafers by dripping deposition and were dried under atmospheric conditions for 12 h.



#### **4.2.5 Particle size distribution**

Particle size distribution of GO and rGO dispersions in basal medium (10 mg/L and pH 7) was measured by dynamic light scattering (DLS) using a Malvern Zetasizer Nano ZS instrument using a refractive index of 1.85 in both cases (Jung et al., 2008).

#### **4.2.6 Batch sludge incubations**

##### **4.2.6.1 Inoculum**

Methanogenic granular sludge was obtained from a full-scale up-flow anaerobic sludge bed reactor treating brewery wastewater (Mahou, Guadalajara, Spain). The sludge was stored at 4°C and it was washed and crushed using a needle gauge 22 G before its use in the incubations. The content of volatile solids (VS) was 6.96 % of wet weight.

##### **4.2.6.2 Acetoclastic and methylotrophic bioassays**

The effect of GO materials on the acetoclastic and methylotrophic methanogenic activity was assessed in batch incubations conducted in triplicate using serological bottles with a total volume of 60 mL. In these experiments, 9 mL of basal medium with acetate or methanol (final concentration of 2 g chemical oxygen demand (COD)/L) and 1.5 g VS/L of sludge were added to each bottle and then flushed with a gas mixture of N<sub>2</sub>/CO<sub>2</sub> (80:20, v/v) for 3 min. Subsequently, bottles were sealed, and the headspace was further flushed using the same gas mixture for 3 min. The bottles were incubated overnight at 30°C in an orbital shaker at 120 rpm. After this period, 1 mL of deionized water was added to the control bottles and 1 mL of the stock of the corresponding GO material in order to get 10 mL in each bottle with a concentration of 10, 50 and 300 mg/L of



each GO material. Once the GO materials were added, the headspace of all bottles was flushed with the N<sub>2</sub>/CO<sub>2</sub> gas mixture for 3 min and incubated at 30°C in an orbital shaker at 120 rpm. Gas samples (100 µL) were periodically taken for methane measurement by gas chromatography, which was conducted under previously reported conditions (Simon-Pascual et al., 2019).

#### **4.2.6.3 Hydrogenotrophic Bioassays**

The effect of GO materials on the hydrogenotrophic methanogenic activity was assessed using the same protocol described above. After establishing anaerobic conditions in the incubations, H<sub>2</sub> was supplied, as H<sub>2</sub>/CO<sub>2</sub> (80:20, v/v), to a final headspace concentration of 0.5 atm.

### **4.3 Results and discussion**

#### **4.3.1 Characterization of graphene materials**

To describe the physical and chemical properties of GO and to verify the development of rGO following the chemical reduction of GO with ascorbic acid, both materials were characterized by several spectroscopic and microscopic techniques. The results showed that the C/O ratio was 2.9 for GO and 4.1 for rGO, which suggests the loss of oxygenated functional groups through the reduction process. The average size of particles shifted from 891.5 nm to 4931 nm for GO and rGO, respectively, which indirectly indicates that rGO is more hydrophobic and, therefore, has a higher trend to agglomerate in aqueous medium. Furthermore, FTIR spectra obtained from rGO (Figure IV-1) showed that the reduction process decreased the intensity of bands related to –C=O, –C–O–C and –C–O functional groups (at 1730, 1200 and 1100 cm<sup>-1</sup>, respectively), evidencing that these groups were removed from GO by reacting with ascorbic acid during the reduction process. In contrast, the C=C band remained unchanged after the reduction process.

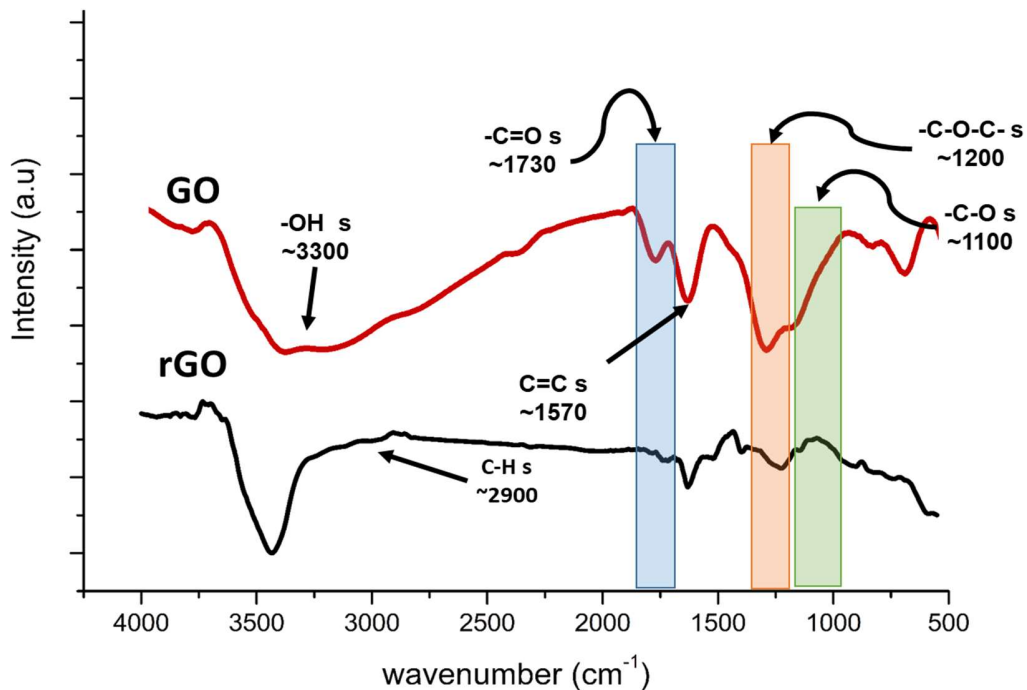


*Figure IV-1. FTIR spectra of GO and rGO. Shaded areas indicate the regions of oxygenated functional groups that underwent changes through the reduction process.*

Moreover, Raman spectra (Figure IV-2) of GO materials displayed the characteristic D and G bands of carbon at  $\sim 1350$  and  $\sim 1600$   $\text{cm}^{-1}$ , respectively. D band is associated with disorder-induced symmetry-breaking effects of  $\text{sp}^2$  network, while G band is related to the ordered structure of graphene hexagons and graphite crystallinity. Furthermore, band 2D at  $\sim 2676$   $\text{cm}^{-1}$  is sensitive to  $\pi$  bonds in the graphitic electronic structure and band D+G at  $\sim 2950$   $\text{cm}^{-1}$  is the combination of band D and G induced by disorder. To get more information about the conductivity and crystallinity, the  $I_{2D}/I_G$  ratio was calculated, since it has been suggested as a better measurement of the graphitic  $\text{sp}^2$  regions and it keeps direct relation with electron mobility (Raza, 2012). The calculated  $I_{2D}/I_G$  ratio was 0.164 and 0.278 for GO and rGO samples, respectively. These values indicate that electrons can move faster in rGO than in GO due to a bigger size of well-ordered graphitic patches.

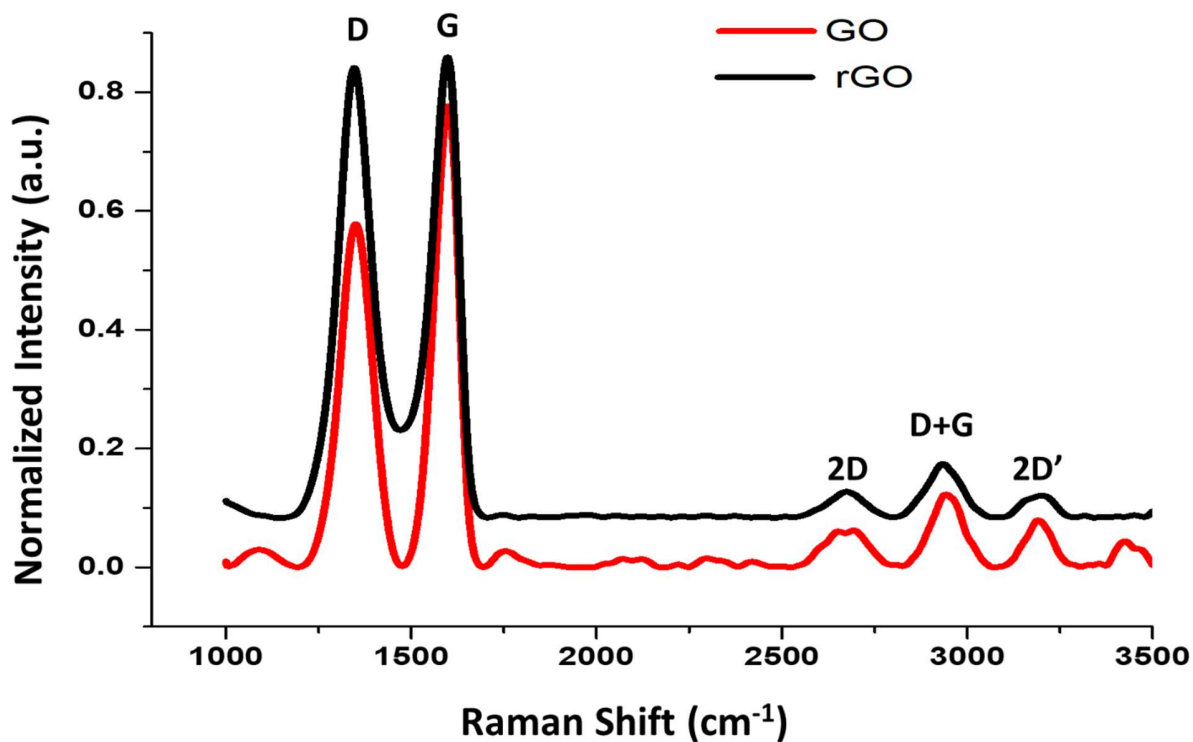


*Figure IV-2. Raman spectra of GO and rGO obtained by chemical reduction using ascorbic acid.*

The peak fitting of C 1s core level of the XPS data of GO (Figure IV-3a.) showed two components; one associated to  $sp^2$  hybridization of the graphitic structure (C=C) at 284.8 eV and another at 285.5 eV assigned to  $sp^3$  hybridization (C-C). Additionally, three components were observed at 287.4, 288.3 and 289.4 eV assigned to C-OH and/or C-O-C, C=O and OH=C-O, respectively (Biniak et al., 1997; Pei and Cheng, 2012). In the case of rGO (Figure IV-3b.), a marked reduction of the components associated to oxygenated functional groups occurred and an important increase on C=C was observed, which agrees with FTIR results.

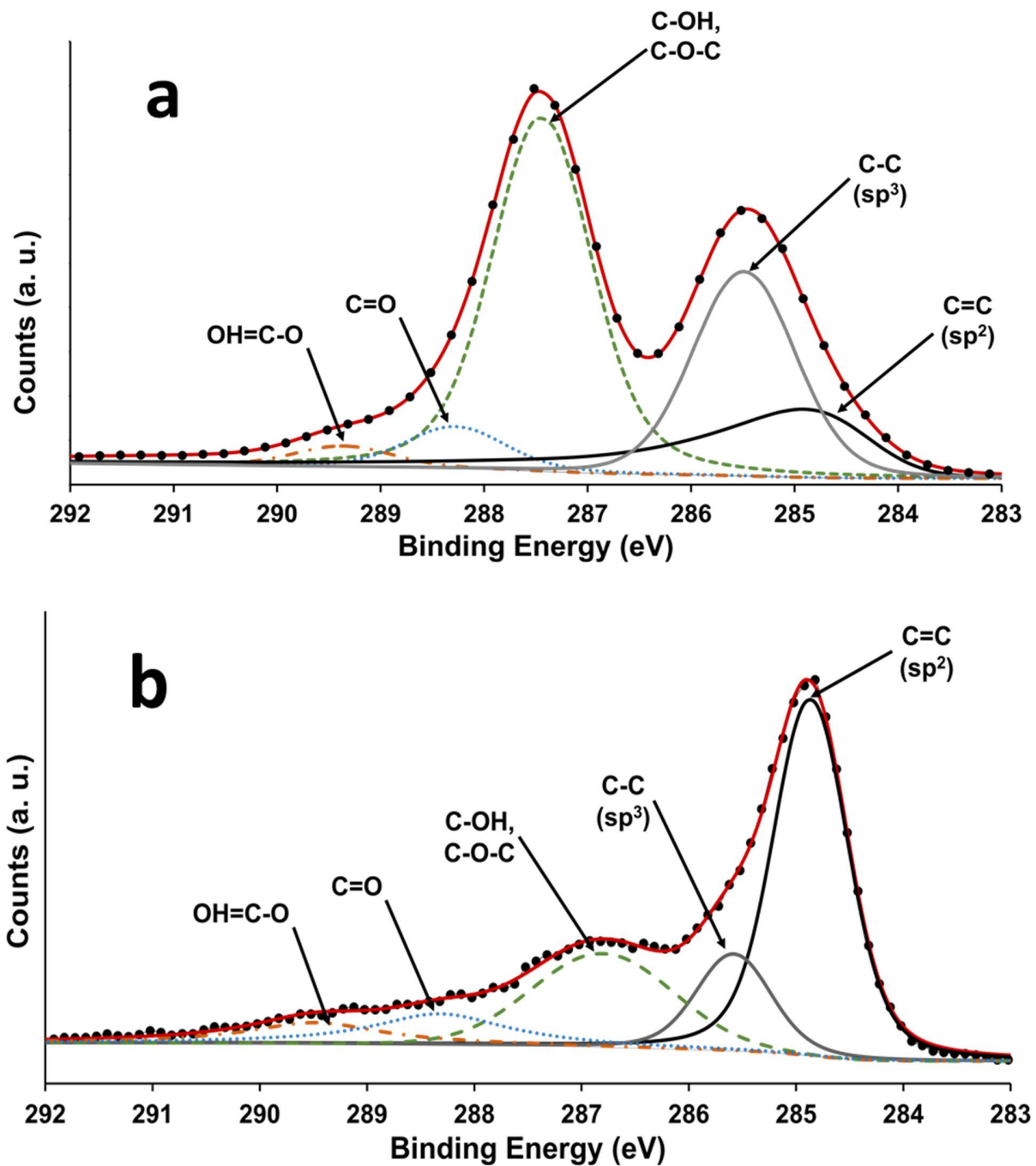


Figure IV-3. Core level C<sub>1s</sub> high resolution XPS spectra of (a) GO, (b) rGO obtained by chemical reduction using ascorbic acid. Dots and black solid line represent the experimental data, while gray and dotted lines are the deconvoluted components.



#### **4.3.2 Effects of GO and rGO on methanogenic activities**

Sludge incubations performed with different concentrations of GO under acetoclastic conditions (Figure IV-4, upper panel) revealed that exposure to low concentrations of GO (10 and 50 mg/L) promoted an increase on the maximum methanogenic activity (MMA, up to 44 %) as compared to the GO-free control. Nevertheless, the acetoclastic MMA decreased by 37 % when the sludge was exposed to the highest concentration of GO tested (300 mg/L). Furthermore, when the sludge was exposed to the reduced form of GO (rGO) under acetoclastic conditions, at concentrations above 50 mg/L, the MMA increased up to 40 % as compared to the control lacking rGO (Table IV-1).

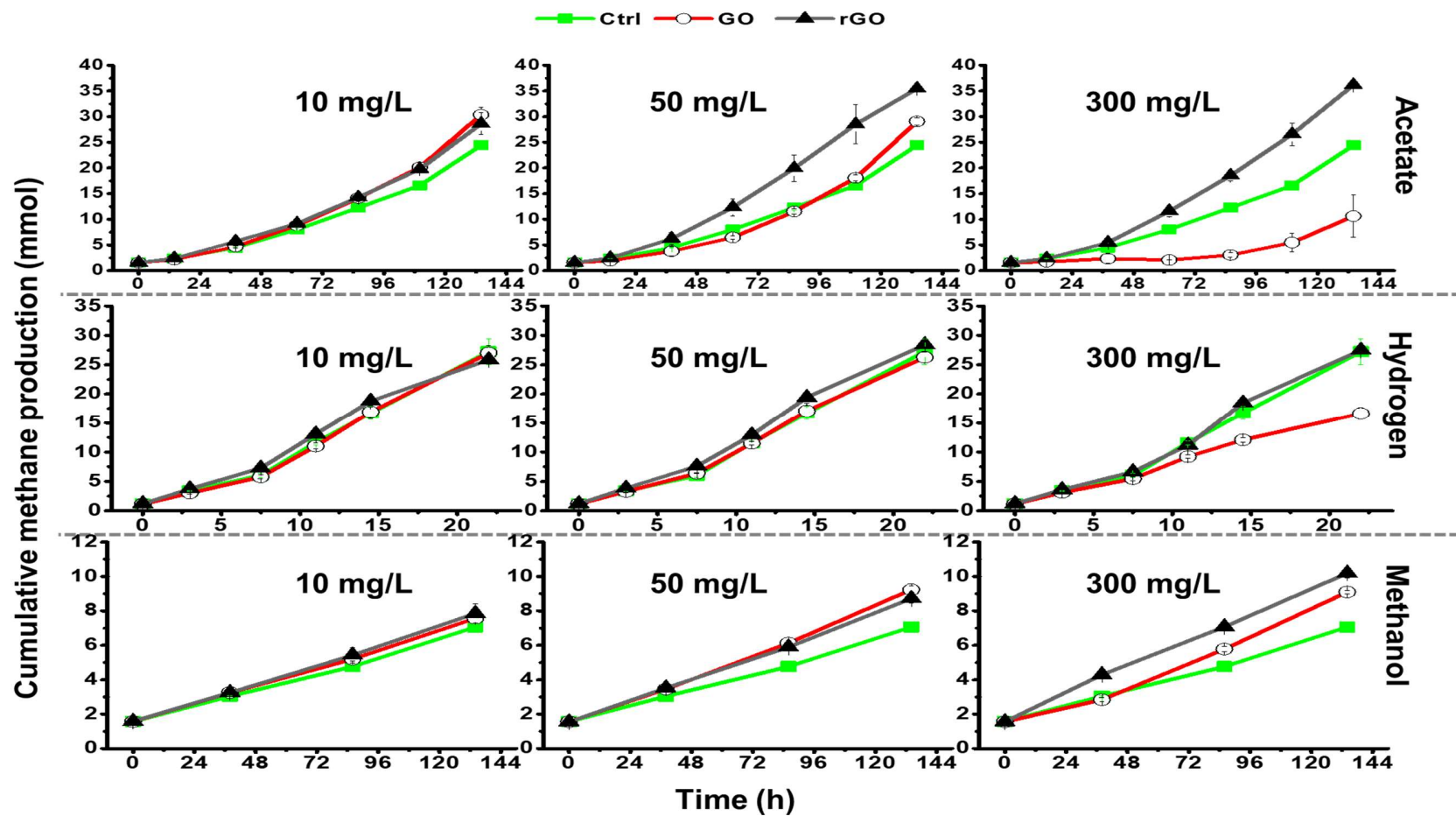


Figure IV-4. Cumulative methane production related to acetoclastic (up), hydrogenotrophic (middle) and methylotrophic (down) activities using different concentrations of graphene oxide (GO) and reduced GO (rGO). Ctrl refers to control incubations performed without GO/rGO. Error bars represent the standard deviation of triplicates.



**Table IV-1.** Calculated maximum methanogenic activity (MMA)<sup>a</sup> observed with different substrates in the presence of GO and rGO

|                | Concentration<br>(mg/L) | Acetate                        |                  | Hydrogen                       |                  | Methanol                       |                  |
|----------------|-------------------------|--------------------------------|------------------|--------------------------------|------------------|--------------------------------|------------------|
|                |                         | MMA ± SD                       | Change           | MMA ± SD                       | Change           | MMA ± SD                       | Change           |
|                |                         | (mmol CH <sub>4</sub> /g VS-h) | (%) <sup>b</sup> | (mmol CH <sub>4</sub> /g VS-h) | (%) <sup>b</sup> | (mmol CH <sub>4</sub> /g VS-h) | (%) <sup>b</sup> |
| <b>Control</b> | --                      | 16.9 ± 0.5                     | --               | 104.4 ± 7.2                    | --               | 2.8 ± 0.1                      | --               |
| <b>GO</b>      | <b>10</b>               | 22.5 ± 1.3                     | 33.4             | 105.9 ± 7.8                    | 1.4              | 3.0 ± 0.2                      | 7.1              |
|                | <b>50</b>               | 24.4 ± 0.4                     | 44.1             | 101.8 ± 8.7                    | -2.5             | 4.0 ± 0.1                      | 43.5             |
|                | <b>300</b>              | 10.5 ± 5.2                     | -37.7            | 64.8 ± 2.8                     | -38.0            | 4.4 ± 0.1                      | 55.7             |
| <b>rGO</b>     | <b>10</b>               | 21.7 ± 0.8                     | 28.4             | 109.9 ± 6.2                    | 5.2              | 3.2 ± 0.4                      | 14.3             |
|                | <b>50</b>               | 24.3 ± 0.3                     | 44.0             | 112.6 ± 9.2                    | 7.8              | 3.6 ± 0.2                      | 29.2             |
|                | <b>300</b>              | 24.5 ± 1.2                     | 45.1             | 112.5 ± 8.7                    | 7.7              | 4.3 ± 0.2                      | 52.1             |

<sup>a</sup>MMA calculated by linear regression from at least three sampling points during the kinetics. <sup>b</sup>Change on MMA with respect to the control incubated without GO/rGO; positive values indicate an increase on MMA, while negative ones, a decrease.



In the case of hydrogenotrophic incubations (Figure IV-4, middle panel), low concentrations of GO (10 mg/L or less) showed negligible effects on the MMA, while the highest concentration of GO tested (300 mg/L) decreased 38 % this activity as compared to the control (Table IV-1). Regarding the experiments performed with rGO, it was observed that its effect was always positive, although to a small extent, increasing the MMA up to 7.8 % as compared to the control lacking rGO.

In contrast to the acetoclastic and hydrogenotrophic pathways, the methylotrophic methanogenic activity was consistently improved by the presence of either GO or rGO in a dose-dependent manner (Figure IV-4, lower panel). Interestingly, the improvement of the methylotrophic activity by GO at concentrations of 50 and 300 mg/L (43.5 % and 55.7 % increase, respectively) was greater than the enhancement observed with rGO at the same concentrations (29.2 % and 52.1 % increase, respectively).

The results suggest that both acetoclastic and hydrogenotrophic pathways may be negatively affected by the presence of GO, particularly at high concentrations (e.g. 300 mg of GO/L). The decrease in methane production could be due to the ability of some anaerobic microorganisms to reduce GO (Akhavan and Ghaderi, 2012; Chen et al., 2017; Raveendran et al., 2013; Salas et al., 2010). Therefore, electrons derived from acetate and hydrogen oxidation might have been deviated from methane synthesis towards the reduction of GO. Additionally, it has been reported that GO inhibits coenzyme F<sub>420</sub> activity (Dong et al., 2019), which could also explain the inhibitory effects observed at high GO concentrations (e.g. 300 mg GO/L).

For methylotrophic experiments, the absence of negative effects could be explained considering that electron-donating bacteria, prefer to use alcohols or fatty acids (Park et al., 2018), and that acetogens can produce acetate or H<sub>2</sub> and CO<sub>2</sub> from methanol, activating the acetoclastic and hydrogenotrophic routes too. These results suggest that GO is reduced faster and, therefore, no negative effects were observed throughout the incubation period. This would suggest that GO recovered from methylotrophic experiments might have presented a higher degree of reduction



---

(Figure IV-5, results discussed below), since all three metabolic pathways might have been involved. In addition, biologically produced rGO could act as a promoter of AD, since it has a great biocompatibility (Zhang et al., 2018) and *in situ* reduction can generate three-dimensional structures, which allow a better interaction between microorganisms and rGO sheets (Shen et al., 2018; Yoshida et al., 2016).

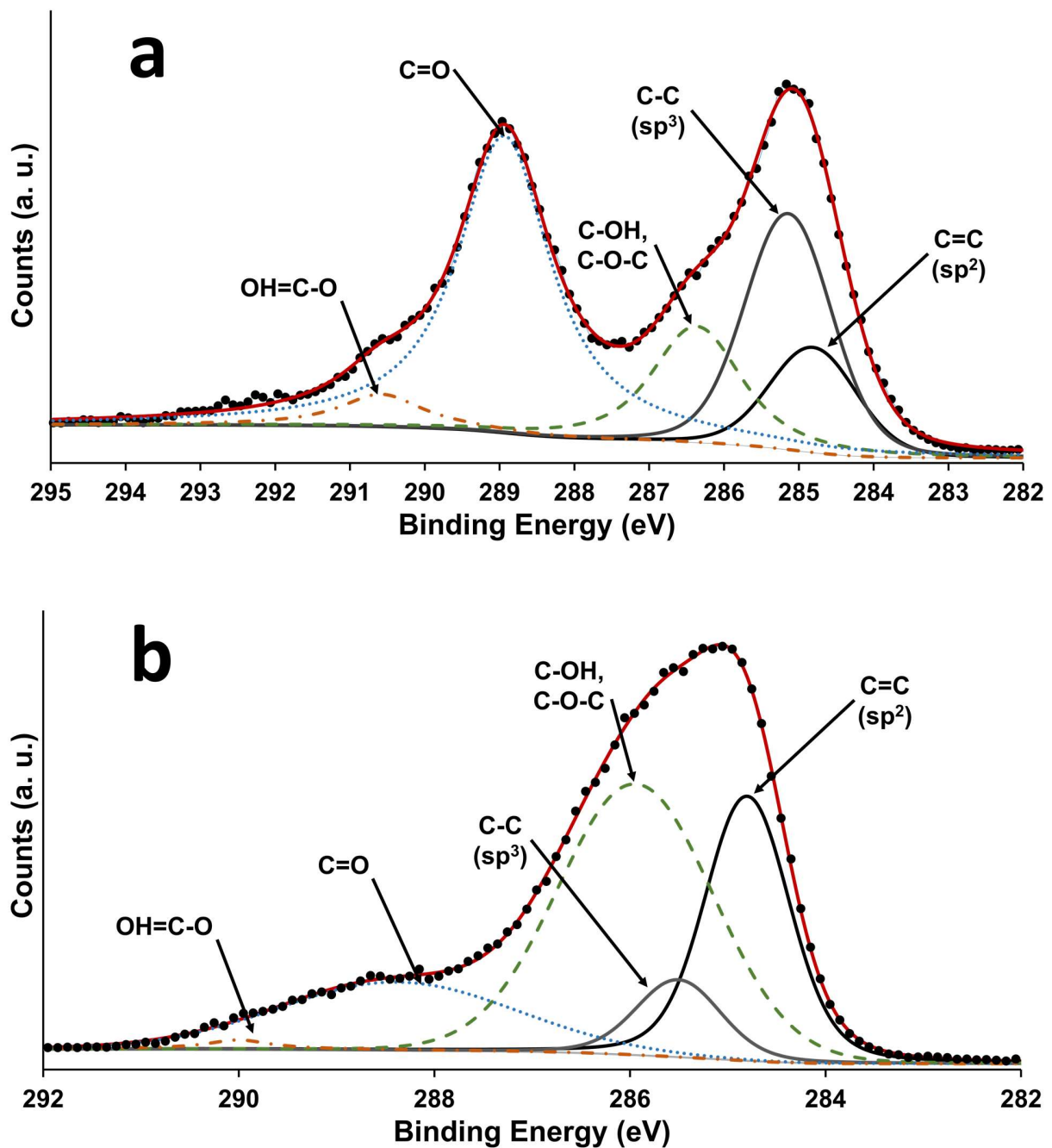


*Figure IV-5. Core level C1s high resolution XPS spectra of GO materials recovered from (a) acetoclastic, and (b) methyloctrophic experiments at the end of the incubation period. Dots and black solid line represent the experimental data, while gray and dotted lines are the deconvoluted components.*



The microbial reduction of GO to rGO was corroborated by XPS spectroscopy both in acetoclastic and methylotrophic experiments (Figure IV-5). In the case of hydrogenotrophic experiments, XPS characterization was excluded because GO showed minor effects on MMA as shown in Table IV-1. Certainly, a decrease in oxygenated functional groups and an increase of the component associated with the graphitic structure was observed in GO collected from acetoclastic experiments at the end of the incubation (Figure IV-5a.) as compared to the original GO (Figure IV-3a). Moreover, GO samples collected from methylotrophic incubations exhibited a considerable decrease of oxygenated functional groups and an intensification of the component related with the  $sp^2$  hybridization (Figure IV-5b.) Interestingly, XPS survey spectra obtained for GO from both acetoclastic and methylotrophic assays showed the peak of N 1s linked to proteins (Edyvean et al., 2008), which suggests possible adsorption of cell components onto GO. However, the results suggest that cell wall was not adsorbed onto GO, since the peak P 2p related to phospholipids (Leone et al., 2006) was absent. Considering the aforementioned, the most important point of comparison to define the reduction extent due to the biological activity was the  $sp^2$  component. The abiotic reduction was discarded by analyzing the FTIR spectra of GO recovered from incubations carried out without sludge (Figure IV-6). These spectra showed negligible changes in the materials recovered as compared to untreated GO, regardless of the substrate used.

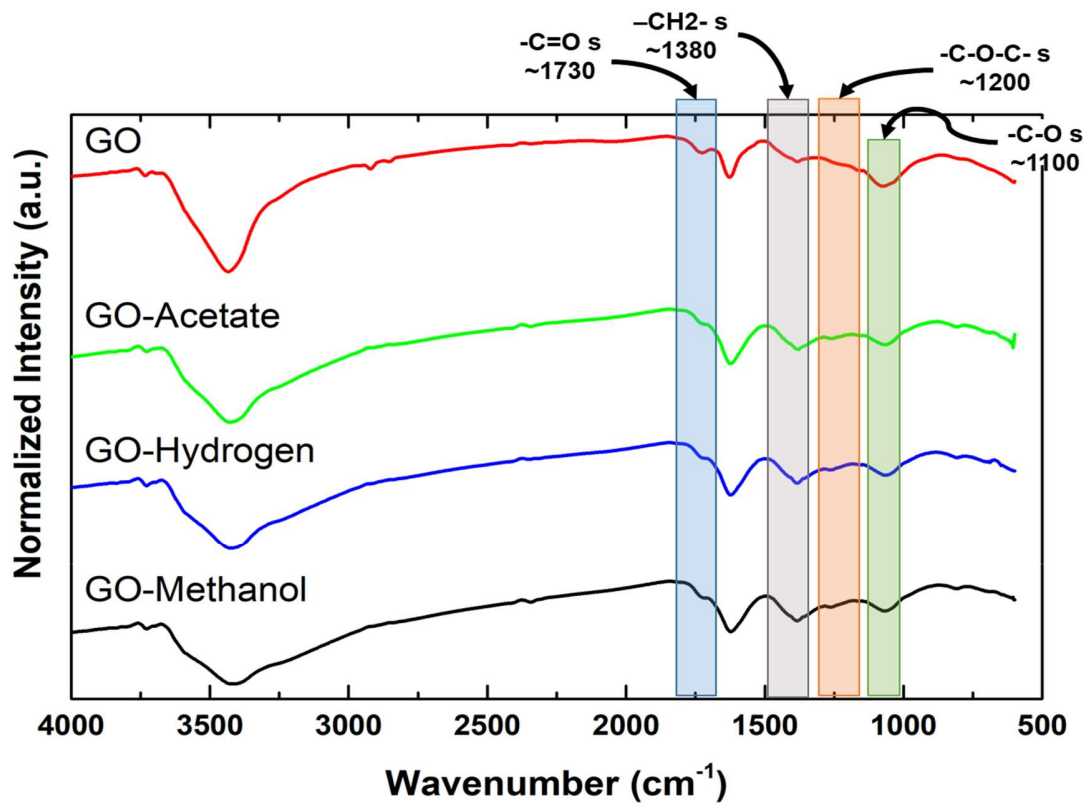


*Figure IV-6. FTIR spectra of GO from abiotic incubations without sludge. Shaded areas highlight the regions of oxygenated functional groups of interest.*

Sludge incubations described up to this point were performed with disintegrated granular sludge. Additional incubations were conducted with granular sludge (Figure IV-7) and results showed that crushing the sludge caused a decrease of the acetoclastic and methylotrophic MMA of 24.1 % and 17.8 %, respectively (Table IV-2 summarize MMA results from granular sludge), for the experiments conducted without GO materials. Although the addition of rGO increased the MMA in incubations with crushed sludge, these methanogenic activities were always lower than in those observed with granular sludge, especially in the case of methanol incubations in which a decrease of around 38 % was observed. In contrast, the hydrogenotrophic activity increased in incubations



---

performed with crushed sludge. In experiments conducted without rGO, the MMA was 36.4 % higher with granular sludge than the activity observed with crushed sludge. Similar results were obtained in the presence of rGO, but the difference in MMA between granular and crushed sludge was 22.8 %. These results make sense considering that in the granule structure, syntrophic bacteria using acetate and methanol are on the external part of the granules, while methanogenic archaea using hydrogen prevail in the inner part of the granules (Lovley, 2011). Thus, crushing the granules allow methanogens to be in contact with hydrogen avoiding diffusional limitations.

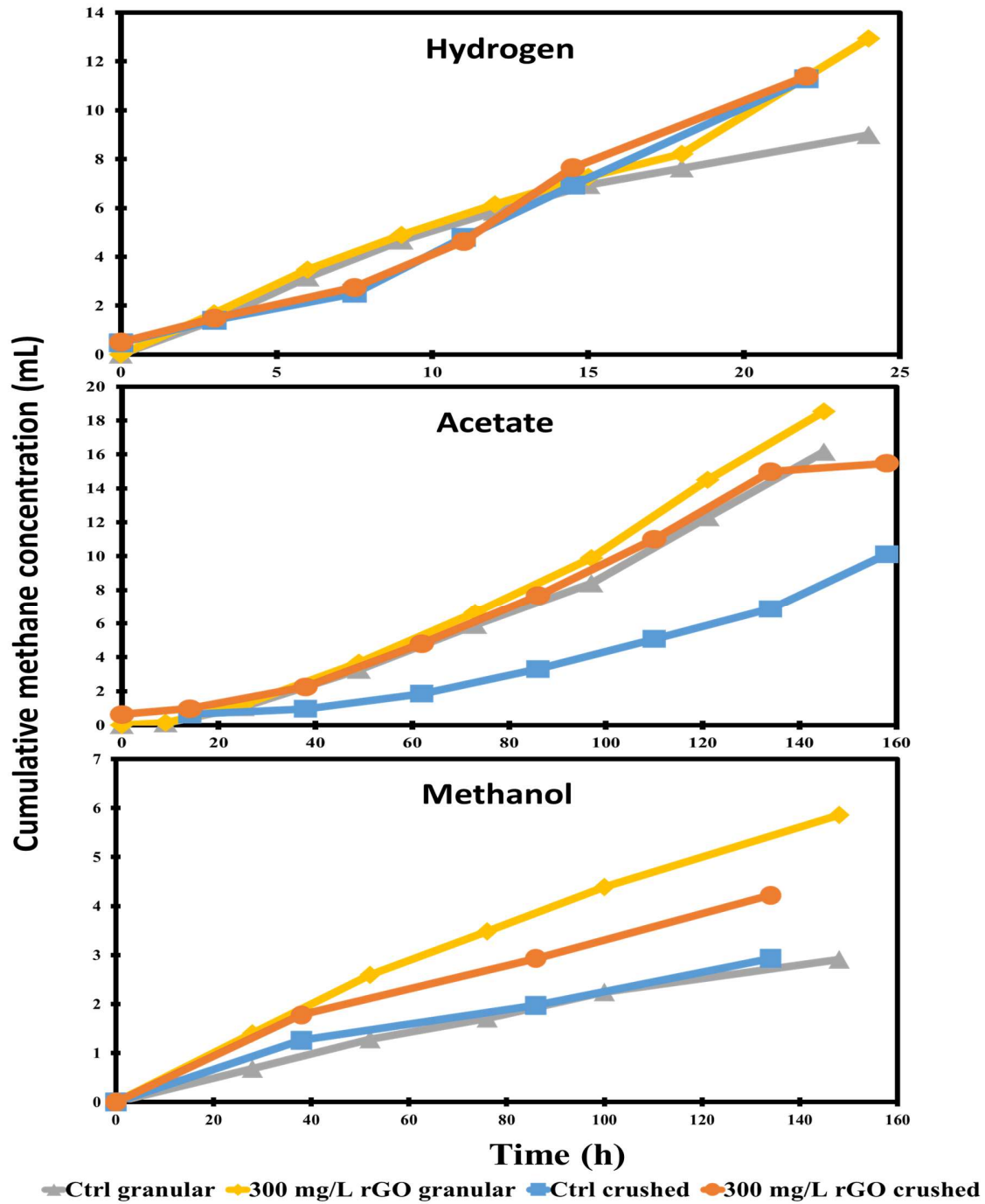


Figure IV-7. Comparative of cumulative methane production using granular sludge, crushed sludge and 300 mg/L of the rGO. Ctrl refers to control incubations performed without rGO.



From the results obtained in the present study, it can be inferred that GO reduction competes for electrons with methanogenesis. Previously, it has been reported that methanogens are able to divert electrons derived from substrates oxidation towards the reduction of quinone moieties in humic substances with the consequent decrease in methane production (Cervantes et al., 2002). Further research is necessary to clarify the long-term effects of GO on anaerobic consortia in anaerobic wastewater treatment systems. However, it is expected that GO would prevail as rGO in such systems, since microorganisms are able to perform GO reduction as evidenced in the present study and in previous reports using pure cultures.

*Table IV-2. Calculated maximum methanogenic activity (MMA)<sup>1</sup> observed with different substrates in the presence and absence of rGO<sup>2</sup> for granular and crushed sludge*

| Substrate | Treatment | Granular sludge | Crushed sludge | Change on MMA <sup>3</sup> (%) |
|-----------|-----------|-----------------|----------------|--------------------------------|
|           |           | MMA ± SD        | MMA ± SD       |                                |
| Acetate   | Control   | 6.46 ± 0.74     | 4.90 ± 0.14    | -24.1                          |
|           | rGO       | 7.31 ± 0.09     | 7.11 ± 0.34    | -2.6                           |
| Hydrogen  | Control   | 22.22 ± 3.70    | 30.30 ± 2.08   | 36.4                           |
|           | rGO       | 26.58 ± 2.54    | 32.64 ± 2.54   | 22.8                           |
| Methanol  | Control   | 0.99 ± 0.07     | 0.81 ± 0.03    | -17.8                          |
|           | rGO       | 2.00 ± 0.03     | 1.23 ± 0.05    | -38.2                          |

<sup>1</sup>MMA calculated by linear regression from at least three sampling points during the kinetics. <sup>2</sup>300 mg/L of rGO was used in all cases; control was incubated in the absence of rGO. <sup>3</sup>Change on MMA, calculated from incubations with crushed sludge respect to those with granular sludge; positive values indicate an increase on MMA, while negative ones, a decrease.



## 4.4 Conclusions

The results obtained in the present study showed that high concentrations of GO negatively affect the hydrogenotrophic and acetoclastic methanogenic activity of an anaerobic consortium. However, the presence of rGO promoted an improvement of up to 40 % of the maximum methanogenic activity achieved with all substrates, except for the hydrogenotrophic pathway that was relatively insensitive to rGO. The methylotrophic pathway seemed to benefit from the presence of either rGO or GO, showing a significant increase of the specific methanogenic activity. Results also suggest that microbial reduction of GO during the incubation period outcompeted methanogenesis, so that electrons derived from substrates oxidation were deviated from methanogenesis towards the reduction of GO, which may explain the decrease in the methanogenic activity observed in the presence of high concentrations of GO. This study provides information to elucidate the effects of GO in anaerobic consortia and the fate of this material in wastewater treatment systems.



---

# **Chapter V**

## **General discussion**



The role of GO in the methanogenic activity of an anaerobic consortium depends strongly on the presence of oxygenated functional groups, which determine whether the effect is negative or positive, as shown by the results obtained in the present dissertation. By reducing GO, the effect shifts from inhibition to stimulation of methanogenesis using both complex (starch) and simple (glucose) substrates as is exemplified in Figure V-1; **Error! No se encuentra el origen de la referencia.** in which the two extremes were compared, in other words, the most oxidized and the most reduced materials were used in the bioassays to measure the effect exerted on the methane production.

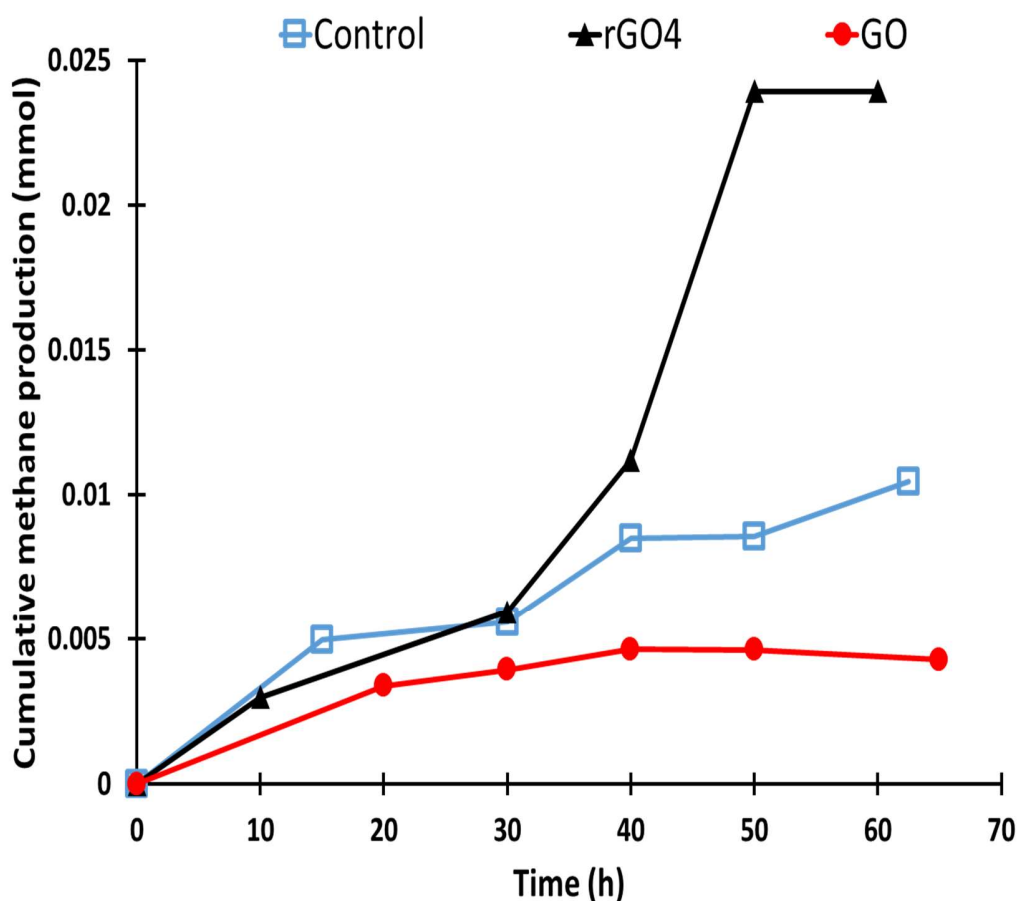
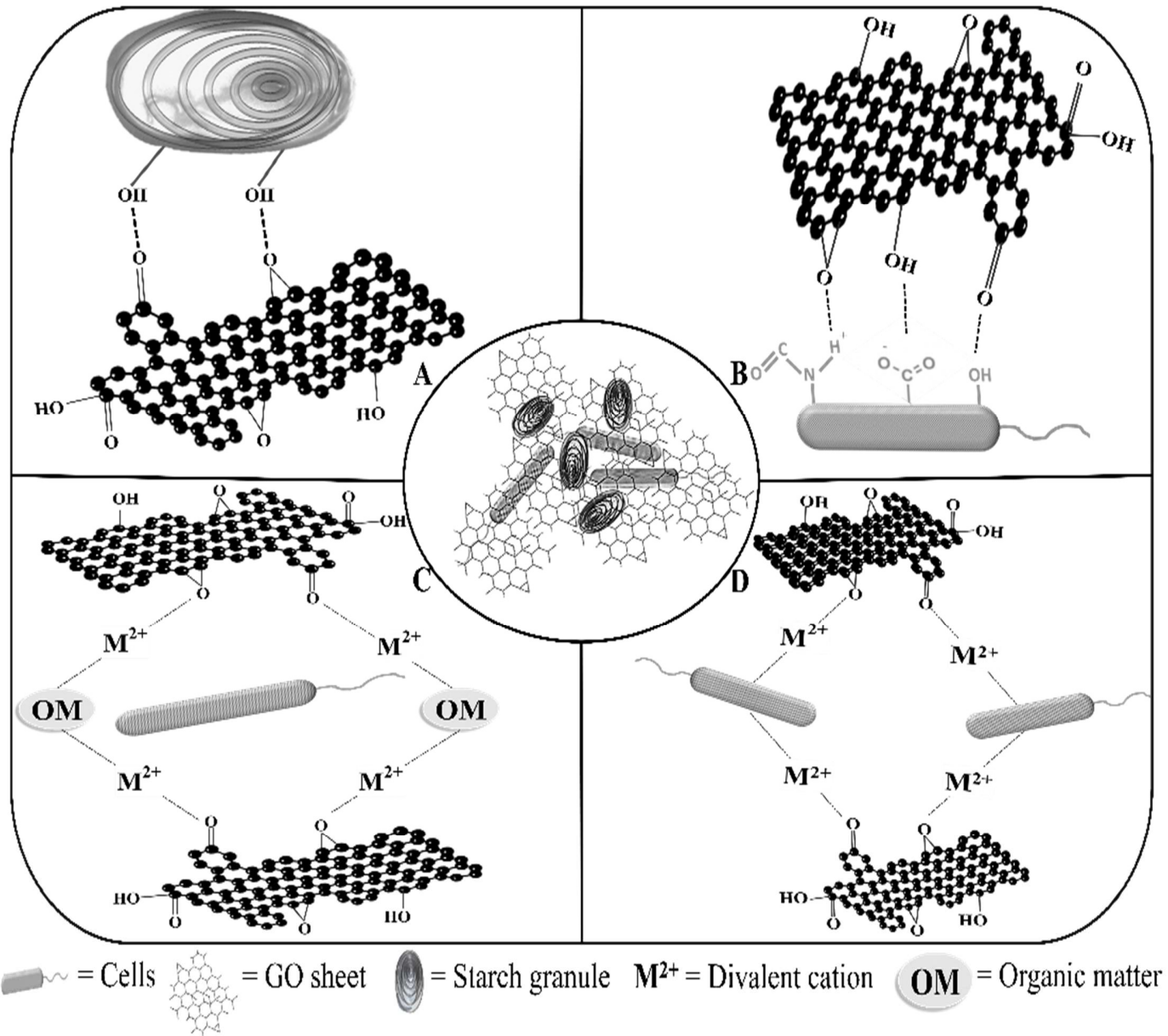


Figure V-1. Comparison of the effect of GO and rGO4 on the anaerobic methanogenic consortium, using 100 mg/L of starch as substrate and 300 mg/L of each graphene material. Control is the treatment without graphene materials.



The results showed that inhibition of starch methanization was due to the envelop of starch granules by GO sheets due to electrostatic interactions, among them hydrogen bridge between hydroxyl groups with positive partial charge of starch and carboxyl and/or epoxy groups with partial negative charge (as outlined in Figure V-2A). Wrapping of starch granules prevents their hydrolysis by mass transfer limitations. Moreover, the inhibition observed with glucose as substrate suggests encapsulation of anaerobic microorganisms due to electrostatic interactions with their functional groups and those of the GO (Figure V-2B). Additionally, the formation of agglomerates of GO due to the bridging phenomenon promoted by the cations of the culture medium and organic matter (Figure V-2C) or live cells (Figure V-2D) could be another inhibitory mechanism during glucose fermentation. However, it cannot be ruled out that cellular damage also occurred because of cutting or extraction of fragments from the external parts of the cells that have been reported in other research works (Liu et al., 2012b; Ou et al., 2016).



**Figure V-2.** Schematic representation of the possible interactions between starch (A) or cells (B) and the GO functional groups; as well as GO agglomeration due to the bridging effect of divalent cations in the basal medium that could involve organic matter (C; e.g. Exopolysaccharides) or cells directly (D).



On the other hand, when rGO is present, the effect observed in the methanogenic process is positive, reaching a maximum improvement of MMA of up to 13.8 % in the case of glucose and 114.1 % for starch as compared to their corresponding controls (Table III-1). The enhancing effect by rGO for the case of starch is attributed to the destabilization of the structure of starch granules by rGO promoting their breakdown into smaller components (Figure III-3). This could have caused an increase of specific surface area with the consequent increase in hydrolysis rate. Meanwhile, in the case of glucose, the evidence seems to indicate that the improvement was due to the increase in the mobility of electrons in the rGO by removing oxygenated groups, such as epoxy, from the basal plane, thus favoring DIET. In addition, these results also showed that the degree of reduction is an important parameter because it determined the amount of remaining functional groups that lead to interactions between rGO and substrate and cells. The reduction process of GO also affects the physical properties of rGO, modifying its particle size (therefore specific surface area) and its resistance to transport electrons. For this reason, it was observed that rGO1 showed a better catalytic performance, in experiments conducted with starch, because it had a greater number of functional groups that can remove amylose and amylopectin structures from the granule and presents a high specific surface area (smaller particle size) within of the culture medium. In the case of glucose, the best material enhancing methanogenesis was rGO2, which was the material presenting a balance between the quantity of oxygenated groups, which allow a good dispersion in the medium and a better conductivity.

Experiments conducted to decipher the specific effects of GO on the different methanogenic routes showed negatively affects by GO on the acetoclastic and hydrogenotrophic pathways, while the opposite occurred in the methylotrophic activity. Based on the evidence found, these results are explained considering that GO is microbially reduced by microorganisms, thus the energy yielded from substrates oxidation is partly used for the reduction of GO instead of the production of methane, particularly for the case of the acetoclastic route. Meanwhile, in the case of the methylotrophic route, the negative effect of GO was quickly reversed by transforming it into rGO and hence an improvement in methane production was observed, which agrees with the results obtained with chemically reduced rGO (Table IV-1). These results indicate that GO selectively



---

inhibits the methanogenic routes and, in addition, the evidence of GO transformation shows that anaerobic consortia can be used for the biological reduction in a dependent manner of the substrate fed.

The results of this work contribute to understanding how wastewater treatment systems, based on anaerobic digestion, can be affected or improved due to the presence of GO and rGO, also provide information on the fate of graphene materials in wastewater treatment systems and in the environment. Moreover, this research provides evidence on the potential use of anaerobic consortia for the biological reduction of GO.



---

# **Chapter VI**

## **Final remarks**



## 6.1 Concluding remarks

Currently, materials such as graphene oxide (GO) and its derivatives have become a central theme in scientific research and have already become part of the products available in the market, which also makes them part of the emerging pollutants. Consequently, knowledge of their effects and how to deal with them is required.

This study clarified, for the first time, mass transfer limitations imposed by GO on the methanogenic activity by an anaerobic consortium. Collected evidence indicated that wrapping of starch granules was the main mechanism involved. The results also revealed that low concentration of GO may enhance the methanogenic activity of the anaerobic consortium studied, presumably driven by DIET, during glucose fermentation.

This study demonstrates that reduced GO (rGO) materials interact with particulate organic matter promoting its disintegration. Thus, the study also presents evidence on the importance of the degree of reduction in the improvement of methanogenesis using simple substrates. The knowledge generated by this study allows predicting the effects of the different materials derived from the GO and apply them for the improvement of biotechnological processes involving anaerobic digestion.

The results obtained in the present study showed negative affectation at high concentrations of GO on the hydrogenotrophic and acetoclastic methanogenic activity of an anaerobic consortium. However, the presence of rGO promoted an improvement of up to 40 % of the maximum methanogenic activity achieved in the acetoclastic and methylotrophic experiments, while the hydrogenotrophic pathway was relatively insensitive to rGO. The methylotrophic pathway seemed to benefit from the presence of either rGO or GO, showing a significant increase of the specific methanogenic activity. Results also suggest that microbial reduction of GO during the incubation period outcompeted methanogenesis, so that electrons derived from substrates oxidation were



---

deviated from methanogenesis towards the reduction of GO, which may explain the decrease in the methanogenic activity observed in the presence of high concentrations of GO.

Finally, a deeper understanding of the variables that give rise to the interactions between graphene oxide and anaerobic digestion systems, as well as the evaluation of the type and magnitude of the effects that may occur, creates a framework of knowledge that can be used to determine the fate of these nanomaterials and to predict their possible effects in the environment.



## 6.2 Perspectives

It was observed that GO wraps starch granules, and this process triggered mass transfer limitations, which decreased the production of methane. Further studies are necessary to assess the effects in a system in which a soluble substrate is also present, which can be used as an energy source for microorganisms to reduce GO as is been evidenced in this work using different types of soluble substrates.

The effects of GO and rGO in anaerobic digestion, studied here, were related to acute exposure, but it is necessary to assess the long-term effects, since the properties of the graphenic materials will change due to the interactions with cells products or byproducts and the bioactivity of microorganisms.

Continuous processes, that are more representative of wastewater treatment systems, need study to understand the effects of GO and rGO, as well as the capacity of these systems to retain those graphenic materials to define bioaccumulation and possible effects of it in the environment.

It is necessary to increase the complexity of the studied systems to mimic real scenarios in anaerobic treatment systems, to better understand the effects of graphene-like materials on anaerobic digestion of real treatment systems.



## 6.3 Scientific products

### 6.3.1 Scientific publications

Bueno-López, J.I., Rangel-Mendez, J.R., Alatraste-Mondragón, F., Pérez-Rodríguez, F., Hernández-Montoya, V., Cervantes, F.J., Graphene oxide triggers mass transfer limitations on the methanogenic activity of an anaerobic consortium with a particulate substrate. *Chemosphere* (2018) 211, 709–716. <https://doi.org/10.1016/j.chemosphere.2018.08.001>.

J. Iván Bueno-López, Chi H. Nguyen, J. Rene Rangel-Mendez, Reyes Sierra-Alvarez, James A. Field, and Francisco J. Cervantes. Effects of graphene oxide and reduced graphene oxide on acetoclastic, hydrogenotrophic and methylotrophic methanogenesis. **Submitted.**

J. Iván Bueno-López, Alejandra Díaz-Hinojosa, J. Rene Rangel-Mendez, Felipe Alatraste-Mondragón, Fátima Pérez-Rodríguez, Virginia Hernández-Montoya and Francisco J. Cervantes. Enhanced methane production promoted by reduced graphene oxide in an anaerobic consortium supplied with particulate and soluble substrates **Submitted.**

### 6.3.2 Congresses and symposia

Bueno-López, J.I., Rangel-Mendez, J.R. Cervantes, F.J. Efecto de las interacciones óxido de grafeno y almidón en el proceso de digestión anaerobia. IX Congreso de la Red Latinoamericana de Ciencias Ambientales (RELACIAM). Octubre 2-6, 2017. San Luis Potosí, SLP, México.



Bueno-López, J.I., Rangel-Mendez, J.R. Cervantes, F.J. Interacciones almidón-óxido de grafeno y sus implicaciones en un proceso metanogénico. 8º Simposio de avances de tesis del posgrado en Ciencias Ambientales. April 20-21, 2017. San Luis Potosí, SLP, México.

Bueno-López, J.I., Rangel-Mendez, J.R. Cervantes, F.J. Efecto de las interacciones óxido de grafeno y almidón en el proceso de digestión anaerobia. 2º Congreso de la Asociación Mexicana del Carbono (AMEXCarb). November 14-17, 2017. San Luis Potosí, SLP, México.

Bueno-López, J.I., Rangel-Mendez, J.R. Cervantes, F.J. Elucidando el papel del óxido de grafeno en la digestión anaerobia. X Simposio de avances de tesis de los posgrados en Ciencias Ambientales. April 25-26, 2019. San Luis Potosí, SLP, México.

Bueno-López, J.I., Rangel-Mendez, J.R. Cervantes, F.J. Acute effects of the reduction degree of graphene oxide on methane production. 16th World Congress on Anaerobic Digestion. Jun 23-27, 2019. Delft, The Netherlands.



## References

- Acik, M., Lee, G., Mattevi, C., Pirkle, A., Wallace, R.M., Chhowalla, M., Cho, K., Chabal, Y., 2011. The Role of Oxygen during Thermal Reduction of Graphene Oxide Studied by Infrared Absorption Spectroscopy. *J. Phys. Chem. C* 115, 19761–19781. <https://doi.org/10.1021/jp2052618>
- Akhavan, O., Ghaderi, E., 2012. Escherichia coli bacteria reduce graphene oxide to bactericidal graphene in a self-limiting manner. *Carbon N. Y.* 50, 1853–1860. <https://doi.org/10.1016/j.carbon.2011.12.035>
- Akhavan, O., Ghaderi, E., Esfandiar, A., 2011. Wrapping Bacteria by Graphene Nanosheets for Isolation from Environment, Reactivation by Sonication, and Inactivation by Near-Infrared Irradiation. *J. Phys. Chem. B* 115, 6279–6288. <https://doi.org/10.1021/jp200686k>
- Amezquita-Garcia, H.J., Rangel-Mendez, J.R., Cervantes, F.J., Razo-Flores, E., 2016. Activated carbon fibers with redox-active functionalities improves the continuous anaerobic biotransformation of 4-nitrophenol. *Chem. Eng. J.* 286, 208–215. <https://doi.org/10.1016/j.cej.2015.10.085>
- Anjum, M., Miandad, R., Waqas, M., Gehany, F., Barakat, M.A., 2016. Remediation of wastewater using various nano-materials. *Arab. J. Chem.* <https://doi.org/10.1016/j.arabjc.2016.10.004>
- Appels, L., Baeyens, J., Degève, J., Dewil, R., 2008. Principles and potential of the anaerobic digestion of waste-activated sludge. *Prog. Energy Combust. Sci.* 34, 755–781. <https://doi.org/10.1016/j.pecs.2008.06.002>
- Arriaga, S., Rosas, I., Alatríste-Mondragón, F., Razo-Flores, E., 2011. Continuous production of hydrogen from oat straw hydrolysate in a biotrickling filter. *Int. J. Hydrogen Energy* 36, 3442–3449. <https://doi.org/10.1016/j.ijhydene.2010.12.019>
- Bagri, A., Mattevi, C., Acik, M., Chabal, Y.J., Chhowalla, M., Shenoy, V.B., 2010. Structural evolution during the reduction of chemically derived graphene oxide. *Nat. Chem.* 2, 581–587.



<https://doi.org/10.1038/nchem.686>

- Bartholy, J., Pongrácz, R., 2018. A brief review of health-related issues occurring in urban areas related to global warming of 1.5°C. *Curr. Opin. Environ. Sustain.* 30, 123–132. <https://doi.org/10.1016/J.COSUST.2018.05.014>
- Barua, S., Dhar, B.R., 2017. Advances towards understanding and engineering direct interspecies electron transfer in anaerobic digestion. *Bioresour. Technol.* 244, 698–707. <https://doi.org/10.1016/j.biortech.2017.08.023>
- Besinis, A., De Peralta, T., Tredwin, C.J., Handy, R.D., 2015. Review of nanomaterials in dentistry: Interactions with the oral microenvironment, clinical applications, hazards, and benefits. *ACS Nano* 9, 2255–2289. <https://doi.org/10.1021/nn505015e>
- Biniak, S., Szymański, G., Siedlewski, J., Świątkowski, A., 1997. The characterization of activated carbons with oxygen and nitrogen surface groups. *Carbon N. Y.* 35, 1799–1810. [https://doi.org/10.1016/S0008-6223\(97\)00096-1](https://doi.org/10.1016/S0008-6223(97)00096-1)
- Bras, J., Dufresne, A., 2010. Starch Nanoparticles: A Review 1139–1153. <https://doi.org/10.1021/bm901428y>
- Bueno-López, J.I., Rangel-Mendez, J.R., Alatríste-Mondragón, F., Pérez-Rodríguez, F., Hernández-Montoya, V., Cervantes, F.J., 2018. Graphene oxide triggers mass transfer limitations on the methanogenic activity of an anaerobic consortium with a particulate substrate. *Chemosphere* 211, 709–716. <https://doi.org/10.1016/j.chemosphere.2018.08.001>
- Bullock, C., 2000. The Archaea—a biochemical perspective. *Biochem. Mol. Biol. Educ.* 28, 186–191. <https://doi.org/10.1111/j.1539-3429.2000.tb00142.x>
- Cai, X., Tan, S., Lin, M., Xie, A., Mai, W., Zhang, X., Lin, Z., Wu, T., Liu, Y., 2011. Synergistic Antibacterial Brilliant Blue/Reduced Graphene Oxide/Quaternary Phosphonium Salt Composite with Excellent Water Solubility and Specific Targeting Capability. *Langmuir* 27, 7828–7835. <https://doi.org/10.1021/la201499s>
- Capson-Tojo, G., Moscoviz, R., Ruiz, D., Santa-Catalina, G., Trably, E., Rouez, M., Crest, M.,



- Steyer, J.-P., Bernet, N., Delgenès, J.-P., Escudié, R., 2018. Addition of granular activated carbon and trace elements to favor volatile fatty acid consumption during anaerobic digestion of food waste. *Bioresour. Technol.* 260, 157–168. <https://doi.org/10.1016/J.BIORTECH.2018.03.097>
- Caruana, D.J., Olsen, A.E. (Eds.), 2016. *Anaerobic digestion: processes, products, and applications*, Naskeo Environment. Nova Science Publishers.
- Castro, K.L.S., Curti, R. V., Araujo, J.R., Landi, S.M., Ferreira, E.H.M., Neves, R.S., Kuznetsov, A., Sena, L.A., Archanjo, B.S., Achete, C.A., 2016. Calcium incorporation in graphene oxide particles: A morphological, chemical, electrical, and thermal study. *Thin Solid Films* 610, 10–18. <https://doi.org/10.1016/j.tsf.2016.04.042>
- Cervantes, F.J., De Bok, F.A.M., Duong-Dac, T., Stams, A.J.M., Lettinga, G., Field, J.A., 2002. Reduction of humic substances by halorespiring, sulphate-reducing and methanogenic microorganisms. *Environ. Microbiol.* 4, 51–57. <https://doi.org/10.1046/j.1462-2920.2002.00258.x>
- Cervantes, F.J., Dos Santos, A.B., 2011. Reduction of azo dyes by anaerobic bacteria: microbiological and biochemical aspects. *Rev. Environ. Sci. Bio/Technology* 10, 125–137. <https://doi.org/10.1007/s11157-011-9228-9>
- Chen, Y., Niu, Y., Tian, T., Zhang, J., Wang, Y., Li, Y., Qin, L.C., 2017. Microbial reduction of graphene oxide by *Azotobacter chroococcum*. *Chem. Phys. Lett.* 677, 143–147. <https://doi.org/10.1016/j.cplett.2017.04.002>
- Cheng, C., Li, S., Thomas, A., Kotov, N.A., Haag, R., 2017. Functional Graphene Nanomaterials Based Architectures: Biointeractions, Fabrications, and Emerging Biological Applications. *Chem. Rev.* 117, 1826–1914. <https://doi.org/10.1021/acs.chemrev.6b00520>
- Cherubini, F., 2010. The biorefinery concept: Using biomass instead of oil for producing energy and chemicals. *Energy Convers. Manag.* 51, 1412–1421. <https://doi.org/10.1016/j.enconman.2010.01.015>



- Chowdhury, I., Mansukhani, N.D., Guiney, L.M., Hersam, M.C., Bouchard, D., 2015. Aggregation and Stability of Reduced Graphene Oxide: Complex Roles of Divalent Cations, pH, and Natural Organic Matter. *Environ. Sci. Technol.* 49, 10886–10893. <https://doi.org/10.1021/acs.est.5b01866>
- Colunga, A., Rangel-Mendez, J.R., Celis, L.B., Cervantes, F.J., 2015. Graphene oxide as electron shuttle for increased redox conversion of contaminants under methanogenic and sulfate-reducing conditions. *Bioresour. Technol.* 175, 309–314. <https://doi.org/10.1016/j.biortech.2014.10.101>
- Costa, K.C., Leigh, J.A., 2014. Metabolic versatility in methanogens. *Curr. Opin. Biotechnol.* 29, 70–75. <https://doi.org/10.1016/j.copbio.2014.02.012>
- De Silva, K.K.H., Huang, H.-H., Joshi, R.K., Yoshimura, M., 2017. Chemical reduction of graphene oxide using green reductants. *Carbon N. Y.* 119, 190–199. <https://doi.org/10.1016/j.carbon.2017.04.025>
- Deppenmeier, U., 2002. Redox-driven proton translocation in methanogenic Archaea. *Cell. Mol. Life Sci.* 59, 1513–1533. <https://doi.org/10.1007/s00018-002-8526-3>
- Dhillon, R.S., von Wuehlisch, G., 2013. Mitigation of global warming through renewable biomass. *Biomass and Bioenergy* 48, 75–89. <https://doi.org/10.1016/J.BIOMBIOE.2012.11.005>
- Dong, B., Xia, Z., Sun, J., Dai, X., Chen, X., Ni, B.J., 2019. The inhibitory impacts of nano-graphene oxide on methane production from waste activated sludge in anaerobic digestion. *Sci. Total Environ.* 646, 1376–1384. <https://doi.org/10.1016/j.scitotenv.2018.07.424>
- Dreyer, D.R., Park, S., Bielawski, C.W., Ruoff, R.S., 2010. The chemistry of graphene oxide. *Chem. Soc. Rev.* 39, 228–240. <https://doi.org/10.1039/b917103g>
- Eduok, S., Martin, B., Villa, R., Nocker, A., Jefferson, B., Coulon, F., 2013. Evaluation of engineered nanoparticle toxic effect on wastewater microorganisms: Current status and challenges. *Ecotoxicol. Environ. Saf.* 95, 1–9. <https://doi.org/10.1016/j.ecoenv.2013.05.022>
- Edyvean, R.G.J., Banwart, S.A., Ojeda, J.J., Romero-González, M.E., Bachmann, R.T., 2008.



- Characterization of the Cell Surface and Cell Wall Chemistry of Drinking Water Bacteria by Combining XPS, FTIR Spectroscopy, Modeling, and Potentiometric Titrations. *Langmuir* 24, 4032–4040. <https://doi.org/10.1021/la702284b>
- Feng, Y., Feng, N., Du, G., 2013. A green reduction of graphene oxide via starch-based materials. *RSC Adv.* 3, 2146621474. <https://doi.org/10.1039/c3ra43025a>
- Ferrari, A.C., 2007. Raman spectroscopy of graphene and graphite: Disorder, electron–phonon coupling, doping and nonadiabatic effects. *Solid State Commun.* 143, 47–57. <https://doi.org/10.1016/J.SSC.2007.03.052>
- Ferrer Polo, J., Seco Torrecillas, A., 2008. Tratamientos biológicos de aguas residuales. Alfaomega.
- Gonzalez-Estrella, J., Sierra-Alvarez, R., Field, J.A., 2013. Toxicity assessment of inorganic nanoparticles to acetoclastic and hydrogenotrophic methanogenic activity in anaerobic granular sludge. *J. Hazard. Mater.* 260, 278–285. <https://doi.org/10.1016/j.jhazmat.2013.05.029>
- Grasso, M., 2019. Oily politics: A critical assessment of the oil and gas industry’s contribution to climate change. *Energy Res. Soc. Sci.* 50, 106–115. <https://doi.org/10.1016/J.ERSS.2018.11.017>
- Guo, J., Peng, Y., Ni, B.J., Han, X., Fan, L., Yuan, Z., 2015. Dissecting microbial community structure and methane-producing pathways of a full-scale anaerobic reactor digesting activated sludge from wastewater treatment by metagenomic sequencing. *Microb. Cell Fact.* 14, 33. <https://doi.org/10.1186/s12934-015-0218-4>
- Guo, Z., Xie, C., Zhang, P., Zhang, J., Wang, G., He, X., Ma, Y., Zhao, B., Zhang, Z., 2017. Toxicity and transformation of graphene oxide and reduced graphene oxide in bacteria biofilm. *Sci. Total Environ.* 580, 1300–1308. <https://doi.org/10.1016/j.scitotenv.2016.12.093>
- Hantsche, H., 1993. High resolution XPS of organic polymers, the scienta ESCA300 database. *Adv. Mater.* 5, 778–778. <https://doi.org/10.1002/adma.19930051035>



- He, X., Aker, W.G., Leszczynski, J., Hwang, H.M., 2014. Using a holistic approach to assess the impact of engineered nanomaterials inducing toxicity in aquatic systems. *J. Food Drug Anal.* 22, 128–146. <https://doi.org/10.1016/j.jfda.2014.01.011>
- Holden, P.A., Gardea-Torresdey, J., Klaessig, F., Turco, R.F., Mortimer, M., Hund-Rinke, K., Cohen Hubal, E.A., Avery, D., Barcelo, D., Behra, R., Cohen, Y., Deydier-Stephan, L., Ferguson, P.L., Fernandes, T.F., Herr Harthorn, B., Henderson, W.M., Hoke, R.A., Hristozov, D., Johnston, J.M., Kane, A.B., Kapustka, L., Keller, A.A., Lenihan, H.S., Lovell, W., Murphy, C.J., Nisbet, R.M., Petersen, E.J., Salinas, E.R., Scheringer, M., Sharma, M., Speed, D.E., Sultan, Y., Westerhoff, P., White, J.C., Wiesner, M.R., Wong, E.M., Xing, B., Steele Horan, M., Godwin, H.A., Nel, A.E., 2016. Considerations of Environmentally Relevant Test Conditions for Improved Evaluation of Ecological Hazards of Engineered Nanomaterials. *Environ. Sci. Technol.* <https://doi.org/10.1021/acs.est.6b00608>
- Hoover, R., 2001. Composition, molecular structure, and physicochemical properties of tuber and root starches: A review. *Carbohydr. Polym.* 45, 253–267. [https://doi.org/10.1016/S0144-8617\(00\)00260-5](https://doi.org/10.1016/S0144-8617(00)00260-5)
- Hu, L., Wan, J., Zeng, G., Chen, A., Chen, G., Huang, Z., He, K., Cheng, M., Zhou, C., Xiong, W., Lai, C., Xu, P., 2017. Comprehensive evaluation of the cytotoxicity of CdSe/ZnS quantum dots in *Phanerochaete chrysosporium* by cellular uptake and oxidative stress. *Environ. Sci. Nano* 4, 2018–2029. <https://doi.org/10.1039/C7EN00517B>
- Hu, X., Li, D., Gao, Y., Mu, L., Zhou, Q., 2016. Knowledge gaps between nanotoxicological research and nanomaterial safety. *Environ. Int.* 94, 8–23. <https://doi.org/10.1016/j.envint.2016.05.001>
- Hu, X., Zhou, Q., 2013. Health and ecosystem risks of graphene. *Chem. Rev.* 113, 3815–3835. <https://doi.org/10.1021/cr300045n>
- International Energy Agency, 2012. Bio-based Chemicals Value Added Products from Biorefineries. Bioenergy-Task42.



- Jagiello, J., Bandosz, T.J., Putyera, K., Schwarz, J.A., 1995. Determination of Proton Affinity Distributions for Chemical Systems in Aqueous Environments Using a Stable Numerical Solution of the Adsorption Integral Equation. *J. Colloid Interface Sci.* 172, 341–346. <https://doi.org/10.1006/jcis.1995.1262>
- Jastrzębska, A.M., Olszyna, A.R., 2015. The ecotoxicity of graphene family materials: current status, knowledge gaps and future needs. *J. Nanoparticle Res.* 17, 40. <https://doi.org/10.1007/s11051-014-2817-0>
- Jung, I., Vaupel, M., Pelton, M., Pinery, R., Dikin, D.A., Stankovich, S., An, J., Ruoff, R.S., 2008. Characterization of thermally reduced graphene oxide by imaging ellipsometry. *J. Phys. Chem. C* 112, 8499–8506. <https://doi.org/10.1021/jp802173m>
- Konkena, B., Vasudevan, S., 2012. Understanding aqueous dispersibility of graphene oxide and reduced graphene oxide through pKa measurements. *J. Phys. Chem. Lett.* 3, 867–872. <https://doi.org/10.1021/jz300236w>
- Le Corre, D., Bras, J., Dufresne, A., 2010. Starch nanoparticles: A review. *Biomacromolecules* 11, 1139–1153. <https://doi.org/10.1021/bm901428y>
- Leone, L., Loring, J., Sjöberg, S., Persson, P., Shchukarev, A., 2006. Surface characterization of the Gram-positive bacteria *Bacillus subtilis*-an XPS study. *Surf. Interface Anal.* 38, 202–205. <https://doi.org/10.1002/sia.2184>
- Levi, G., Senneca, O., Causà, M., Salatino, P., Lacovig, P., Lizzit, S., 2015. Probing the chemical nature of surface oxides during coal char oxidation by high-resolution XPS. *Carbon N. Y.* 90, 181–196. <https://doi.org/10.1016/j.carbon.2015.04.003>
- Li, R., Liu, C., Ma, J., 2011. Studies on the properties of graphene oxide-reinforced starch biocomposites. *Carbohydr. Polym.* 84, 631–637. <https://doi.org/10.1016/j.carbpol.2010.12.041>
- Lin, L.-C., Grossman, J.C., 2015. Atomistic understandings of reduced graphene oxide as an ultrathin-film nanoporous membrane for separations. *Nat. Commun.* 6.



<https://doi.org/10.1038/ncomms9335>

- Lin, R., Cheng, J., Zhang, J., Zhou, J., Cen, K., Murphy, J.D., 2017a. Boosting biomethane yield and production rate with graphene: The potential of direct interspecies electron transfer in anaerobic digestion. *Bioresour. Technol.* 239, 345–352. <https://doi.org/10.1016/j.biortech.2017.05.017>
- Lin, R., Cheng, J., Zhang, J., Zhou, J., Cen, K., Murphy, J.D., 2017b. Boosting biomethane yield and production rate with graphene: The potential of direct interspecies electron transfer in anaerobic digestion. *Bioresour. Technol.* 239, 345–352. <https://doi.org/10.1016/j.biortech.2017.05.017>
- Liu, S., Hu, M., Zeng, T.H., Wu, R., Jiang, R., Wei, J., Wang, L., Kong, J., Chen, Y., 2012a. Lateral Dimension Dependent Antibacterial Activity of Graphene Oxide Sheets. *Langmuir*. <https://doi.org/10.1021/la3023908>
- Liu, S., Hu, M., Zeng, T.H., Wu, R., Jiang, R., Wei, J., Wang, L., Kong, J., Chen, Y., 2012b. Lateral Dimension-Dependent Antibacterial Activity of Graphene Oxide Sheets. *Langmuir* 28, 12364–12372. <https://doi.org/10.1021/la3023908>
- Lovley, D.R., 2011. Live wires: direct extracellular electron exchange for bioenergy and the bioremediation of energy-related contamination. *Energy Environ. Sci.* 4, 4896. <https://doi.org/10.1039/c1ee02229f>
- Lü, F., Guo, K.J., Duan, H.W., Shao, L.M., He, P.J., 2018. Exploit Carbon Materials to Accelerate Initiation and Enhance Process Stability of CO Anaerobic Open-Culture Fermentation. *ACS Sustain. Chem. Eng.* 6, 2787–2796. <https://doi.org/10.1021/acssuschemeng.7b04589>
- Lu, X., Zhen, G., Estrada, A.L., Chen, M., Ni, J., Hojo, T., Kubota, K., Li, Y.-Y., 2015. Operation performance and granule characterization of upflow anaerobic sludge blanket (UASB) reactor treating wastewater with starch as the sole carbon source. *Bioresour. Technol.* 180, 264–273. <https://doi.org/10.1016/j.biortech.2015.01.010>
- Luo, Y., Yang, X., Tan, X., Xu, L., Liu, Z., Xiao, J., Peng, R., 2016. Functionalized graphene



- oxide in microbial engineering: An effective stimulator for bacterial growth. *Carbon* N. Y. 103, 172–180. <https://doi.org/10.1016/j.carbon.2016.03.012>
- Ma, J., Quan, X., Si, X., Wu, Y., 2013. Responses of anaerobic granule and flocculent sludge to ceria nanoparticles and toxic mechanisms. *Bioresour. Technol.* 149, 346–352. <https://doi.org/10.1016/j.biortech.2013.09.080>
- Ma, T., Chang, P.R., Zheng, P., Ma, X., 2013. The composites based on plasticized starch and graphene oxide/reduced graphene oxide. *Carbohydr. Polym.* 94, 63–70. <https://doi.org/10.1016/j.carbpol.2013.01.007>
- Mao, S.S., Shen, S., Guo, L., 2012. Nanomaterials for renewable hydrogen production, storage and utilization. *Prog. Nat. Sci. Mater. Int.* 22, 522–534. <https://doi.org/10.1016/j.pnsc.2012.12.003>
- Marcoux, M.A., Matias, M., Olivier, F., Keck, G., 2013. Review and prospect of emerging contaminants in waste - Key issues and challenges linked to their presence in waste treatment schemes: General aspects and focus on nanoparticles. *Waste Manag.* 33, 2147–2156. <https://doi.org/10.1016/j.wasman.2013.06.022>
- Martins, G., Salvador, A.F., Pereira, L., Alves, M.M., 2018. Methane Production and Conductive Materials: A Critical Review. *Environ. Sci. Technol.* 52, 10241–10253. <https://doi.org/10.1021/acs.est.8b01913>
- Mattevi, C., Eda, G., Agnoli, S., Miller, S., Mkhoyan, K.A., Celik, O., Mastrogiovanni, D., Granozzi, G., Carfunkel, E., Chhowalla, M., 2009. Evolution of electrical, chemical, and structural properties of transparent and conducting chemically derived graphene thin films. *Adv. Funct. Mater.* 19, 2577–2583. <https://doi.org/10.1002/adfm.200900166>
- Mohammadinejad, R., Karimi, S., Irvani, S., Varma, R.S., 2016. Plant-derived nanostructures: types and applications. *Green Chem* 18. <https://doi.org/10.1039/c5gc01403d>
- National Centers for Environmental Information, 2019. State of the Climate: Global Climate Report for March 2019, published online.



- NOAA Earth System Research Laboratory, 2005. ESRL Global Monitoring Division - Global Greenhouse Gas [WWW Document]. URL <https://www.esrl.noaa.gov/gmd/ccgg/trends/> (accessed 5.8.19).
- Novoselov, K.S., Fal'ko, V.I., Colombo, L., Gellert, P.R., Schwab, M.G., Kim, K., 2012. A roadmap for graphene. *Nature* 490, 192–200. <https://doi.org/10.1038/nature11458>
- Ohara, H., 2003. Biorefinery. *Appl. Microbiol. Biotechnol.* 62, 474–477. <https://doi.org/10.1007/s00253-003-1383-7>
- Otero-González, L., Field, J.A., Sierra-Alvarez, R., 2014. Fate and long-term inhibitory impact of ZnO nanoparticles during high-rate anaerobic wastewater treatment. *J. Environ. Manage.* 135, 110–117. <https://doi.org/10.1016/j.jenvman.2014.01.025>
- Ou, L., Song, B., Liang, H., Liu, J., Feng, X., Deng, B., Sun, T., Shao, L., 2016. Toxicity of graphene-family nanoparticles: A general review of the origins and mechanisms. Part. *Fibre Toxicol.* <https://doi.org/10.1186/s12989-016-0168-y>
- Park, J.-H., Kang, H.-J., Park, K.-H., Park, H.-D., 2018. Direct interspecies electron transfer via conductive materials: A perspective for anaerobic digestion applications. *Bioresour. Technol.* 254, 300–311. <https://doi.org/10.1016/j.biortech.2018.01.095>
- Park, M.V.D.Z., Bleeker, E.A.J., Brand, W., Cassee, F.R., Van Elk, M., Gosens, I., De Jong, W.H., Meesters, J.A.J., Peijnenburg, W.J.G.M., Quik, J.T.K., Vandebriel, R.J., Sips, A.J.A.M., 2017. Considerations for Safe Innovation: The Case of Graphene. *ACS Nano.* <https://doi.org/10.1021/acsnano.7b04120>
- Patrón-Soberano, A., Núñez-Luna, B.P., Casas-Flores, S., De Las Peñas, A., Domínguez-Espíndola, R.B., Rodríguez-González, V., 2017. Photochemical & Photobiological Sciences Photo-assisted inactivation of *Escherichia coli* bacteria by silver functionalized titanate nanotubes,  $\text{Ag/H}_2\text{Ti}_2\text{O}_5 \cdot \text{H}_2\text{O}$ . *Photochem. Photobiol. Sci.* 16. <https://doi.org/10.1039/c6pp00237d>
- Pei, S., Cheng, H.-M., 2012. The reduction of graphene oxide. *Carbon* N. Y. 50, 3210–3228.



<https://doi.org/10.1016/j.carbon.2011.11.010>

Pérez, S., Bertoft, E., 2010. The molecular structures of starch components and their contribution to the architecture of starch granules: A comprehensive review. *Starch/Staerke*. <https://doi.org/10.1002/star.201000013>

Pradeep, T., Anshup, 2009. Noble metal nanoparticles for water purification: A critical review. *Thin Solid Films* 517, 6441–6478. <https://doi.org/10.1016/j.tsf.2009.03.195>

Puziy, A.M., Poddubnaya, O.I., Socha, R.P., Gurgul, J., Wisniewski, M., 2008. XPS and NMR studies of phosphoric acid activated carbons. *Carbon N. Y.* 46, 2113–2123. <https://doi.org/10.1016/j.carbon.2008.09.010>

Rabaçal, M., Ferreira, A.F., Silva, C.A.M., Editors, M.C., 2017. *Biorefineries Targeting Energy, High Value Products and Waste Valorisation, Lecture Notes in Energy*. Springer International Publishing AG. <https://doi.org/10.1007/978-3-319-48288-0>

Raveendran, S., Chauhan, N., Nakajima, Y., Toshiaki, H., Kurosu, S., Tanizawa, Y., Tero, R., Yoshida, Y., Hanajiri, T., Maekawa, T., Ajayan, P.M., Sandhu, A., Kumar, D.S., 2013. Ecofriendly Route for the Synthesis of Highly Conductive Graphene Using Extremophiles for Green Electronics and Bioscience. *Part. Part. Syst. Charact.* 30, 573–578. <https://doi.org/10.1002/ppsc.201200126>

Raza, H. (Ed.), 2012. *Graphene Nanoelectronics, NanoScience and Technology*. Springer Berlin Heidelberg, Berlin, Heidelberg. <https://doi.org/10.1007/978-3-642-22984-8>

Rogala, M., Dabrowski, P., Kowalczyk, P.J., Wlasny, I., Kozłowski, W., Busiakiewicz, A., Karaduman, I., Lipinska, L., Baranowski, J.M., Klusek, Z., 2016. The observer effect in graphene oxide – How the standard measurements affect the chemical and electronic structure. *Carbon N. Y.* 103, 235–241. <https://doi.org/10.1016/j.carbon.2016.03.015>

Salas, E.C., Sun, Z., Lüttge, A., Tour, J.M., 2010. Reduction of Graphene Oxide via Bacterial Respiration. *ACS Nano* 4, 4852–4856. <https://doi.org/10.1021/nn101081t>

Salvador, A.F., Martins, G., Melle-Franco, M., Serpa, R., Stams, A.J.M., Cavaleiro, A.J., Pereira,



- M.A., Alves, M.M., 2017. Carbon nanotubes accelerate methane production in pure cultures of methanogens and in a syntrophic coculture. *Environ. Microbiol.* 19, 2727–2739. <https://doi.org/10.1111/1462-2920.13774>
- Şentürk, E., Ince, M., Engin, G.O., 2010. Kinetic evaluation and performance of a mesophilic anaerobic contact reactor treating medium-strength food-processing wastewater. *Bioresour. Technol.* 101, 3970–3977. <https://doi.org/10.1016/j.biortech.2010.01.034>
- Shen, L., Jin, Z., Wang, D., Wang, Y., Lu, Y., 2018. Enhance wastewater biological treatment through the bacteria induced graphene oxide hydrogel. *Chemosphere* 190, 201–210. <https://doi.org/10.1016/j.chemosphere.2017.09.105>
- Simon-Pascual, A., Sierra-Alvarez, R., Field, J.A., 2019. Platinum(II) reduction to platinum nanoparticles in anaerobic sludge. *J. Chem. Technol. Biotechnol.* 94, 468–474. <https://doi.org/10.1002/jctb.5791>
- Socrates, G., 2004. *Infrared and Raman Characteristic Group Frequencies: Tables and Charts*, 3rd ed. John Wiley and Sons.
- Song, Y., Qu, K., Zhao, C., Ren, J., Qu, X., 2010. Graphene oxide: Intrinsic peroxidase catalytic activity and its application to glucose detection. *Adv. Mater.* 22, 2206–2210. <https://doi.org/10.1002/adma.200903783>
- Su, C., Acik, M., Takai, K., Lu, J., Hao, S., Zheng, Y., Wu, P., Bao, Q., Enoki, T., Chabal, Y.J., Ping Loh, K., 2012. Probing the catalytic activity of porous graphene oxide and the origin of this behaviour. *Nat. Commun.* 3, 1298. <https://doi.org/10.1038/ncomms2315>
- Thakur, S., Karak, N., 2015. Alternative methods and nature-based reagents for the reduction of graphene oxide: A review. *Carbon N. Y.* 94, 224–242. <https://doi.org/10.1016/j.carbon.2015.06.030>
- Tian, T., Qiao, S., Li, X., Zhang, M., Zhou, J., 2017a. Nano-graphene induced positive effects on methanogenesis in anaerobic digestion. *Bioresour. Technol.* 224, 41–47. <https://doi.org/10.1016/j.biortech.2016.10.058>



- Tian, T., Qiao, S., Li, X., Zhang, M., Zhou, J., 2017b. Nano-graphene induced positive effects on methanogenesis in anaerobic digestion. <https://doi.org/10.1016/j.biortech.2016.10.058>
- Tiwari, A., 2013. Innovative Graphene Technologies: Developments & Characterisation. Smithers Information Limited.
- Toral-Sánchez, E., Ascacio Valdés, J.A., Aguilar, C.N., Cervantes, F.J., Rangel-Mendez, J.R., 2016. Role of the intrinsic properties of partially reduced graphene oxides on the chemical transformation of iopromide. *Carbon* N. Y. 99, 456–465. <https://doi.org/10.1016/j.carbon.2015.12.067>
- Toral-Sánchez, E., Rangel-Mendez, J.R., Ascacio Valdés, J.A., Aguilar, C.N., Cervantes, F.J., 2017. Tailoring partially reduced graphene oxide as redox mediator for enhanced biotransformation of iopromide under methanogenic and sulfate-reducing conditions. *Bioresour. Technol.* 223, 269–276. <https://doi.org/10.1016/j.biortech.2016.10.062>
- Trujillo-Reyes, J., Peralta-Videa, J.R., Gardea-Torresdey, J.L., 2014. Supported and unsupported nanomaterials for water and soil remediation: Are they a useful solution for worldwide pollution? *J. Hazard. Mater.* 280, 487–503. <https://doi.org/10.1016/j.jhazmat.2014.08.029>
- Valenzuela, E.I., Prieto-Davó, A., López-Lozano, N.E., Hernández-Eligio, A., Vega-Alvarado, L., Juárez, K., García-González, A.S., López, M.G., Cervantes, F.J., 2017. Anaerobic Methane Oxidation Driven by Microbial Reduction of Natural Organic Matter in a Tropical Wetland. *Appl. Environ. Microbiol.* 83, AEM.00645-17. <https://doi.org/10.1128/AEM.00645-17>
- Vance, M.E., Kuiken, T., Vejerano, E.P., McGinnis, S.P., Hochella, M.F., Hull, D.R., 2015. Nanotechnology in the real world: Redeveloping the nanomaterial consumer products inventory. *Beilstein J. Nanotechnol.* 6, 1769–1780. <https://doi.org/10.3762/bjnano.6.181>
- Vanier, N.L., El Halal, S.L.M., Dias, A.R.G., da Rosa Zavareze, E., 2017. Molecular structure, functionality and applications of oxidized starches: A review. *Food Chem.* 221, 1546–1559. <https://doi.org/10.1016/j.foodchem.2016.10.138>
- Vasileva, P., Donkova, B., Karadjova, I., Dushkin, C., 2011. Synthesis of starch-stabilized silver



- nanoparticles and their application as a surface plasmon resonance-based sensor of hydrogen peroxide. *Colloids Surfaces A Physicochem. Eng. Asp.* 382, 203–210. <https://doi.org/10.1016/j.colsurfa.2010.11.060>
- Walsh, B.S., Parratt, S.R., Hoffmann, A.A., Atkinson, D., Snook, R.R., Bretman, A., Price, T.A.R., 2019. The Impact of Climate Change on Fertility. *Trends Ecol. Evol.* 34, 249–259. <https://doi.org/10.1016/J.TREE.2018.12.002>
- Wang, G., Qian, F., Saltikov, C.W., Jiao, Y., Li, Y., 2011. Microbial reduction of graphene oxide by *Shewanella*. *Nano Res.* 4, 563–570. <https://doi.org/10.1007/s12274-011-0112-2>
- Wang, H., Yuan, X., Wu, Y., Huang, H., Peng, X., Zeng, G., Zhong, H., Liang, J., Ren, M.M., 2013. Graphene-based materials: Fabrication, characterization and application for the decontamination of wastewater and wastegas and hydrogen storage/generation. *Adv. Colloid Interface Sci.* 195–196, 19–40. <https://doi.org/10.1016/j.cis.2013.03.009>
- Wang, J., Wang, D., Liu, G., Jin, R., Lu, H., 2014. Enhanced nitrobenzene biotransformation by graphene-anaerobic sludge composite. *J. Chem. Technol. Biotechnol.* 89, 750–755. <https://doi.org/10.1002/jctb.4182>
- Xie, F., Pollet, E., Halley, P.J., Avérous, L., 2013. Starch-based nano-biocomposites. *Prog. Polym. Sci.* 38, 1590–1628. <https://doi.org/10.1016/j.progpolymsci.2013.05.002>
- Xu, H., Xie, L., Wu, D., Hakkarainen, M., 2016. Immobilized Graphene Oxide Nanosheets as Thin but Strong Nanointerfaces in Biocomposites. *ACS Sustain. Chem. Eng.* 4, 2211–2222. <https://doi.org/10.1021/acssuschemeng.5b01703>
- Xu, S., He, C., Luo, L., Lü, F., He, P., Cui, L., 2015. Comparing activated carbon of different particle sizes on enhancing methane generation in upflow anaerobic digester. *Bioresour. Technol.* 196, 606–612. <https://doi.org/10.1016/j.biortech.2015.08.018>
- Yang, Y., Yu, Z., Nosaka, T., Doudrick, K., Hristovski, K., Herckes, P., Westerhoff, P., 2015. Interaction of carbonaceous nanomaterials with wastewater biomass. *Front. Environ. Sci. Eng.* 9, 823–831. <https://doi.org/10.1007/s11783-015-0787-9>



- Yoshida, N., Miyata, Y., Doi, K., Goto, Y., Nagao, Y., Tero, R., Hiraishi, A., 2016. Graphene oxide-dependent growth and self-Aggregation into a hydrogel complex of exoelectrogenic bacteria. *Sci. Rep.* 6, 21867. <https://doi.org/10.1038/srep21867>
- Zhang, H., Da, Z., Feng, Y., Wang, Y., Cai, L., Cui, H., 2018. Enhancing the electricity generation and sludge reduction of sludge microbial fuel cell with graphene oxide and reduced graphene oxide. *J. Clean. Prod.* 186, 104–112. <https://doi.org/10.1016/j.jclepro.2018.02.159>
- Zhang, H., Yu, X., Guo, D., Qu, B., Zhang, M., Li, Q., Wang, T., 2013. Synthesis of Bacteria Promoted Reduced Graphene Oxide-Nickel Sulfide Networks for Advanced Supercapacitors. *ACS Appl. Mater. Interfaces* 5, 7335–7340. <https://doi.org/10.1021/am401680m>
- Zhao, J., Wang, Z., White, J.C., Xing, B., 2014. Graphene in the aquatic environment: Adsorption, dispersion, toxicity and transformation. *Environ. Sci. Technol.* 48, 9995–10009. <https://doi.org/10.1021/es5022679>
- Zhao, Z., Zhang, Y., Woodard, T.L., Nevin, K.P., Lovley, D.R., 2015. Enhancing syntrophic metabolism in up-flow anaerobic sludge blanket reactors with conductive carbon materials. *Bioresour. Technol.* 191, 140–145. <https://doi.org/10.1016/J.BIORTECH.2015.05.007>
- Zou, X., Zhang, L., Wang, Z., Luo, Y., 2016. Mechanisms of the Antimicrobial Activities of Graphene Materials. *J. Am. Chem. Soc.* 138, 2064–2077. <https://doi.org/10.1021/jacs.5b11411>

